

# JGR Space Physics

## REVIEW ARTICLE

10.1029/2020JA029097

### Special Section:

Solar and Heliospheric Plasma Structures: Waves, Turbulence, and Dissipation

### Key Points:

- Physics of waves in solar chromosphere
- Heating of the chromosphere by waves and instabilities
- Wave propagation through the solar chromosphere

### Correspondence to:

A. K. Srivastava,  
asrivastava.app@iitbhu.ac.in








### Citation:

Srivastava, A. K., Ballester, J. L., Cally, P. S., Carlsson, M., Goossens, M., Jess, D. B., et al. (2021). Chromospheric heating by magnetohydrodynamic waves and instabilities. *Journal of Geophysical Research: Space Physics*, 126, e2020JA029097. <https://doi.org/10.1029/2020JA029097>

Received 5 JAN 2021

Accepted 2 APR 2021

## Chromospheric Heating by Magnetohydrodynamic Waves and Instabilities

A. K. Srivastava<sup>1</sup> , J. L. Ballester<sup>2,3</sup> , P. S. Cally<sup>4</sup> , M. Carlsson<sup>5,6</sup> , M. Goossens<sup>7</sup>,  
D. B. Jess<sup>8</sup> , E. Khomenko<sup>9,10</sup>, M. Mathioudakis<sup>8</sup>, K. Murawski<sup>11</sup> , and  
T. V. Zaqarashvili<sup>12,13,14</sup> 

<sup>1</sup>Department of Physics, Indian Institute of Technology (BHU), Varanasi, India, <sup>2</sup>Departament de Física, Universitat de les Illes Balears, Palma de Mallorca, Spain, <sup>3</sup>Institut d'Aplicacions Computacionals de Codi Comunitari (IAC3), Universitat de les Illes Balears, Palma de Mallorca, Spain, <sup>4</sup>School of Mathematics, Monash University, Clayton, Australia, <sup>5</sup>Institute of Theoretical Astrophysics, University of Oslo, Oslo, Norway, <sup>6</sup>Roseland Center for Solar Physics, University of Oslo, Oslo, Norway, <sup>7</sup>Centre for Mathematical Plasma Astrophysics (CmPA), KU Leuven, Leuven, Belgium, <sup>8</sup>Astrophysics Research Centre, School of Mathematics and Physics, Queen's University Belfast, Belfast, UK, <sup>9</sup>Instituto de Astrofísica de Canarias, La Laguna, Spain, <sup>10</sup>Departamento de Astrofísica, Universidad de La Laguna, La Laguna, Spain, <sup>11</sup>Institute of Physics, University of M. Curie-Skłodowska, Lublin, Poland, <sup>12</sup>IGAM, Institute für Physik, University of Graz, Graz, Austria, <sup>13</sup>Ilia State University, Tbilisi, Georgia, <sup>14</sup>Abastumani Astrophysical Observatory, Abastumani, Georgia

**Abstract** The importance of the chromosphere in the mass and energy transport within the solar atmosphere is now widely recognized. This review discusses the physics of magnetohydrodynamic waves and instabilities in large-scale chromospheric structures as well as in magnetic flux tubes. We highlight a number of key observational aspects that have helped our understanding of the role of the solar chromosphere in various dynamic processes and wave phenomena, and the heating scenario of the solar chromosphere is also discussed. The review focuses on the physics of waves and invokes the basics of plasma instabilities in the context of this important layer of the solar atmosphere. Potential implications, future trends and outstanding questions are also delineated.

### 1. Introduction

The complex magnetic field of the solar chromosphere exerts significant effects on the propagation and dissipation of magnetohydrodynamic (MHD) waves. The chromosphere channels mechanical energy from the photosphere into the transition region (TR) and corona, leading to several physical processes such as wave reflection and mode-conversion, which depend on the magnetic field strength and the local plasma properties (e.g., Ballester et al., 2020; Cally & Khomenko, 2019; Srivastava et al., 2008; Vecchio et al., 2007). In the quiet-Sun the magnetic field is rooted in the intergranular lanes forming intense flux tubes which are subjected to continuous motions of their footpoints. The physical nature of the drivers near the footpoints of the flux tubes results in a variety of wave modes which evolve as they travel through the solar photosphere and lower chromosphere. Such MHD waves may also be evolved in situ in the chromosphere and can propagate into TR and inner corona imparting some Poynting energy flux to overcome their radiative losses, as recently observed in a variety of chromospheric structures (e.g., Jess et al., 2009, 2020; Kukhianidze et al., 2006; Kuridze et al., 2013; Morton et al., 2012; Srivastava et al., 2017; Zaqarashvili et al., 2007). For example these MHD modes include: (i) kink waves excited by the horizontal buffeting motions, (ii) slow waves due to pressure fluctuations, (iii) torsional Alfvén waves generated by the twisting motions; or/otherwise important in the long-wavelength limit fast and slow magnetoacoustic-gravity waves as well as their hybrid consisting of coupled Alfvén and magnetoacoustic-gravity waves (e.g., De Pontieu et al., 2007; Hasan et al., 2003; Jess et al., 2009, 2015; Khomenko, Collados, & Felipe, 2008; Liu et al., 2019; Mathioudakis et al., 2013; McIntosh et al., 2011; Morton et al., 2012; Srivastava et al., 2017; Ulmschneider et al., 1991).

The MHD waves and oscillations are also associated with the active region sunspots. The chromospheric plasma, which is a low-lying and rather strongly magnetized region above these spots, possesses exotic physical processes and their subsequent effects on the wave propagation. Wave excitation mechanisms above these spots, mode conversion, the formation of shocks, frequency dependent reflection from the transition region, the effects of complex magnetic structuring and inhomogeneities in the penumbra, put forward a

multitude of physical processes that affect the evolution and dissipation of MHD wave modes and determine their role in chromospheric and coronal heating (e.g., Botha et al., 2011; Cho & Chae, 2020; Crouch & Cally, 2005; Grant et al., 2018; Kang et al., 2019; Khomenko & Cally, 2012; Khomenko & Collados, 2015; Srivastava et al., 2018; Tian et al., 2014). While the complex structuring of plasma and magnetic field above sunspots influence highly the evolutionary and dissipative properties of MHD waves over the large-scale environment at long-wavelength limits, there is an ample evidence that these strongly magnetized structures can act as a MHD wave-guide for the excited tubular modes (e.g., kink, sausage, and torsional modes) which transport the significant amount of energy upwards into the overlying corona possibly for its heating (e.g., Grant et al., 2015; Jess et al., 2017; Keys et al., 2018; Moreels, Van Doorselaere, et al., 2015).

The plasma of solar prominences has properties similar to the properties of the chromospheric plasma, apart from the superstrong magnetic field in the intense flux tubes. These structures are treated as thermally and pressure isolated, enveloped inside a Prominence-Corona-Transition-Region (PCTR) and are made-up of partially ionized plasma (Parenti, 2014). It has been proposed that the excitation and dissipation of MHD waves in prominences can contribute to their heating in addition to the more dominant radiative heating (Arregui, 2015). Complex and turbulent flows, strong inhomogeneities in plasma and magnetic field properties under the presence of gravity also yield some typical instabilities in such isolated chromospheric plasma systems, e.g., Rayleigh-Taylor (R-T), Kelvin-Helmholtz (K-H) instabilities (e.g., T. E. Berger et al., 2008; Ryutova et al., 2010; T. E. Berger et al., 2010; Hillier et al., 2011; Innes et al., 2012; T. Berger et al., 2017; Mishra & Srivastava, 2019; Mishra et al., 2018). As a result of the existence of waves and a wide variety of plasma flows induced by their nonlinear behavior in the prominences, which are strongly influenced by the large magnetic Reynolds numbers of the ambient system, such solar prominences may develop turbulence that further contribute significantly to the heating rate of these large-scale structures (Hillier & Polito, 2018).

The solar chromosphere is different from the corona as far as MHD wave modes, instabilities, and heating are concerned. It requires higher amounts of energy input ( $10^6$ – $10^7$  erg cm<sup>-2</sup>s<sup>-1</sup>) to balance its radiative losses compared to the solar corona ( $10^4$ – $10^6$  erg cm<sup>-2</sup>s<sup>-1</sup>). Realistic models of the chromospheric plasma involve a multi-fluid approach with a finite plasma-beta and accommodate the additional physical effects of partial ionisation and radiative transfer in non-local thermodynamic equilibrium (e.g., Ballai et al., 2019; Hansteen et al., 2007; Martínez-Sykora et al., 2015; Soler et al., 2012; Soler et al., 2019). Although the single continuum fluid consideration at MHD length and time scales will suffice in dealing with the various wave modes or instabilities in the solar chromosphere, we do not invoke some additional frequency dependent physics of the region, for example., wave damping by ion-neutral collisions, etc., there (Ballester et al., 2018).

Alternatively, the direct dissipation of electric current facilitated by the magnetic reconnection provides a stringent physical scenario about another significant mechanism to heat the solar atmosphere (e.g., nano-flare heating; bulk plasma heating; liberating energy through twists and braiding of the magnetic field lines, etc.) (e.g., Cargill & Klimchuk, 2004; Klimchuk, 2015; Srivastava et al., 2019; Winebarger et al., 2013; Xue et al., 2016). Apart from the magnetic reconnection generated heating, when we consider the two- or multi-fluid scales and relevant physical scenario especially in the context of the solar chromosphere, regardless of the waves the frictional heating can be significant as it simply accounts for the case where the ions are moving relatively to the neutrals and the friction between them can be significant (e.g., Al Shidi et al., 2019). The similar physical scenario is true for the waves and instabilities also in the frame-work of the solar chromosphere where the deviation from MHD scales to fluid scales lead the additional physics (e.g., ion-neutral collisions; ambipolar diffusion, etc) leading the evolution and dissipation of the perturbations at much smaller spatial scales (e.g., Díaz et al., 2012; Soler et al., 2013; Khomenko & Collados, 2012; Khomenko, Díaz, et al., 2014; Martínez-Gómez et al., 2018; Soler, Ballester, & Zaqarashvili, 2015; Soler, Carbonell, & Ballester, 2015; Soler et al., 2012; Zaqarashvili et al., 2013). Complementing the alternative physical scenario significant for the chromospheric heating and multitude of its dynamical plasma processes, we conjecture herewith that the present article review the role of the waves and instability in MHD environment of the solar chromosphere.

There have been several reviews that discuss the key observations and theoretical developments on MHD waves in the solar chromosphere and corona and their contribution to heating (e.g., Arregui, 2015; Aschwanden, 2019; Jess et al., 2015; Mathioudakis et al., 2013; Narain & Ulmschneider, 1996; Van Doorselaere et al., 2020; Zaqarashvili & Erdélyi, 2009). In the present review, we aim to discuss the physics of MHD

waves and instabilities in the chromospheric plasma, and their heating capabilities. The description of shocks is also included in the context of chromospheric heating. Key updates on new observational results of these physical phenomena are also elucidated. In Section 2, we address the physical behavior of MHD waves in the large-scale chromosphere, and depict recent progress on this important topic. Section 3 describes the physics and current trend of the research of various MHD waves in the structured chromosphere and its magnetic fluxtubes. We demonstrate the overall development in the understanding of solar chromospheric heating in Section 4. Thermally isolated chromospheric plasma structures, that is, solar prominences, are illustrated in Section 5. We discuss the evolution and observational aspects of instabilities that may have significant impact on the chromospheric plasma systems, including their contribution to heating and dynamics. In the last section, we present discussion and conclusions. Here, we also list a number of outstanding questions that could be addressed with the use of existing high-resolution and upcoming ultra high-resolution ground (e.g., 4m-Daniel K. Inouye Solar Telescope (DKIST), upcoming 4m-EST, 2m-NLST) and space (e.g., SDO, IRIS, Parker Solar Probe, Solar Orbiter, upcoming Aditya-L1, Solar-C, etc) borne observations, which will also ensure one-to-one continuous refinements of the theoretical understanding.

## 2. Magnetohydrodynamic Waves in the Large-Scale Chromosphere

MHD waves take their simplest linear form in a uniform ideal fully ionized magnetofluid, providing three restoring forces: gas pressure, magnetic pressure, and magnetic tension. The Alfvén wave, in its pure form, is driven by tension alone (though see the discussion in Section 3.3 for a more nuanced view), whilst the two magnetoacoustic waves, fast and slow, result from the combination of all three.

However, the solar chromosphere is very far from simple. To these basic forces, we must add the effects of magnetic structure, including current sheets, gravitational stratification, giving rise to refraction, reflection, steepening and buoyancy; nonlinearity; partial ionization; radiation; non-LTE; and substantial background flows. Under these conditions, the simple fast/slow/Alfvén categorization may be inadequate, or at least not globally valid.

There are also various sources of the wave motions, such as the Sun's internal oscillations, the p-modes; granulation at the photosphere; small reconnection events, etc. <sup>1</sup> (The net horizontal velocities in granules at the photosphere are of order  $0.5 \text{ km s}^{-1}$ , with the corresponding vertical velocities being about half that (Mattig et al., 1981). For comparison, the combined p-mode oscillation velocity amplitude in the five-minute range is also about  $0.5 \text{ km s}^{-1}$ , mostly vertical, though this is made up of millions of individual modes whose individual amplitudes do not exceed  $10 \text{ cm s}^{-1}$  (Christensen-Dalsgaard, 2002)). A commonly invoked wave driver is photospheric granulation. Although it has been argued that granulation is a part of a Kolmogorov turbulent spectrum (Espagnet et al., 1993), this has been strenuously disputed by Nordlund et al. (1997) on the basis that the turbulence is non-steady and full properties cannot be inferred from a single snapshot. Nevertheless, a granular scale of 1–2 Mm is prominent, and timescales of a few minutes are typical. Cranmer and van Ballegoijen (2005) famously based a whole-heliosphere Alfvén wave model on such granular and supergranular driving with peak “kink-mode wave energy” power at periods of 5–10 min, inferred from observed Magnetic Bright Point (MBP) motions.

The Sun's internal normal modes, the p- and f-modes, have a similar timescale, peaked around five minutes, though their horizontal length scales are far larger. A typical granule size of 1 Mm corresponds to a very high spherical harmonic degree  $\ell \approx 4,400$ , but nearly all p-mode power lies at much smaller  $\ell$ , so these drivers of atmospheric waves are quite distinct.

Using the Coronal Multi-Channel Polarimeter (CoMP) to observe a region of bright active region coronal loops in the FeXIII 1,074.7 nm emission line, Tomczyk et al. (2007) detected a distinct peak in oscillatory power around 3.5 mHz, which they associated with the Sun's internal p-modes. The power peak correlates well with both the position and width of the average power spectrum of intermediate degree photospheric seismic oscillations. These coronal oscillations were initially identified as Alfvén waves, but are more likely kink magnetoacoustic waves (Erdélyi & Fedun, 2007; Van Doorsselaere et al., 2008) if sufficient flux tube structuring is available to support them.

It is also possible that the 3.5 mHz peak is characteristic of coronal loop resonant frequencies rather than p-modes. Nechaeva et al. (2019) identify a large number of decaying kink oscillations with periods in the range of roughly 2–26 min (their Table 1), that is, frequencies between 0.6 and 8 mHz. See also the proposed self-oscillatory mechanism of Nakariakov, Anfinogentov et al. (2016). However, this frequency range seems much broader than the CoMP observations suggest. Their persistence across all coronal magnetic field topologies, even in open field, argues in favor of p-mode origins; see Morton et al. (2015, 2016 and 2019) for further details. Despite these indications, the role of p-modes in driving coronal oscillations remains an open question.

However, if p-modes are the cause, this poses the question of how these Alfvén or Alfvénic (near transverse and near incompressible) waves propagate through the chromosphere, and how they penetrate the transition region with enough amplitude to explain the observed transverse coronal oscillations (McIntosh & De Pontieu, 2012; McIntosh et al., 2011).

The energy carried by these coronal waves was estimated by McIntosh et al. (2011) and McIntosh and De Pontieu (2012), using more resolved observations from *Hinode*/SOT and SDO/AIA, to provide substantial coronal heating and solar wind acceleration. However, this was based on wave flux formulae relevant to Alfvén waves in a uniform plasma. It is now more widely believed that the observed oscillations are kink waves on discrete flux tubes, for which filling-factor considerations reduce the calculated fluxes by factors of 10–50 (Goossens et al., 2013a, 2013b).

Waves in and on magnetic structures such as spicules may contribute to coronal heating and solar wind origin, but in this section the focus is on the large scale in which the horizontal length scales are far larger than the typically 100–200 km vertically imposed by gravity. Due to the very weak ionization levels in the photosphere (typically of order  $10^{-4}$ ) there has been some doubt that Alfvén waves could be directly excited there to any significant amplitude (Vranjes et al., 2008), though this has been disputed. The knob of the discrepancy is that only the ionized fluid is given any initial velocity in the analysis of Vranjes et al., whereas Tsap et al. (2011) effectively give the ionized and neutral fluids the same initial velocity. Energy is therefore spread very thinly when it is used to accelerate the predominant neutral fluid in the model of Vranjes et al., thereby greatly reducing amplitude (Soler et al., 2013).

In any case, the p-mode component of any atmospheric wave driving in quiet Sun is predominantly acoustic and vertical at the photosphere, and clearly not Alfvénic. How does this ultimately register as transverse waves in the transition region and corona? Let us discuss the route taken by initially acoustic waves in traversing the chromosphere.

Two characteristic frequencies associated with an atmosphere determine the behavior of acoustic and acoustic-gravity waves: the Brunt-Väisälä or buoyancy frequency  $N$  defined by  $N^2 = g / H - g^2 / c_s^2$ , where  $g$  is the gravitational acceleration,  $H$  is the density scale height, and  $c_s$  is the sound speed, and the acoustic cutoff frequency  $\omega_c$ .

Acoustic cutoff frequency is a very fragile quantity, with different formulae resulting from using different variables in describing the equations (Schmitz & Fleck, 1998, 2003). In a non-magnetic plane-stratified atmosphere, introducing dependent variable  $\Psi = \rho^{1/2} c_s^2 \nabla \cdot \mathbf{v}$  (Deubner & Gough, 1984) and assuming  $\exp[i(k_x x + k_y y - \omega t)]$  dependence, the linearized wave equations may be reduced to the form

$$\frac{d^2 \Psi}{dz^2} + \left( \frac{\omega^2 - \omega_c^2}{c_s^2} + \frac{N^2}{\omega^2} k_h^2 - k_h^2 \right) \Psi = 0, \quad (1)$$

where  $k_h = \sqrt{k_x^2 + k_y^2}$  is the horizontal wave number, and  $\omega_c^2 = (c_s^2 / 4H^2)(1 - 2H')$ . Although mathematically elegant, the form of  $\omega_c$  in this formulation is a computational nightmare when used for calculations in a tabulated empirical atmosphere such as the widely used VAL C (Vernazza et al., 1981) (a tabulation of proton density, electron density, pressure, temperature, etc., in a one-dimensional stationary quiet chromosphere model based on non-LTE radiative transfer and many atomic and ionic species). It yields very noisy results because of the second derivative of density implicit in the  $H'$  term. Nevertheless, in an isothermal atmosphere, where  $H' = 0$ , the unambiguously correct “isothermal acoustic cutoff”  $\omega_{ci} = c_s / 2H$  is recovered.

Identifying the term in the bracket in Equation 1 as the square of the vertical wavenumber  $k_z$ , the dispersion relation for these non-magnetic waves is  $c_s^2 k_z^2 = \omega^2(\omega^2 - \omega_c^2) - (\omega^2 - N^2)c_s^2 k_h^2$ , which allows propagation vertically only if the right hand side is positive, that is, if

$$\omega^2 \geq \frac{1}{2} \left[ c_s^2 k_h^2 + \omega_c^2 \pm \sqrt{(c_s^2 k_h^2 + \omega_c^2)^2 - 4c_s^2 N^2 k_h^2} \right], \quad (2)$$

corresponding respectively to acoustic waves (upper signs  $>$  and  $+$ ) and gravity waves (lower signs  $<$  and  $-$ ). Between the two, the waves are vertically evanescent and do not propagate. In particular, if  $k_h = 0$ , propagation occurs only for frequencies  $\omega > \omega_c$ , which explains the name “cutoff frequency.” Typically, the acoustic cutoff frequency in the solar chromosphere is around 5 mHz, so by rights, sound waves should not be able to propagate upward below this frequency.

This provides an opportunity for trapping waves between two heights, corresponding to a cavity. A 3-min chromospheric cavity is reasonably well-established in sunspot atmospheres (e.g., Botha et al., 2011; Jess et al., 2020), although different interpretations can often be provided by considering line formation heights (Bogdan & Judge, 2006). There is evidence of a very small number of trapped “chromospheric eigen modes” in the quiet Sun too (Deubner et al., 1996), though Fleck and Schmitz (1991) attribute 3-min chromospheric oscillations to resonant excitation of an acoustic cutoff frequency mode that exists even in isothermal models where the acoustic cutoff frequency is constant. On the other hand, the chromosphere may be so dynamic that discussion of cavities is moot (Carlsson & Stein, 1998).

However, the chromosphere is magnetic (Carlsson & Stein, 1995). The acoustic cutoff effect is ameliorated by sufficiently strong magnetic field (Bel & Leroy, 1977), allowing propagation with a traveling (non-evanescent) vertical component if  $\omega > \omega_c \cos \theta$ , where  $\theta$  is the inclination angle of the magnetic field from the vertical. This opens “magnetic portals” (Jefferies et al., 2006) in the low atmosphere that allow waves well below 5 mHz to propagate into the upper atmosphere. This is sometimes called the “ramp effect”, and is most effective in quiet Sun in strong small scale magnetic elements such as supergranular network where  $\beta \lesssim 1$ . Of course, it is very effective in active regions.

A crucial insight is that the three MHD wave types: slow, Alfvén and fast, are not fixed across inhomogeneous atmospheres. They may be unambiguously one of these types over much of the atmosphere, but change to another type where the phase velocities of the two waves nearly match. This became apparent with the exact two-dimensional (2D) solutions for ideal magnetoacoustic waves in an isothermal gravitationally stratified atmosphere with uniform inclined magnetic field (Zhugzhda & Dzhaliyov, 1984 in terms of Meijer-G functions, or Cally, 2009 in terms of the more elementary  ${}_2F_3$  hypergeometric functions), where exact fast/slow coupling coefficients may be found. The Alfvén wave is strictly decoupled in 2D where the wave propagates in the plane defined by gravity and the magnetic field.

Two rather different types of mode conversion play a significant role. The first is fast/slow conversion at any Alfvén-acoustic equipartition surface  $v_A = c_s$ , where  $v_A$  is the Alfvén speed. In the quiet solar chromosphere this might typically be at heights of a few hundred kilometres, though in sunspots it can be below the photosphere. Above this region the Alfvén speed increases roughly exponentially, due to the exponential decrease in density with height, whilst the sound speed varies only slowly until the transition region is reached.

Fast/slow conversion is a very compact process. In a 2D scenario, Schunker and Cally (2006) show that the energy transmission coefficient is (to a good approximation) given by

$$T = \exp \left[ - \frac{\pi h k^2 k_{\perp}^2}{|k_z| (k^2 + k_{\perp}^2)} \right]_{v_A=c_s} = \exp \left[ - \frac{\pi h k^2 \sin^2 \alpha}{|k_z| (1 + \sin^2 \alpha)} \right]_{v_A=c_s}, \quad (3)$$

where  $k = |\mathbf{k}|$  is the total wave number,  $k_{\perp}$  is the component of wave vector  $\mathbf{k}$  perpendicular to the magnetic field,  $h = [d(v_A^2 / c_s^2) / dz]^{-1}$  is the equipartition layer scale height, and  $\alpha$  is the attack angle between the wave vector and the magnetic field (so  $k_{\perp} = k \sin \alpha$ ). The corresponding conversion coefficient is  $C = 1 - T$  (ignoring the phase). Note that transmission is total ( $T = 1$ ) for zero attack angle, meaning that a field-aligned fast wave from  $v_A < c_s$  (making it predominantly acoustic in nature) passes perfectly through to



$v_A > c_s$  still as acoustic wave (now the slow wave), with no conversion to a magnetically dominated (fast) wave. On the other hand, at non-zero attack angle, the incident wave splits into a combination of slow and fast waves. This is seen in numerous simulations (e.g., Felipe et al., 2010), and even persists for shock waves (Pennicott & Cally, 2019). Figure 1 illustrates the two mode conversion processes both schematically (upper) and through  $z - k_z$  dispersion diagrams for representative cases.

The other important mode conversion process is fast-to-Alfvén, which only occurs in 3D where gravity, the magnetic field lines and the wave vector are not co-planar. This discussion is predicated on the assumption that vertical gravitational stratification, typically with scale height of order 150 km in the chromosphere, is the dominant inhomogeneity. It would be altered in the presence of similar or smaller horizontal magnetic scales, though the general principles persist. High in the chromosphere, after (magnetically dominated) fast waves have been generated by mode conversion at  $v_A = c_s$  they propagate rapidly up into the region where  $v_A \gg c_s$  and their dispersion relation is  $\omega^2 \approx v_A^2(k_h^2 + k_z^2)$ . They then reflect ( $k_z = 0$ ) at around where the horizontal phase speed equals the Alfvén speed. It is near this point, but typically distributed over several scale heights, that the fast wave partially loses energy to generate an Alfvén wave, that either travels upwards along the field lines if those field lines are inclined in the direction of propagation, or downward if the field is inclined counter to the direction of wave propagation (Cally & Hansen, 2011). Both mode conversion processes are confirmed computationally by Cally and Goossens (2008). Fast-to-Alfvén conversion is found to enhance Alfvén wave penetration of the transition region compared to Alfvén waves generated at the photosphere (Hansen & Cally, 2012).

These two mode conversion processes are confirmed by simulations in model sunspots (Felipe, 2012; Khomeenko & Cally, 2012). By its very nature, mode conversion is not something that can be observed locally with telescopes and instruments, since the process happens where elsewhere-distinct wave types (fast, slow, and Alfvén) become almost degenerate and indistinguishable. In the language of Goossens et al. (2019), they exhibit “mixed properties”. This makes simulation particularly valuable in verifying and exploring the process in realistic atmospheres. From an observational viewpoint, mode conversion is best observed through its effects: the disappearance of p-modes hitting sunspots (Braun et al., 1987); the signatures of transverse waves in the corona associated with the 5-min oscillations (Tomczyk et al., 2007); the acoustic halos surrounding sunspots that bear the hallmarks of returning fast waves from above (Khomeenko & Collados, 2009; Rajaguru et al., 2013; Rijs et al., 2016); the influence of magnetic field inclination on chromospheric waves (Rajaguru et al., 2019); etc. As far as the chromosphere goes, the effects of mode conversion are potentially profound, providing rungs of a ladder for energy propagation from the photosphere to the corona. More detail about links between mode conversion and chromospheric wave heating may be found in Section 4.

In summary, above the acoustic cutoff frequency (about 5 mHz), acoustic waves from the surface or sub-surface, including those due to p-modes, may partially convert to magnetically dominated fast waves at  $v_A = c_s$ , and then, although these fast waves reflect and do not reach the corona, they may pass on considerable energy to Alfvén waves, and these can penetrate the transition region. However, below  $\omega_c$  they would need to enter via magnetic portals in inclined intense supergranular network flux elements, where they will encounter an  $v_A = c_s$  equipartition layer much lower in the atmosphere than in the broader canopy (Bogdan et al., 2003), perhaps several times as the Alfvén speed may decrease with height due to rapid field-line spread before increasing again as the density decreases. The picture is complicated further by a significant fraction of internetwork field (around half) that also joins the network field that reaches the corona (Schrijver & Title, 2003). This three-stage process may help explain the observational link between the Sun’s sub-surface seismic wavefield and the ubiquitous Alfvénic oscillations in the corona (Morton et al., 2015).

We have seen that the Sun’s internal normal modes, the p- and f-modes, can drive chromospheric oscillations, and perhaps even be detected in the corona. It is also well-established that the chromosphere affects the subsurface global seismology, particularly as activity varies across a solar cycle. Models are explored by Campbell and Roberts (1989); Evans and Roberts (1991) and reviewed at length by Erdélyi (2006), who asks “Can the tail wag the dog?” Furthermore, chromospheric waves can affect internal local seismology via a combination of the mechanisms discussed above, especially in and around active regions. Time-distance analysis of simulations by Cally and Moradi (2013) reveals that significant “travel time” discrepancies of up to 40 s are introduced around active regions by reflected and mode-converted waves re-entering the subphotosphere, thereby polluting the wavefield and making it more difficult to infer subsurface features

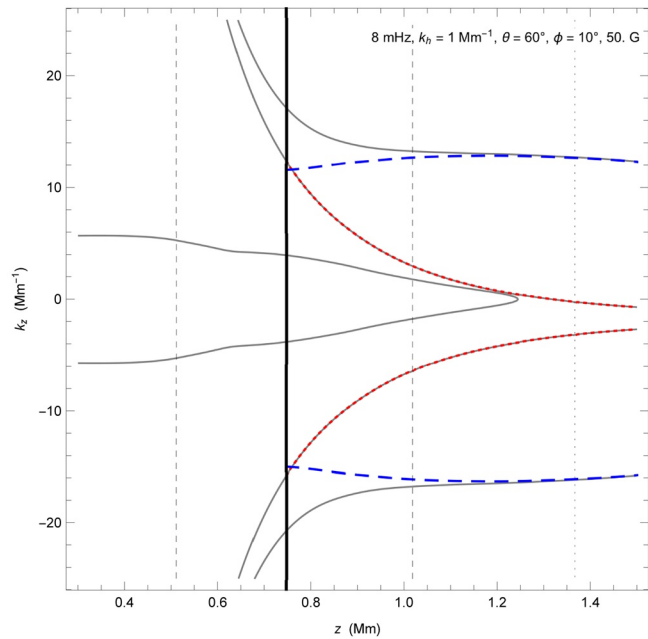
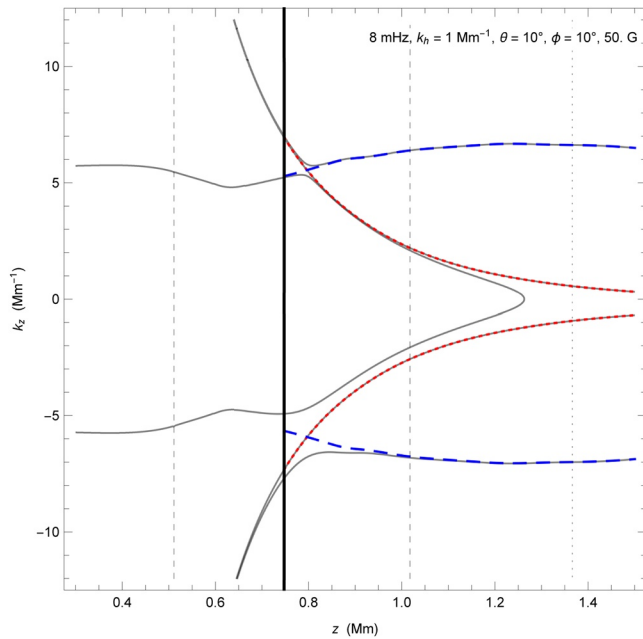
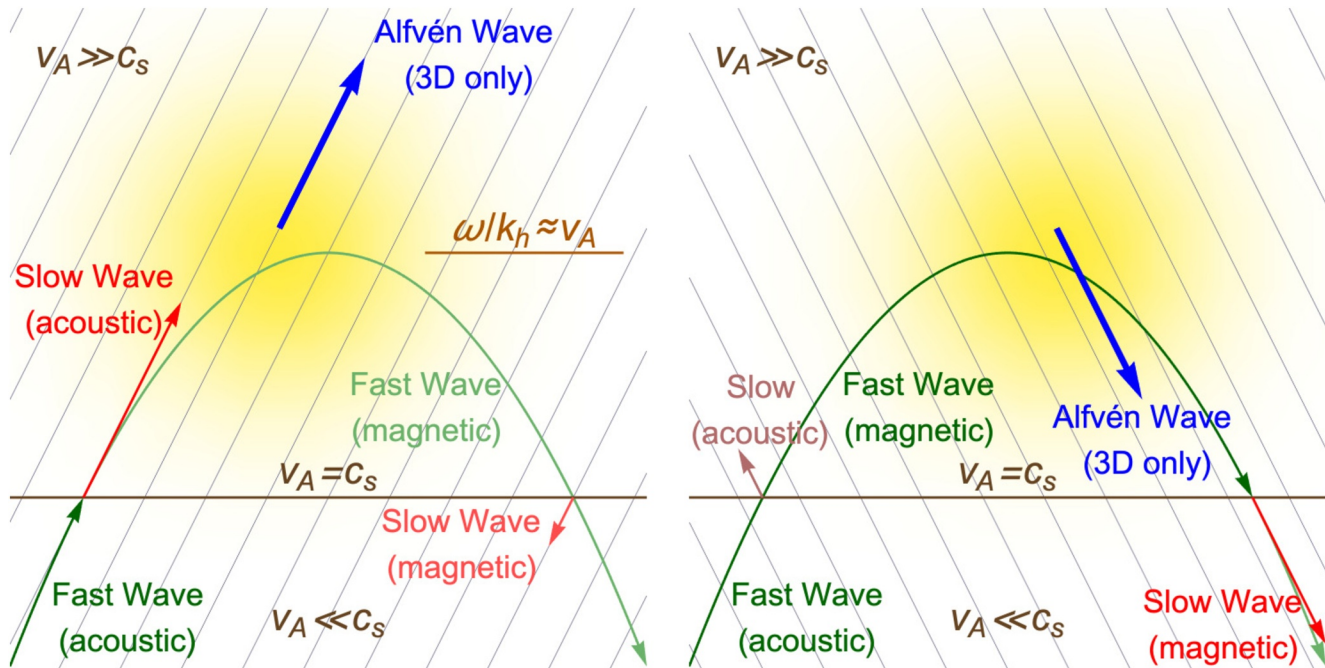


**Figure 1.** Top left: schematic diagram of an injected fast (acoustic) ray incident from bottom left traveling upward and passing through the Alfvén-acoustic equipartition level  $v_A = c_s$ , mostly transmitting as a slow wave but partly converting to a fast wave. The fast wave reflects near where its horizontal phase speed matches the Alfvén speed, where it partially converts to an upgoing Alfvén wave (three-dimensional [3D] only). Top right: same, except the magnetic field is inclined contrary to the propagation direction, so most energy at  $v_A = c_s$  goes into the fast wave, with subsequent conversion to a downward Alfvén wave. Bottom left:  $z - k_z$  dispersion diagram for an 8 mHz,  $k_h = 1 \text{ Mm}^{-1}$  wave in uniform 50 G magnetic field inclined  $\theta = 10^\circ$  from the vertical and oriented  $\phi = 10^\circ$  out of the  $x - z$  plane. The ray enters at the bottom on the fast branch with  $k_z \approx 6 \text{ Mm}^{-1}$ , reaches  $v_A = c_s$  around  $z = 0.75 \text{ Mm}$  (thick vertical line), and passes very close to the slow branch. Partial mode conversion happens at this avoided crossing. The subsequent fast ray continues upward and reflects around  $z = 1.3 \text{ Mm}$ , but experiences a long near-correspondence with the intermediate (Alfvén) mode and again partially converts. The blue dashed line indicates the asymptotic  $v_A \gg c_s$  slow (acoustic) wave and the red dashed curve is the asymptotic Alfvén wave. The atmosphere is VAL C. Bottom right: the same, but with  $\theta = 60^\circ$ , for which case the fast-Alfvén conversion occurs much closer to the fast wave apex. The upper part of this figure is adapted from Khomenko and Cally (2012).

from local seismic data. Rijs et al. (2016) also demonstrate via simulations that the observed acoustic halo around active regions is due to fast waves returning from the chromosphere.

A further feature of the photosphere and low chromosphere that affects wave propagation is the very low ionization fraction there, as low as  $10^{-4}$ . This has several effects. First, by increasing the mean molecular weight it profoundly alters the hydrostatic pressure and density structure of the equilibrium atmosphere, compared to a fully ionized model. Second, it introduces further physics, notably the Hall effect and ambipolar diffusion (Khomenko, Collados, et al., 2014). Although the Hall term is conventionally written in terms of a diffusivity  $\eta_H = B/(en_e\mu)$ , where  $e$  is the elemental charge,  $n_e$  is the electron number density and  $\mu$  is the magnetic permeability, it is not in fact diffusive (it does not contribute to the thermal energy). Instead, it induces a continuous oscillation between fast and Alfvén waves in the form of a precession of the polarization (Cally & Khomenko, 2015). However, the dimensionless Hall parameter for a wave of frequency  $\omega$ ,  $\epsilon = \omega/(f\Omega_i)$  where  $f = \rho_i/\rho$  is the ionization fraction and  $\Omega_i$  is the ion gyroradius, is insignificant in the solar chromosphere for all but weak fields (a few Gauss) and very high frequencies (of order 1 Hz or above). Simulations by González-Morales et al. (2019) confirm that Alfvén waves are indeed generated by Hall coupling at these high frequencies, and reach amplitudes sufficient to play a role in coronal heating.

In one-fluid descriptions, the ambipolar diffusivity is  $\eta_A = \xi_n^2 B^2 / (\alpha_n \mu)$ , where  $\xi_n = \rho_n/\rho = 1 - f$  is the fractional contribution of the neutrals to the density and  $\alpha_n$  is the neutral collisional parameter (a density-weighted collision frequency of neutrals with electrons and ions). Linear and nonlinear simulations of 10 mHz waves in an inclined rectangular packed ensemble of flux tubes with an internal/external field strength contrast of a few percent (Khomenko & Cally, 2019) reveal that linear scattering greatly enhances the production of Alfvén waves compared to the horizontally uniform case; that nonlinear effects become important in the upper chromosphere; that the flux tube structuring enhances Poynting flux reaching the corona by about 35% and reduces reflection at the transition region by 50%; and that ambipolar diffusion, though notionally weak at this frequency, does have some effect in thermalizing a small fraction of fast waves in the chromosphere (see also Cally & Khomenko, 2019) due to the steep gradients that develop there in the magnetically structured model, though this is not fully resolved numerically (10 km) and may in reality be stronger. Recently, Al Shidi et al. (2019) have shown that ion-neutral frictional heating can be significant in the chromosphere, and lead to the generation of jets.

The influence of partial ionization on chromospheric waves is not restricted to processes in the chromosphere only. Gonzalez-Morales et al. (2020) find that ambipolar diffusion near-surface battery-excited dynamo reduces the flux of Alfvén waves generated, whilst the Hall effect substantially enhances chromospheric Alfvén fluxes. Heating aspects of waves in the large-scale solar chromosphere is discussed in details in Section 4.

In the next-section, we review the evolution of the waves in the fine structured chromospheric flux tubes.

### 3. Waves in Structured Flux Tubes in the Chromosphere

In Section 2, we have described the detailed physics of the slow, fast, and Alfvén waves in the homogeneous and unbounded solar plasma, and discussed especially the role of the solar chromosphere on their propagation. In the present Section 3, we discuss the physics of MHD wave modes (e.g., kink, sausage, and torsional waves) in the fine structured tubes, and the recent trends of research in the frame-work of the solar chromosphere.

#### 3.1. Various MHD Modes and Kink Waves in Structured Non-Uniform Flux Tubes

Kink waves in cylindrical plasmas are non-axisymmetric waves that correspond in a system of cylindrical coordinates to the azimuthal wave number  $m = 1$ . They are important because they displace the flux tube as a whole. This phenomenon is well-known for uniform flux tubes with piecewise constant density. When the flux tube is non-uniform there are strong rotational motions in addition to this translational motion. The starting point of its physical description can be two papers from 1970s by Ionson (1978) and Wentzel (1979) and a book by Hasegawa and Uberoi (1982). Wentzel (1979) studied hydromagnetic surface waves on cylindrical flux tubes. He pointed out that these surface waves differ qualitatively and quantitatively from ordinary magnetohydrodynamic waves (e.g., Alfvén, slow, fast waves; Section 2). Wentzel solved the linear



MHD equations for arbitrary azimuthal wave number  $m$ . The  $m = 1$  corresponds to kink waves. Wentzel (1979) recalled that Ionson (1978) proposed a theory for heating coronal loops by Alfvénic surface waves. He derived the waves for a plane surface and assumed  $k_y = 1/R$  for a cylinder. The  $k_y = 1/R$  corresponds to  $m = 1$  in cylindrical geometry, that is, kink waves. Resonant absorption requires smooth non-uniformity. It does not work for discontinuous profiles. Hasegawa and Uberoi (1982) emphasized that  $P'$  (pressure perturbation) plays a special role for MHD waves in a non-uniform plasma. They noted that “The basic characteristic of the ideal Alfvén wave is that the total pressure in the fluid remains constant during the passage of the wave as a consequence of the incompressibility condition. For inhomogeneous medium, however, the total pressure, in general, couples with the dynamics of the motion, and the assumption of neglect of pressure perturbations becomes invalid.” Often the results for MHD waves on a uniform plasma of infinite extent are used as guidelines. The MHD waves can be separated in Alfvén waves and magnetoacoustic waves. The Alfvén waves propagate parallel vorticity and are incompressible. The magnetoacoustic waves are compressible and do not propagate parallel vorticity. However, when the equilibrium configuration is changed either by a discontinuous variation of the equilibrium quantities or by a continuous variation in a non-uniform layer, deviations from this classification occur.

After this very fundamental illustration, now we focus on the linear MHD waves superimposed on a 1-D cylindrical plasma column of radius  $R$  in static equilibrium. It basically describes a plasma cylinder of a circular cross-section, extended along the field, and smoothly non-uniform in the radial direction. The equilibrium density  $\rho_0(r)$ , equilibrium pressure  $p_0(r)$  and the components of the equilibrium magnetic field  $B_{z,0}(r)$ ,  $B_{\varphi,0}(r)$  are functions of  $r$  or constant. Since the equilibrium quantities are independent of  $\varphi$  and  $z$  the wave variables can be put proportional to the exponential factor  $\exp(i(m\varphi + k_z z))$  with  $m$ ,  $k_z$  the azimuthal and axial wave numbers,  $m$  is an integer. Kink waves correspond to  $m = 1$ .

The linear MHD waves superimposed on this 1-D cylindrical plasma column can be described by two ordinary differential equations for the radial component of the Lagrangian displacement  $\xi_r$ , and the Eulerian perturbation of total pressure  $P'$  (Sakurai et al., 1991). The components of the Lagrangian displacement in the magnetic surfaces perpendicular and parallel to the magnetic field lines  $\xi_{\perp}$ ,  $\xi_{\parallel}$ , compression  $\nabla \cdot \vec{\xi}$  and vorticity ( $\nabla \times \vec{\xi}$ ) can be given by expressions in terms of  $\xi_r$  and  $P'$  and their derivatives. Algebraic expressions for  $\xi_{\perp}$ ,  $\xi_{\parallel}$ ,  $\nabla \cdot \vec{\xi}$  can be found in Sakurai et al. (1991). Equations for the components of ( $\nabla \times \vec{\xi}$ ) can be found in Goossens et al. (2019). The components of vorticity are in general non-zero. All of the wave variables are coupled. The MHD waves have mixed properties, they propagate both compression and parallel vorticity and have non-zero radial, perpendicular and parallel components of displacement and vorticity. A situation in which a subset of the wave variables is not coupled to the other wave variables is an exception. Such a situation appears for axisymmetric motions in the presence of a straight field. In general, the clear division into Alfvén waves and magneto-sonic waves that exists for a uniform plasma of infinite extent does not any longer hold.

Let us now focus on MHD waves in presence of a straight field. For a straight field ( $B_{\varphi,0} = 0$ ) the magnetic surfaces are cylinders:  $r = \text{constant}$ . The  $\varphi$ - and  $z$ - directions are the directions in the magnetic surfaces respectively perpendicular and parallel to the magnetic field lines. The  $r$ -direction is normal to the magnetic surfaces. The equations to be used are e.g., Equation 45 of Goossens et al. (2019) for the components of the displacement  $\vec{\xi}$  and compression  $\nabla \cdot \vec{\xi}$

$$\begin{aligned}\xi_r &= \frac{1}{\rho_0(\omega^2 - \omega_A^2)} \frac{dP'}{dr}, \\ \xi_{\perp} &= \xi_{\varphi} = i \frac{m}{r} \frac{1}{\rho_0(\omega^2 - \omega_A^2)} P', \\ \xi_{\parallel} &= \xi_z = ik_z \frac{c_s^2}{c_s^2 + v_A^2} \frac{1}{\rho_0(\omega^2 - \omega_C^2)} P', \\ \nabla \cdot \vec{\xi} &= \frac{-\omega^2 P'}{\rho_0(c_s^2 + v_A^2)(\omega^2 - \omega_C^2)}\end{aligned}\tag{4}$$

The local Alfvén frequency  $\omega_A$  and the local cusp frequency  $\omega_C$  are defined as

$$\omega_A^2 = k_z^2 v_A^2 = k_{\parallel} v_A^2, \quad \omega_C^2 = \frac{c_s^2}{c_s^2 + v_A^2} \omega_A^2 \quad (5)$$

In a non-uniform plasma  $\omega_A$  and  $\omega_C$  are function of position. For a given set of wave numbers ( $m, k_z$ ) they map out two ranges of frequencies known as the Alfvén continuum and the cusp continuum. The  $v_A, c_s$  are the velocity of sound and the Alfvén velocity.

$$v_A^2 = \frac{B_0^2}{\mu \rho_0}, \quad c_s^2 = \frac{\gamma P_0}{\rho_0} \quad (6)$$

For axi-symmetric motions with  $m = 0$  the equation for  $\xi_{\perp} = \xi_{\phi}$

$$(\omega^2 - \omega_A^2) \xi_{\phi} = 0 \quad (7)$$

is decoupled from the remaining equations. The axi-symmetric MHD waves are separated in axi-symmetric Alfvén waves with  $\xi_{\phi} \neq 0, P' = 0$  and sausage magneto-acoustic waves with  $\xi_{\phi} = 0, P' \neq 0$ . The pure sausage modes in a straight cylindrical flux-tube will be discussed in sub-section 3.2. For an axi-symmetric non-uniform 1-dimensional cylindrical plasma this is the only case where pure Alfvén waves show up in the analysis. Each magnetic surface oscillates with its own local Alfvén frequency. In what follows we shall not be concerned with axi-symmetric Alfvén waves.

Similarly use Equation 53 of Goossens et al. (2019) for the components of  $\nabla \times \vec{\xi}$ . Because of limitations of space we only list the parallel component

$$(\nabla \times \vec{\xi})_z = -i \frac{m}{r} \frac{1}{\{\rho_0(\omega^2 - \omega_A^2)\}^2} \frac{d}{dr} \left\{ \rho_0(\omega^2 - \omega_A^2) \right\} P' \quad (8)$$

Equations 4 and 8 clearly show that  $P'$  plays the role of coupling function (see also Hasegawa & Uberoi, 1982). The horizontal components of vorticity  $(\nabla \times \vec{\xi})_r$  and  $(\nabla \times \vec{\xi})_{\phi}$  are always non-zero. The parallel component  $(\nabla \times \vec{\xi})_{\parallel} = (\nabla \times \vec{\xi})_z$ , which can be considered as a marker for Alfvén wave behavior, is non-zero when

$$\frac{d}{dr} \left\{ \rho_0(\omega^2 - \omega_A^2) \right\} \neq 0 \quad (9)$$

Non-uniformity generates wave behavior that is reminiscent of Alfvén waves. In addition compression is non-zero and the wave has a mixed Alfvén-magneto-acoustic behavior. MHD waves with frequencies in the Alfvén continuum undergo resonant Alfvén wave damping. These waves have non-zero parallel vorticity in the non-uniform region and parallel vorticity becomes very big in absolute value when we move closer to the resonant position  $r_A$  where  $\omega_A(r_A) = \omega$ . For a resonantly damped wave the frequency is complex and there is not a singularity on the real axis but parallel vorticity becomes very big anyway. Close to the ideal resonant position the Alfvén behavior dominates over the magnetoacoustic behavior. The wave is an Alfvénic wave. Kink waves are non-axisymmetric waves with azimuthal wave number  $m = 1$ . Hence the properties discussed in above apply to kink waves. Kink waves are important because they produce translational motions and are invoked to explain the transverse waves observed in flux tubes. Although this manifestation of kink wave is universally valid, however, if we consider such oscillations in the chromosphere, there are few scientific papers that report the observations of kink waves (Jafarzadeh et al., 2017; Kухianidze et al., 2006; Kuridze et al., 2013; Morton et al., 2012, 2014; Stangalini et al., 2017; Zaqarashvili et al., 2007). A striking property of transverse MHD waves on magnetic tubes is their fast damping with damping times that are of the order of a few periods. It should be noted that this property is eventually an observational fact. Actually, the theory predicts that the damping time can take many oscillation periods too, if the profile of the perpendicular non-uniformity is steep. A possible mechanism to explain the rapid damping of the

transverse motions is resonant absorption (Goossens et al., 1992, 2002; Hollweg & Yang, 1988; Ruderman & Roberts, 2002). Although, the below mentioned descriptions are universally valid for the radially and longitudinally structured magnetic flux tubes, however, here we analyze them in MHD regime in connection to the chromospheric tubes where the wave modes are evolved naturally.

Goossens et al. (2009) studied forces and analyzed dispersion relations for several cases. In their Section 3, they found that kink waves do not disappear in incompressible MHD. This subject was studied in greater detail by Goossens et al. (2012). In subsection 4.2.2 of their study, they studied kink wave ( $m = 1$ ) on a cylinder with piece-wise constant density. When they considered the incompressible limit they found that all radial overtones disappeared but that the fundamental radial mode survived (See their Figure 1). The fundamental radial mode of kink waves does not need compressibility. It is hard to call it a fast mode. It behaves very similar to surface Alfvén waves in a Cartesian system as already emphasized by Wentzel (1979). In the low beta limit the fundamental radial mode of kink waves has mixed properties. It is compressible as a magnetoacoustic wave but has also non-zero parallel vorticity as an Alfvén waves. This is explained in, for example, Goossens et al. (2021). When the discontinuous variation of density is replaced by a continuous variation in a transitional layer Goossens et al. (2012) found that the fundamental radial mode of kink waves is resonantly damped but has both non-zero Eulerian perturbation of total pressure everywhere and non-zero parallel vorticity in the non-uniform transitional layer. So it is a Alfvénic surface wave with mixed properties. The ratio of parallel vorticity to compression depends on position. So the nature of the wave changes when it propagates through the plasma. Goossens et al. (2009) compared the force due to magnetic tension and the gradient total pressure force. They found that the magnetic tension force is the dominant force especially in the non-uniform layer. The fundamental radial mode of kink waves is clearly identified as an Alfvénic wave that has both non-zero total pressure and non-zero parallel vorticity. The observation by Wentzel (1979) that surface waves differ from the ordinary hydromagnetic waves (Alfvén, slow, and fast magnetosonic waves) is indeed correct. The energy content and propagation of kink MHD waves are investigated by Goossens et al. (2013a). Again behavior of kink MHD waves differs substantially from that of bulk Alfvén waves and of magneto-acoustic waves.

As for the motion associated with the fundamental radial mode of kink waves we first consider the thin tube approximation of a piece-wise constant density flux tube. The Lagrangian displacement in horizontal planes inside the flux tube ( $0 \leq r \leq R$ ) is (we suppress the dependence on  $z$  and  $t$ ; see Goossens et al., 2009, 2014).

$$\vec{\xi}_h(r, \varphi) = C (\cos \varphi \vec{1}_r - \sin \varphi \vec{1}_\varphi) = C \vec{1}_x = \vec{\xi}_{TR} \quad (10)$$

Equation 10 describes a uniform motion of the entire internal plasma along the  $x$ -axis. The reason for this result is that  $\xi_r$  and  $\xi_\varphi$  have equal amplitudes and  $\xi_\varphi$  is a quarter of period ahead of  $\xi_r$ . In the thin tube approximation, the square of the frequency of the kink wave is

$$\omega^2 = \frac{\rho_i \omega_{Ai}^2 + \rho_e \omega_{Ae}^2}{\rho_i + \rho_e} = \omega_k^2. \quad (11)$$

The density is piece wise constant and for that reason parallel vorticity is a  $\delta$ -function centered at the boundary explained in Goossens et al. (2012). The displacement field is shown in Figure 2 of Goossens et al. (2014). Damping due to resonant absorption requires non-uniformity. When the discontinuous variation of equilibrium density is replaced by a continuous variation of density from its internal value  $\rho_i$  to its external value  $\rho_e$  in a transitional layer of thickness  $l$  then the eigenvalue of the kink wave is in the Alfvén continuum and the kink wave is resonantly damped (Goossens et al., 1992). In addition, the non-uniformity generates parallel vorticity that is largest in absolute value at the resonant position. The  $\xi_r$  and  $\xi_\varphi$  no longer have equal amplitudes. The result is that the motion of the flux tube is a translation combined with a rotational motion. The displacement field of a flux tube with a non-uniform transitional layer is shown on Figure 2 (left-panel) that is equivalent to Figure 11 of Goossens et al. (2014). In the vicinity of the resonant surface the motion resembles the motion depicted in Figure 1 of Spruit (1981) for a non-axisymmetric  $m = 1$  Alfvén wave in a uniform cylinder. Compression and the components of vorticity are shown in Figures 1 and 2 of Goossens et al. (2020). Compression is non-zero everywhere. Parallel vorticity is zero in the uniform part of the flux tube. It is non-zero in the non-uniform part and becomes large as we move closer

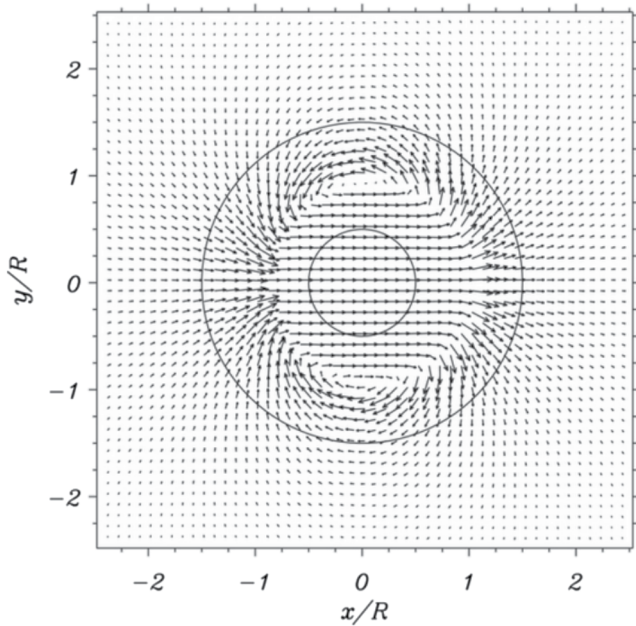


**Figure 2.** The displacement field of a magnetized flux tube with a non-uniform transitional layer during the kink mode oscillations. This figure is adapted from Goossens et al. (2014) (©AAS Reproduced with permission).

to the resonant position. The temporal evolution of a flux tube that is initially given a translational motion is shown in four snapshots in Figure 12 of Goossens et al. (2014). The initial translational motion is transformed into a motion that is dominated by rotational motions. The dissipationless damping by resonant absorption is due to a transformation of energy of translational motions to energy of rotational motions as explained in Goossens et al. (2014).

### 3.2. Sausage Waves

In sub-section 3.1, we have discussed the concept of all possible MHD modes and their properties in non-uniform and structured magnetic flux tubes. In the present sub-section, we discuss the physics and recent trends of sausage waves evolved individually in magnetic flux tubes in the solar chromosphere where we do not consider radial non-uniformity. Sausage waves are axisymmetric modes in magnetic flux tubes with the azimuthal wave number  $m = 0$  (see Section 3.1). The waves modify the tube cross sections and hence density, therefore they have been frequently observed by radio observations in flaring coronal loops (Aschwanden et al., 2004), though additional efforts should be taken into account (Gruszecki et al., 2012; Reznikova et al., 2015). The sausage waves also modify plasma emission intensity, therefore can be revealed by imaging observations in the whole solar atmosphere, and also in solar chromospheric structures (Grant et al., 2015; Morton et al., 2012; Srivastava et al., 2008).

#### 3.2.1. Linear Sausage Waves

Sausage waves in magnetic tubes are divided into fast and slow waves corresponding to the fast and the slow MHD modes (Edwin & Roberts, 1983). Fast and slow sausage waves may have surface (with one velocity node at the tube center) and body (more than one velocity node along the radial direction) modes depending on the plasma parameters inside and outside the tube. In photospheric conditions, fast body sausage modes are absent (Edwin & Roberts, 1983). The upper left panel of Figure 3 shows the dispersion diagram of fast and slow sausage waves under the conditions  $v_A = 2c_s$ ,  $v_{Ae} = 0.5c_s$  and  $c_{se} = 1.5c_s$ . Besides the phase speed, another important difference between the fast and slow sausage modes is the phase relation of the oscillations in cross sectional area and intensity. Fast surface sausage waves display anti-phase relation between the tube cross section and the emission intensity, while the slow surface and body waves show in-phase relation (Moreels et al., 2013). Therefore, the imaging observations may show the distinction between fast and slow modes. Another important feature of sausage waves is the cut-off wavenumber for fast surface sausage waves (Aschwanden et al., 2004)

$$k = k_c = \left[ \frac{(c_s^2 + v_A^2)(v_{Ae}^2 - v_T^2)}{(v_{Ae}^2 - v_A^2)(v_{Ae}^2 - c_s^2)} \right]^{1/2} \frac{j_{0,s}}{R}, \quad (12)$$

where  $v_T$  is the tube speed,  $R$  is the tube radius and  $j_{0,s} = (2.40, 5.52\dots)$  are the zeros of the Bessel function  $J_0$ . In photospheric conditions only the fast surface wave is allowed, therefore  $j_{0,1} = 2.40$ .

The sausage waves may carry energy from the photosphere upwards into the chromosphere and corona contributing to the plasma heating processes. Therefore, the observation of waves at different levels of the solar atmosphere is of great importance. The first possible identification of linear sausage waves in photospheric magnetic pores was made by Dorotovič et al. (2008) as oscillations of the cross sectional area of pores with periods of 20–70 min<sup>2</sup> (However such long periods require much longer vertical wave length than the width of the photosphere-chromosphere, therefore the interpretation of the observation in terms of sausage waves may be doubtful.) Morton et al. (2011) have found an observational evidence of high frequency sau-



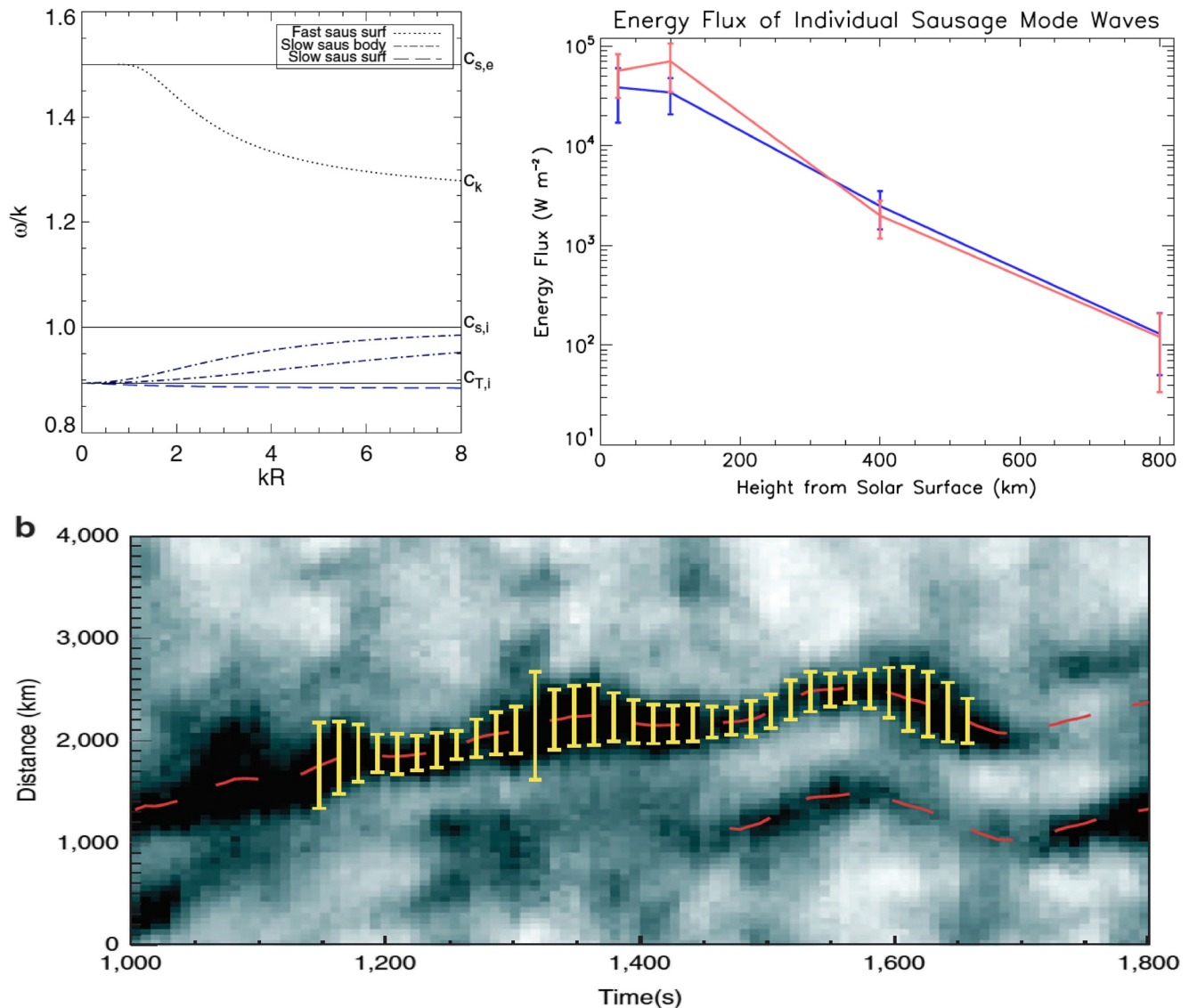


**Figure 3.** Upper left panel: Phase speed diagram of sausage waves under photospheric conditions:  $v_A = 2v_s$ ,  $v_{Ae} = 0.5v_s$  and  $v_{se} = 1.5v_s$ . Fast body waves are absent in these conditions. This panel is adapted from Moreels et al. (2013; © ESO Reproduced with permission). Upper right panel: The calculated energy flux of 210 s (red) and 290 s (blue) sausage mode oscillations versus height from the solar surface observed by the Dunn Solar Telescope. Rapid decrease of energy flux of both oscillations with height are clearly seen. This figure panel is adapted from Grant et al. (2015; © AAS Reproduced with permission). Lower panel: Time-distance plot from ROSA observations showing simultaneous propagation of kink and sausage modes in chromospheric structures. Transverse displacement corresponds to the kink wave and the variation of structure width corresponds to the sausage wave. This panel is adapted from Morton et al. (2012) (Credit and Permissions:- R. Morton; Springer Nature).

sage waves with periods from 50 to 600 s. Fujimura and Tsuneta (2009) reported possible spectro-polarimetric observations of slow sausage waves in magnetic pores with Hinode.

Grant et al. (2015) presented multi wavelength observations of magnetic pores using Dunn Solar Telescope at Sacramento Peak, New Mexico. They used simultaneous observations of continuum, G-band, Na  $ID_1$  and Ca II  $K$  lines covering up to 800 km heights from the Sun's surface. Sausage mode oscillations with periods from 180 to 412 s, with an average period of 290 s, were detected in both intensity and area fluctuations. The phase difference between different wavelength bands showed upward propagation of sausage mode waves with a phase speed of  $\sim 3 km s^{-1}$ . In-phase relation between oscillations in cross sectional area and intensity categorizes the waves as slow sausage waves. The energy flux of the waves was estimated at different heights using the theoretical tool of Moreels, Freij, et al. (2015). They found the energy flux of the waves at the solar

surface to be  $35 \text{ kW m}^{-2}$ , which rapidly decreased to  $100 \text{ W m}^{-2}$  at the height of 800 km (see the upper right panel of Figure 3). The observed rapid reduction of the waves is not yet fully explained (Gilchrist-Millar et al., 2021; Riedl et al., 2021). Neither resonant absorption of slow sausage waves nor the electric resistivity is efficient enough to explain the observed damping (Chen et al., 2018; Yu et al., 2017). Ion-neutral collisions through Cowling resistivity may have a stronger effect, but it is generally much smaller in longitudinal slow waves than in transverse fast waves (Zaqarashvili, Khodachenko, & Rucker, 2011). Therefore, ion-neutral damping can probably not explain these observations. Another possibility is slow mode conversion into fast/Alfvén modes in linear (Bogdan et al., 2003) and nonlinear (Kuridze & Zaqarashvili, 2008; Ulmschneider et al., 1991; Zaqarashvili & Roberts, 2006) regimes. However, estimates show that the observed drop of energy flux occurred within one-quarter of the wavelength of the waves, therefore none of the damping/conversion mechanisms may explain the huge drop of the energy flux.

Observations reveal simultaneous propagation of sausage and kink waves in chromospheric structures, which may indicate their mutual coupling/conversion. Using the Dunn Solar Telescope, McAteer et al. (2003) observed propagating transverse kink (with frequency of 1.3, 1.9 mHz) and longitudinal sausage (with frequency of 2.6, 3.8 mHz) waves in the chromospheric network. These observations clearly showed the coupling of transverse and longitudinal oscillations with  $\omega_l = 2\omega_t$ , where  $\omega_t$  and  $\omega_l$  are the transverse (kink) and the longitudinal (sausage) wave frequencies, respectively. This may indicate nonlinear coupling of transverse and longitudinal waves, which satisfy the theoretical frequency relation of coupled waves (Ulmschneider et al., 1991; Zaqarashvili & Roberts, 2006). Morton et al. (2012) detected clear coupling of kink and sausage waves in chromospheric structures (see lower panel of Figure 3). Clear anti-phase relation between oscillations of structure width and emission intensity ranked the sausage waves as fast waves. The observed periods of kink and sausage waves were estimated as  $232 \pm 8 \text{ s}$  and  $197 \pm 8 \text{ s}$ , which are clearly out of nonlinear resonant conditions, probably indicating linear coupling of the waves.

Dorotovič et al. (2014) detected fast and slow sausage waves with periods from 4 to 65 min in photospheric magnetic waveguides using the Swedish 1-m Solar Telescope. The period ratio of the oscillations indicated that they are part of a group of standing harmonics in a flux tube that is non-homogeneous and bound by the photosphere and the transition region. Later Freij et al. (2016) confirmed the existence of standing harmonics of slow sausage waves, which enabled the estimation of tube expansion factor that was in good agreement with numerical simulations (see also Moreels, Freij, et al., 2015).

Keys et al. (2018) presented direct evidence of surface and body sausage waves in numerous magnetic pores at the solar photosphere. The authors found surface modes more frequently than body modes in the data. Observed wave frequencies were in the range of  $\sim 2\text{--}12 \text{ mHz}$ , where the body mode frequency reached up to 11 mHz, but no surface modes were found above 10 mHz. The authors estimated that  $35 \text{ kW m}^{-2}$  at the photospheric level the surface modes transport at least twice the average energy flux ( $22 \pm 10 \text{ kW m}^{-2}$ ) as the observed body modes ( $11 \pm 5 \text{ kW m}^{-2}$ ). This may be significant in determining which mode contributes more to localized atmospheric heating as a function of waveguide height.

Gafeira et al. (2017) reported the detection of high-frequency oscillations in slender Ca II H fibrils from high-resolution observations acquired with the SUNRISE balloon-borne solar observatory. The fibrils show obvious predominantly anti-phase oscillations in their intensity and width, which classifies the waves as fast sausage modes. The obtained distributions have median values of the period of  $32 \pm 17 \text{ s}$  and  $36 \pm 25 \text{ s}$ , respectively.

As seen above, the recent high-resolution observations detect the presence of sausage waves in the chromosphere that are carrying substantial energy flux to heat it and the overlying corona. Another exclusive feature, which is rarely observed, but could be an another important aspect of the hydrodynamic response of solar chromosphere, is the slow sausage solitons. We describe it briefly in the next sub-section.

### 3.2.2. Slow Sausage Solitons

When slow sausage pulses propagate from the photosphere upwards they may quickly steepen into shocks due to the rapid decrease of density. In certain conditions, the tube dispersive effects may prevent the non-linear steepening leading to the formation of a soliton, which is a stable structure propagating without significant change of shape. The formation of sausage solitons in magnetic tubes was first suggested by Roberts and Mangeney (1982), which was followed by several papers about weakly nonlinear waves and

solitons (Barbulescu & Erdélyi, 2016; Erdélyi & Fedun, 2006; Nakariakov & Roberts, 1999; Zhugzhda, 2005; Zhugzhda & Nakariakov, 1997). The solution of a slow sausage surface soliton in magnetic slabs with width  $2d$  is given by the following expression (Ruderman, 2003)

$$\eta = \frac{al^2}{l^2 + |z - st|^2} \quad (13)$$

where  $\eta$  is the displacement of the slab boundary,  $a$  is the soliton amplitude and

$$s = v_T + \frac{1}{4} \frac{ab}{d}, l = 4 \frac{\kappa d}{ab} \quad (14)$$

are the soliton speed and the spatial scale, respectively. The parameters  $b$  and  $\kappa$  are expressed as

$$b = \frac{v_A^4 [3c_s^2 + (\gamma + 1)v_A^2]}{2v_T(v_A^2 + c_s^2)^2}, \kappa = \frac{d \rho_e v_T c_s^2 (v_T^2 - v_{Ae}^2)}{2 \rho_i m_e v_A^2 (c_s^2 + v_A^2)} \quad (15)$$

The typical symbols of characteristic speeds, densities, etc have their usual meanings as we have followed throughout in this review article ( $v_T = v_A c_s / (v_A + c_s)$  is the tube speed). Barbulescu and Erdélyi (2016) studied the nonlinear sausage waves in magnetic flux tubes and concluded that the slow sausage soliton can be formed in certain conditions.

Zaqarashvili, Kukhianidze, and Khodachenko (2010) analyzed a time series of the Ca II H line obtained at the solar limb with the Solar Optical Telescope (SOT) on board Hinode (see also Zaqarashvili, Murawski, et al., 2011). Observations showed an intensity blob propagating from 500 to 1,700 km above the solar surface with a mean apparent speed of  $35 \text{ km s}^{-1}$ . The speed was much higher than the expected local sound speed, therefore the blob could not be a simple pressure pulse. The authors found that the blob speed, length-to-width ratio and relative intensity were characteristic of a slow sausage soliton propagating along a magnetic tube. The blob width increased with height corresponding to the magnetic tube expansion in a stratified atmosphere. The authors suggested that the propagation of the intensity blob may be the first observational evidence of a slow sausage soliton in the solar atmosphere.

In the next section, we emphasize the basic physics of torsional modes in the solar chromosphere, and the recent trend of scientific research keeping the view of solar chromosphere at the central place.

### 3.3. Torsional Waves

The presence of Alfvén waves in the Earth's magnetosphere is unquestionable, with their role in magnetosphere-ionosphere coupling, energy transportation, field line resonance, and particle acceleration at the forefront of solar terrestrial physics (Keiling, 2009). Contrarily, Alfvén waves have long been one of the most elusive waveforms in the solar atmosphere (Mathioudakis et al., 2013). However, the desire to identify and benchmark the capabilities of Alfvén waves manifesting throughout the Sun's atmosphere stems from the original pioneering work by Alfvén (1942), who put forward the idea that these waveforms may be responsible for the elevated temperatures found in the solar corona (Alfvén, 1947).

Such speculation is a result of the intrinsic properties of Alfvén waves, whereby their relative incompressibility (when compared to other MHD waves, including fast and slow magnetoacoustic modes) allows them to propagate much further before being dissipated. The incompressibility of Alfvén waves is the result of magnetic tension providing the only restoring force when driven by linear perturbations. Hence, to achieve dissipation of the energy embodied in Alfvén waves in order to provide thermal energy to the outer solar atmosphere, specific mechanisms must be invoked, including phase mixing (Ebadi et al., 2012; Heyvaerts & Priest, 1983; Ofman & Aschwanden, 2002; Prokopyshyn & Hood, 2019; Van Damme et al., 2020), resonant absorption (Davila, 1987; Giagkiozis et al., 2016; Goossens et al., 2006, 2011; Howson et al., 2019; Ionson, 1978; Ofman et al., 1994, 1995; Poedts et al., 1989, 1990), mode conversion (Cally & Khomenko, 2015; Crouch & Cally, 2005; Pagano & De Moortel, 2017; Suzuki & Inutsuka, 2005), and Alfvén turbulence (Cranmer & van Ballegoijen, 2005; van Ballegoijen et al., 2017, 2011; van Ballegoijen & Asgari-Targhi, 2016;

Oran et al., 2017; Dinesh Singh & Singh Jatav, 2019). Indeed, Chitta et al. (2012) compared the velocity fluctuations corresponding to small-scale magnetic elements in the lower solar atmosphere and found significant Fourier power associated with high-frequency ( $\sim 20$  mHz) horizontal motions, hence providing indirect evidence for the creation of a turbulent environment that can efficiently provide Alfvén wave dissipation. Furthermore, it is also possible for linear Alfvén waves to dissipate their initial energy through the process of parametric decay, which combines a weakly turbulent environment with the coupling of Alfvén waves to other compressible magnetoacoustic modes (Malara & Velli, 1996). In this regime, the initial energy of the Alfvén wave is gradually transferred to daughter species, resulting in the destruction of the initially coherent state. This form of energy transfer has been identified in the solar wind (Del Zanna, 2001; Malara et al., 2000; Primavera et al., 2019; Tenerani & Velli, 2013), but has yet to be fully documented in the confines of the solar atmosphere.

In sub-section 3.1, we have discussed the physics of all possible MHD modes (kink, sausage, and Alfvénic) and their properties in non-uniform and structured magnetic flux tubes. In the present sub-section, we describe only physics and recent research on pure incompressible torsional Alfvén waves that are generated individually in the magnetic flux tubes (over iso-frequency magnetic surfaces) where no radial non-uniformities exist. Here, we use the term “radial” to indicate the direction perpendicular to the magnetic field vector. We essentially exclude the concept of Alfvénic waves (mixed mode of radial kink waves with surface Alfvén waves) in such physical conditions, and the pure Alfvén waves are likely evolved in the magnetized solar chromosphere. In such a situation, once the driving forces that underpin the Alfvén waves become sufficiently non-linear, magnetic tension still remains the dominant restoring force, but the validity of incompressibility may become compromised. For circularly polarised Alfvén waves, they remain incompressible due to the strict rotation of their magnetic field vector around the direction of propagation (Ferraro, 1955). However, linearly or elliptically polarised non-linear Alfvén waves create density perturbations in the local plasma due to the operation of ponderomotive forces, with the resulting dynamics governed by the derivative of the non-linear Schrödinger equation (Laming, 2009; Medvedev, 1999),

$$\frac{\partial b}{\partial \tau} + \frac{1}{4(1-\beta)} \frac{\partial}{\partial z} (|b|^2 b) \pm i \frac{v_A^2}{2\Omega_i} \frac{\partial^2 b}{\partial z^2} = 0, \quad (16)$$

where  $b = B_{\perp}/B_z$  is the relative amplitude of transverse magnetic field perturbations along a straight unperturbed magnetic field,  $B_z$ ,  $\Omega_i$  is the ion cyclotron frequency,  $\tau = (B_z / B_{\perp})^2 t$  is the extended time, and  $\beta \propto c_s^2 / v_A^2$  is the ratio of the plasma pressure to the magnetic pressure, where  $v_A$  and  $c_s$  are the local Alfvén and sound speeds, respectively. Within the lower solar atmosphere, the ion-cyclotron frequency has values on the order of  $10^5$ – $10^6$  Hz (Khomenko, Collados, et al., 2014), which helps to alleviate wave dispersion and simplifies Equation 16 to,

$$\frac{\partial b}{\partial \tau} + \frac{1}{4(1-\beta)} \frac{\partial}{\partial z} (|b|^2 b) = 0. \quad (17)$$

Hence, non-linear Alfvén waves are able to steepen into shocks (Cohen & Kulsrud, 1974; Murawski et al., 2015; Shestov et al., 2017; Snow et al., 2018), with such steepening being expedited when the Alfvén speed is approximately equal to the local sound speed (i.e., the plasma- $\beta \sim 1$ ; Montgomery, 1959). Of course, it is important at this stage to highlight the differences between the non-linear evolution of plane shear Alfvén waves and torsional oscillations in magnetic flux tubes. For both cases, Vasheghani Farahani et al. (2012) found that a non-linear self-interaction resulted in the steepening of the waves. However, in the case of a finite plasma- $\beta$ , the non-linear steepening of torsional Alfvén waves develops more slowly than their plane shear wave counterparts. Interestingly, Vasheghani Farahani et al. (2011) found that the precise value of the plasma- $\beta$  had no effect on the creation of compressive perturbations in propagating torsional Alfvén waves, something that was linked to the inherent tube speed (i.e., the natural speed of the longitudinal compressive perturbations) always being lower than both the local Alfvén and sound speeds. Recent evidence for such Alfvén wave steepening has been put forward by Grant et al. (2018), who employed a combination of imaging spectroscopy and inversion routines to examine the temperature fluctuations of chromospheric plasma when Alfvén wave signals were present.



However, conclusively detecting the presence of Alfvén waves is a challenging endeavour. It is common to detect the appearance of MHD wave modes (e.g., the slow magnetoacoustic mode) through the intensity fluctuations generated by the compressions and rarefactions of the propagating wave signal. Unfortunately, the lack of compressibility for linear and circularly polarised Alfvén waves means that there are no associated periodic signatures in the intensity signal being emitted by the wavetrain. Thankfully, the lower solar atmosphere provides structures and driving mechanisms that should result in an abundance of Alfvén waves. For example, the most basic form of Alfvén waves, the torsional mode with an azimuthal wavenumber  $m = 0$ , can be readily generated in axially symmetric structures synonymous with sunspots, magnetic pores, spicules, and filaments through the ubiquitous buffeting motions present at the footpoints of these omnipresent features (Fedun, Shelyag, & Erdélyi, 2011; Luo et al., 2002; Matsumoto & Shibata, 2010; Ruderman, 1999; Ruderman et al., 1997; Vigeesh et al., 2012). Indeed, Shelyag and Przybylski (2014) employed simulated photospheric Fe I 6,302 Å observations generated by the MURaM (Vögler et al., 2005) MHD code to search for the presence of Alfvén waves at the base of the photosphere. The authors found an abundance of evidence for Alfvén waves manifesting in magnetic elements in the intergranular lanes, however, these signatures disappeared when the simulated observations were degraded to the resolution of the Solar Optical Telescope (SOT; Tsuneta et al., 2008) onboard the Hinode (Kosugi et al., 2007) spacecraft, hence highlighting the need for high resolution observations of the solar photosphere and chromosphere to study Alfvén wave generation and propagation.

With cutting-edge simulations verifying the mechanisms responsible for generating ubiquitous Alfvén waves in the lower solar atmosphere, attention naturally turns to the identification of these features in modern ground- and space-based observations. As highlighted above, the relative incompressibility of Alfvén modes means that intensity fluctuations cannot be harnessed to provide evidence of such waves. Instead, attention needs to be turned to spectroscopy. An  $m = 0$  torsional Alfvén wave propagating along a magnetic flux tube can be visualized as a set of rotating magnetic iso-surfaces (left panel of Figure 4). When the waveguide is viewed from the side, the rotation of the iso-surfaces manifest in equal, yet opposite Doppler shifts due to one side of the flux tube rotating toward the observer, while the other side of the flux tube rotates away from the observer. If the Alfvén waveguide is well resolved spatially, then the observer will be able to detect the induced blue- and red-shifted Doppler velocities manifesting at opposite edges of the flux tube (Kohutova et al., 2020; Mathioudakis et al., 2013; Srivastava et al., 2017). However, if the Alfvén waveguide is below the resolution element of the telescope instrumentation, then the opposing Doppler shifts will become blended and result in periodic fluctuations in the full-width at half-maximum (FWHM) of the measured spectral line (McClements et al., 1991; Zaqarashvili, 2003). The magnitude of such non-thermal line broadening will be dependent on both the velocity amplitude of the Alfvén wave, as well as the inclination angle of the waveguide with respect to the observer's line-of-sight (i.e., the cos term will modulate the degree of Doppler-induced broadening visible to the observer). Furthermore, turbulence and/or bulk flows embedded within the flux tube may also mask the presence of FWHM oscillations caused by Alfvén waves (Jess & Verth, 2016). As a result, a combination of high spatial resolution observations and high precision spectroscopy is required to unequivocally detect the presence of Alfvén waves manifesting in the lower solar atmosphere.

Employing Solar Optical Universal Polarimeter (SOU; Title, 1984) observations of the chromospheric H $\alpha$  absorption line, Jess et al. (2009) provided the first detection of Alfvén waves in the solar chromosphere. Through examination of a magnetic flux tube anchored above a photospheric magnetic bright point, Jess et al. (2009) measured the amplitude of H $\alpha$  non-thermal line broadening to be  $\sim 0.05$  Å (or a velocity amplitude on the order of  $2.5 \text{ km s}^{-1}$ ; upper-right panel of Figure 4), and when combined with a plasma density of  $\sim 10^{-9} \text{ g cm}^{-3}$  and a local Alfvén speed of  $\sim 22 \text{ km s}^{-1}$ , provided a wave energy flux equal to  $\sim 150,000 \text{ W m}^{-2}$ . While this quantity of energy is far in excess of the amount required to balance chromospheric radiative losses (Withbroe & Noyes, 1977), Verth and Jess (2016) hypothesized that the filling factor of such waves needs to be evaluated before the true importance of their existence can be evaluated. With this in mind, Fedun, Verth, et al. (2011) harnessed the numerical Sheffield Advanced Code (SAC; Shelyag et al., 2008) and placed a vortex-type driver at the photospheric boundary, before examining the torsional effects and higher atmospheric heights. Comparing the outputs from the SAC code with the observational findings of Jess et al. (2009) and Fedun, Verth, et al. (2011) revealed how the geometry of magnetic flux concentrations that make up realistic solar structures (e.g., magnetic bright points, pores, etc.) acts as a spatial frequency filter

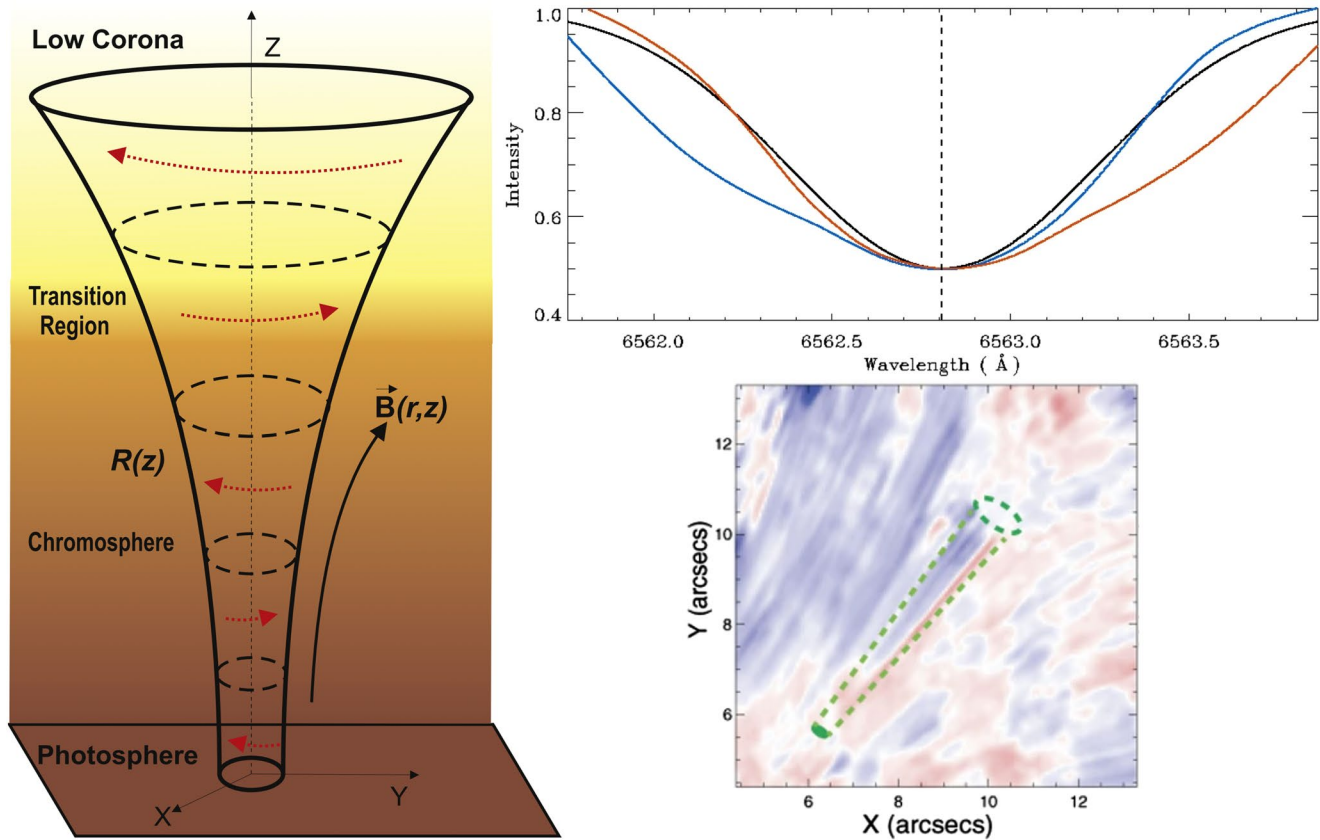


**Figure 4.** Left: A cartoon schematic of Alfvén wave propagation in an expanding waveguide, where the rotation of magnetic isosurfaces synonymous with the presence of torsional Alfvén waves is highlighted using dotted red arrows (image reproduced from Soler et al., 2017; © AAS Reproduced with permission). Upper-right: Sample  $H\alpha$  spectra corresponding to heavily blue-wing broadened (blue line), quiescent (black line), and heavily red-wing broadened (red line) profiles that demonstrate the non-thermal broadening characteristics consistent with the presence of torsional Alfvén waves. Here, the blue, black, and red  $H\alpha$  profiles were acquired simultaneously by the SOUP instrument at the Swedish 1-m Solar Telescope (SST) and correspond to the spectra obtained at the center (black line) and opposite edges (blue and red lines) of the chromospheric waveguide (image adapted from Jess et al., 2009; Mathioudakis et al., 2013; © AAS Reproduced with permission). Lower-right: Line-of-sight  $H\alpha$  Doppler velocities acquired by the CRISP instrument at the SST, where the dashed green lines outline the boundaries of a chromospheric magnetic flux tube and the axes represent heliocentric coordinates. The asymmetric red (down flowing) and blue (up flowing) velocities across the diameter of the waveguide indicate the presence of torsional Alfvén waves embedded within the magnetic structure (image adapted from Srivastava et al., 2017). CRISP, Crisp Imaging Spectropolarimeter; SOUP, Solar Optical Universal Polarimeter; SST, Swedish 1-m Solar Telescope.

that modulates the observable wave signatures, hence providing a novel method to map solar magnetism as a function of atmospheric height by capturing torsional Alfvén waves in different spectral lines with corresponding differences in their formation heights.

While the work of Jess et al. (2009) examined Alfvén waves present in long-lived magnetic flux tubes extending upwards from the photosphere, De Pontieu et al. (2012) turned attention toward much more dynamic and rapidly evolving chromospheric features in the form of Type-ii spicules (Kuridze et al., 2015; Langangen et al., 2007; Rouppe van der Voort et al., 2009). Harnessing a combination of both the Crisp Imaging Spectropolarimeter (CRISP; Scharmer et al., 2008) and the TRI-Port Polarimetric Echelle-Littrow (TRIPPEL; Kiselman et al., 2011) spectrograph on the SST, De Pontieu et al. (2012) found evidence that the dominant majority of Type-ii spicules undergo large torsional twists that represent the signatures of Alfvénic waves propagating toward the corona at several hundred  $\text{km s}^{-1}$ . This interpretation was reached due to the ability of the CRISP and TRIPPEL instruments to resolve the red-blue Doppler velocity asymmetries across the diameter of the Type-ii spicules in both Ca ii H and  $H\alpha$  observations. In this work, the term “Alfvénic” is used to categorize the embedded wave motion since Type-ii spicules also demonstrate large-amplitude transverse (kink) waves in addition to their torsional (with respect to the axis of the magnetic field) motions. Goossens et al. (2009); Goossens et al. (2012) revealed that plasma compression is limited in the case of thin magnetic flux tubes (such as for Type-ii spicules), and hence the resulting wave motion is more closely

aligned with Alfvén waves than typical fast magneto-sonic waves. Hence, the term “Alfvénic” was coined (Goossens et al., 2009) to impart a caveat that pure theoretical Alfvén waves (as described by Alfvén, 1942) can only exist in a uniform plasma of infinite extent. Goossens et al. (2014) also highlighted that the derived velocity profiles of transverse kink waves can lead to similar Doppler characteristics that would be expected for torsional Alfvén waves, and therefore the viewing angle of the solar structures must be taken into consideration to reach a firm conclusion regarding the captured wave mode. The details of the key theoretical developments on Alfvénic waves originally proposed by M. Goossens and fellow scientists over the last two decades are summarized in sub-section 3.1.

Following the launch of the Interface Region Imaging Spectrograph (IRIS; De Pontieu, Title, et al., 2014, De Pontieu, Rouppe van der Voort, et al., 2014) examined high spatial resolution ( $\approx 0.33$  arcsec) UV spectra and found that the chromosphere and transition region was replete with small-scale torsional motions. Importantly, De Pontieu, Rouppe van der Voort, et al. (2014) found that such torsional motion was readily present in quiet Sun, active region, and coronal hole locations, highlighting the omnipresent nature of torsional behavior in the solar chromosphere. Utilizing the multi-thermal capabilities of the IRIS instrument, it was found that the chromospheric structures undergoing torsional motions were rapidly heated to transition region temperatures, which was hypothesized to be compatible with the heating expected from the dissipation of torsional Alfvén waves generated by small-scale photospheric vortices (Asgari-Targhi & van Ballegooijen, 2012; Shelyag & Przybylski, 2014; van Ballegooijen et al., 2011). If the chromosphere is indeed permeated by torsional Alfvén waves, then they are required to propagate through the temperature minimum region. Here, ion-neutral effects are likely to play an important role (Khomenko & Collados, 2012; Khomenko et al., 2018), with theoretical work revealing that short period ( $< 5$  s) Alfvén waves damp very rapidly in the chromospheric network as a result of ion-neutral collisions (Zaqarashvili et al., 2013). Hence, in order to probe the heating effects of torsional Alfvén waves, the community is turning its attention toward the highest frequencies currently achievable with modern instrumentation.

Recently, Srivastava et al. (2017) utilized the high-precision CRISP instrument on the SST to search for high-frequency torsional Alfvén waves. Nine wavelength steps across the H $\alpha$  absorption line were chosen to maximize the spectral cadence ( $\approx 3.9$  s), with the resulting images reconstructed using the multi-object multi-frame blind deconvolution (MOMFBD; van Noort et al., 2005) code to ensure the smallest spatial scales were visible. Following analyses using Fourier cross-correlation and wavelet techniques, Srivastava et al. (2017) uncovered evidence for the presence of torsional Alfvén waves with frequencies in the range of 12–42 mHz, providing periodicities (24 – 83 s) approximately one order-of-magnitude more rapid than previously uncovered (Jess et al., 2009). The high spatial resolution of the CRISP instrument allowed the blue and red Doppler shifts associated with the rotating magnetic iso-surfaces to be examined (see the lower-right panel of Figure 4). Numerical models, including the use of the FLASH code (Lee & Deane, 2009), revealed that the necessary high-frequency photospheric wave drivers were able to generate and supply vast Alfvén wave energy flux ( $\sim 10^5$  W m $^{-2}$ ) into the solar chromosphere, consistent with previous analytical estimations (Murawski et al., 2015). Importantly, Srivastava et al. (2017) concluded that even accounting for partial reflections at the transition region interface, more than  $\sim 10^3$  W m $^{-2}$  would be transmitted into the overlying corona. This has significant implications for studies into both the heating of the multi-million degree corona and the generation of the supersonic solar wind.

Over the last decade, torsional Alfvén waves manifesting in the lower solar atmosphere have gone from elusive through to ubiquitously detectable in modern observing sequences (e.g., Grant et al., 2018; Jess et al., 2009; Liu et al., 2019; Srivastava et al., 2017). This success has arisen from a combination of more sensitive instrumentation, better wave detection techniques, alongside more refined MHD wave theory. Looking toward the future, we have already been stepping into an era of ultra-high precision solar physics with the advent of the 4-m DKIST (Rimmele et al., 2020) that has already seen its first light in 2020 and now releasing unprecedented fine details of the solar atmosphere. It will now become possible to examine the Doppler velocity asymmetries synonymous with torsional Alfvén waves on unprecedented spatial scales as small as  $\approx 20$  km (Rast et al., 2021). A current challenge is understanding the precise observables we will be able to detect at these small spatial scales. For example, when the magnetic flux tube supporting a torsional Alfvén wave is non-uniform (e.g., there are non-uniformities in the radial direction away from the central axis of the magnetic field), then elements of phase mixing will need to be considered (e.g., Browning &

Priest, 1984; Díaz-Suárez & Soler, 2021; Heyvaerts & Priest, 1983; Shestov et al., 2017). Here, the variable phase velocities of the embedded Alfvén waves cause refraction and hence create large gradients in the direction perpendicular to the magnetic field (Ruderman et al., 1999). When structures with reduced opacities (e.g., coronal loops) are examined, this naturally results in mixed observational signatures that may be difficult to disentangle. However, this concern may be less important in the optically thick chromosphere, where observations of fibrillar-type features more closely align with the outermost shells of the structure, hence providing less mixed signals due to larger local opacities (Bose et al., 2019). Nevertheless, phase mixing is able to produce Kelvin-Helmholtz instabilities in the observed plasma (Guo et al., 2019), which may need to be taken into consideration for accurate scientific interpretations. High resolution observations, combined with next-generation instrumentation capable of high cadence data acquisition, will make it possible to probe the ion-neutral effects of Alfvén wave dissipation at periodicities less than 5 s. As a result, the community looks forward to making rapid advancements in the understanding of torsional Alfvén waves and their role in supplying energy at high frequencies to the outer regions of the solar atmosphere.

In Section 3, we have discussed the physical properties of various MHD modes and their possible contributions in heating the solar chromosphere. In the next section we will discuss the overarching scenario of chromospheric heating, keeping a central view on MHD waves.

## 4. Heating of the Chromosphere

In Section 3, it is noticed that MHD waves carry substantial energy in the solar chromosphere, therefore, in the context of the wider physical implications of the heating of this layer the role of these waves should be explicitly studied and explored. In this Section 4, we evaluate the heating aspects of the MHD waves in the solar chromosphere. In sub-section 4.1, we discuss in general the heating aspects of the large-scale chromosphere, while in the sub-section 4.2 we will depict the energy budget of MHD waves in chromospheric localized flux tubes and thereby their heating capabilities. In the sub-section 4.3 we describe the wave heating of solar prominence plasma.

### 4.1. Wave Heating of the Large-Scale Chromosphere

No generally accepted theory of the formation of the hot solar chromosphere exists so far. The total radiative losses of the quiet chromosphere are of the order of  $4,300 \text{ W m}^{-1}$  (Avrett, 1981) and up to a factor of 2–4 higher in active regions (Withbroe & Noyes, 1977). Heating by waves falls into one of the most popular categories of chromospheric heating models, and it can be sub-divided into the heating by acoustic waves (without involving the magnetic fields) and heating by different kinds of MHD waves (Sections 2 and 3). The latter involves interactions of acoustic waves generated in sub-photospheric layers with magnetic structures present at the surface. In order to understand wave heating mechanisms in the chromosphere one needs first to understand which processes can help bringing the wave energy in sufficient amount to these layers and then to provide efficient dissipation mechanisms for these waves. Wave energy transport and dissipation are frequency-dependent, and their efficiency is different for high- and low-frequency waves. The maxima of the observed solar wave spectra fall into the 3–5 mHz range, depending on the height. This low-frequency part of the solar photospheric spectrum has been extensively studied both theoretically and observationally (Gizon & Birch, 2005). The high-frequency part of the spectrum still represents a challenge from an observational point of view, while theoretically there is increasing evidence that high-frequency wave phenomena may play a relevant role in energizing the solar chromosphere.

Heating of the quiet chromosphere can be done by acoustic waves (see Section 2). These waves are continuously produced by convection (e.g., Balmforth, 1992; Goldreich & Keeley, 1977; Nordlund & Stein, 2001; Stein & Nordlund, 2001). The amount of energy contained in acoustic waves is sufficiently high to heat the upper chromosphere and corona if all this energy could reach these high layers and be converted into heat there (e.g., Biermann, 1946; Narain & Ulmschneider, 1996; Schwarzschild, 1948; Stein, 1968). The change of the atmospheric properties in the vertical direction in a gravitationally stratified solar atmosphere leads to a steepening of the vertically propagating acoustic waves into shocks. The energy of the propagating shock waves is then dissipated near their fronts due to radiation or viscosity, converting it into the thermal energy. Such an energy deposit process has a stochastic character due to the stochastic nature of the excited



acoustic waves (e.g., Carlsson & Stein, 1997; Ulmschneider, 1971a, 1971b, 1978). According to Carlsson and Stein (1995, 1997), who modeled time-dependent acoustic waves propagation including non-LTE radiative losses in the chromosphere, the chromosphere is not necessarily hot at all times and locations. In their simulations, there are observed short intervals of very high temperature caused by acoustic shocks but the average chromospheric temperature continued to decrease with height. The heights where the shock formation and dissipation happen depend on the wave frequency and amplitude. Higher-frequency acoustic waves (periods around  $10^1$  s) shock rather low in the atmosphere (Ulmschneider, 1971a, 1971b; Narain & Ulmschneider, 1996), and therefore must not be the best candidates for heating the upper atmosphere. Lower frequency waves (periods of  $10^2$  s) could propagate the energy higher up, but this process is limited by the presence of the acoustic cut-off frequency around 3 mHz at the bottom of the photosphere. Thus, acoustic waves with maximum energy in the spectrum are unable to transport this energy to the chromosphere.

On their way to the upper atmosphere, the acoustic waves suffer multiple changes of their physics, related to the presence of magnetic structures in these layers. The magnetic field concentrations embedded in solar granulation suffer foot point motions and this drives waves in these structures through the solar atmosphere, as was shown in numerous “idealized” simulations of the wave dynamics (see Khomenko & Calvo Santamaria, 2013; Khomenko & Collados, 2015). As the waves propagate upwards they find obstacles, such as the equipartition layer where the acoustic,  $c_s$  and the Alfvén,  $v_A$ , speeds coincide  $c_s = v_A$  (equivalent to plasma  $\beta = 1$ ), the layer where the local acoustic cut-off frequency is equal to the wave frequency, the steep temperature gradient at the transition region, etc. In these regions waves suffer transformations, refraction, and reflection. Some of these processes prevent the wave energy reaching the upper chromosphere and corona, but others can favor wave energy transmission. It is important to take into account the location of these critical layers with respect to the height of formation of the observed spectral lines, see e.g., Moretti et al. (2007). The efficiency of the wave-related heating mechanisms will depend on the structure and topology of the magnetic fields in a given solar region.

Vast theoretical effort has been dedicated to understanding how low-frequency waves (3–5 mHz) can reach the chromosphere and corona with the help of magnetic field concentrations, and what are the mechanisms of efficient energy dissipation of the different wave mode types, present in magnetic structures. From the theoretical point of view, wave mode transformation theory has been frequently invoked (Cally, 2006; Schunker & Cally, 2006). According to this theory, acoustic waves (or  $p$ -modes) propagating from sub-photospheric regions suffer conversion into fast and slow magneto-acoustic waves at the equipartition layer. This way, a part of the low-frequency  $p$ -mode energy can escape to the chromosphere in the form of the slow magneto-acoustic mode along the inclined magnetic field lines (Jefferies et al., 2006; Stangalini et al., 2011), frequently called “magnetic portals.” Since these slow magneto-acoustic waves propagate field aligned in the  $\beta < 1$  atmosphere, they “see” the local cutoff frequency reduced through the ramp effect as the gravity is lowered by  $g \rightarrow g \cos(\theta)$ . The fast magneto-acoustic mode in the  $\beta < 1$  atmosphere will refract due to the gradients of the Alfvén speed, and its energy will return to the sub-surface layers. The efficiency of the mode transformation mechanism in transmitting the wave energy to the chromosphere depends on the relative inclination between the wave propagation direction and the direction of the magnetic field, being most efficient for the fields inclined by about  $30^\circ$  (Cally, 2006; Schunker & Cally, 2006). As far as we concerned about the tube waves (see Section 3 also), in the regions of the magnetic portals with low beta plasma, the effective gravity on a particular magnetic field will be modified by the cosine of the angle subtended by that field line with respect to the direction of the gravity, further causing reduced cut-off and allowing the wave propagation (McIntosh & Jefferies, 2006). More specifically, the effects of inclination, magnetic field, and non-uniformity of the medium along with the gravity stratification lead reduction of the cut-off and propagation of the waves (Afanasyev & Nakariakov, 2015; Spruit & Roberts, 1983).

Alfvén waves are one of the best candidates to bring the energy to the upper atmosphere because they do not shock at lower layers, and due to their incompressibility they are not affected by damping through viscosity or radiation (see Section 3). Efficient damping of these waves can be achieved through ion-neutral effects in the partially ionized chromospheric plasma (e.g., ambipolar diffusion mechanism, as discussed by Goodman, 1996, 2011; Goodman & Kazeminezhad, 2010; Martínez-Sykora et al., 2016; Song & Vasyliūnas, 2011, 2014; Shelyag et al., 2016 see below). One of the ways of producing Alfvén waves is through the geometrical mode transformation. At heights where fast magnetic waves refract and reflect (typically located in the

upper photosphere and chromosphere), these can be partially converted into Alfvén waves (Cally & Goossens, 2008; Cally & Hansen, 2011). The most efficient conversion is achieved for strongly inclined magnetic fields as those in sunspot penumbra or the upper chromosphere at the interiors of the network elements. Such a typical scenario of the Alfvén wave propagation in the large-scale chromosphere above a sunspot was recently observed by Grant et al. (2018).

The wave energy transport is extensively studied in observations. A number of studies points that the mode transformation mechanism is indeed acting in the Sun (Grant et al., 2018; Kontogiannis et al., 2016, 2014; Moretti et al., 2007; Rajaguru et al., 2013, 2019). In particular, one of the most prominent phenomena that is now believed to be essentially due to the mode transformation is the presence of high frequency acoustic halos surrounding active regions (Khomenko & Collados, 2009; Rijs et al., 2016). According to Moretti et al. (2007), the same type of magneto-acoustic wave is required to explain both the phenomena of *p*-mode absorption in sunspots and power halos at magnetic canopies. Kontogiannis et al. (2014, 2016) showed that the measured magneto-acoustic wave power in the quiet Sun depends on the magnetic field inclination as predicted by theoretical models of the mode conversion. Long-period waves were observed to be channeled to the chromospheric layers along the inclined magnetic field lines, while the short-period waves were refracted and reflected back at the inclined canopy of a network region, producing magnetic shadows. This behavior certainly affects the amount of the wave power reaching the chromosphere. Rajaguru et al. (2019) demonstrated that the energy flux of acoustic waves within magnetic structures, both in active and quiet regions, peaks around magnetic inclination of 60°, in agreement with the action of the mode-conversion process. Mode conversion was also observed to be important for driving Type I spicule oscillations (Jess et al., 2012). Their data provide evidence for magneto-acoustic oscillations, propagating from the surface to above undergoing longitudinal-to-transverse mode conversion into waves at twice the initial driving frequency. The energy flux to the chromosphere was estimated to be  $3 \times 10^5 \text{ W m}^{-2}$  which is sufficiently high even to heat the corona and to accelerate the solar wind. Some observational inference of such a mode conversion above an EUV bright point is reported by Srivastava and Dwivedi (2010). Direct observational confirmations of the conversion to Alfvén waves are still missing. Nevertheless recently, Grant et al. (2018) used HMI/SDO data to provide observational evidences of Alfvén waves heating chromospheric plasma in a sunspot umbra. The velocity showed tangential signatures, and the observed temperature enhancements were suggested to be consistent with mode-converted Alfvén waves, after their conversion from magneto-acoustic waves.

Many observational works have been dedicated to try to detect heating process related to traveling waves of different nature. Carlsson and Stein (1997) demonstrated that the transient bright grains seen in the core of Ca II H and K lines are due to acoustic waves forming shocks. Beck et al. (2009) found that the acoustic flux in the quiet areas can maintain the temperature of semi-empirical models only below 500 km, but is insufficient at heights above 800–1,200 km. The temperature in the quiet chromosphere oscillates between an atmosphere in radiative equilibrium and one with a moderate chromospheric temperature rise, and horizontal canopy structure reflects itself in temperature maps at heights in the low chromosphere (Beck et al., 2013). Using Ca II 853.2 IBIS data, Abbasvand, Sobotka, Heinzel, et al. (2020) found that the deposited magneto-acoustic wave energy balances 30%–50% radiative losses in the quiet chromosphere and 50%–60% of the losses in a plage with vertical field, rising up to 70%–90% in the plage regions with inclined field. This way, significant portions of the radiative losses could be compensated via acoustic wave flux which has been previously converted to magneto-acoustic wave flux in the regions with the inclined fields. Abbasvand, Sobotka, Švanda, et al. (2020) concluded that the flux contained in magneto-acoustic waves with frequencies up to 20 mHz is sufficient to balance the radiative losses of the quiet chromosphere up to 1,000–1,400 km height. The difference with the previous results can be attributed to the existence of magnetic shadows (areas with reduced wave power at a given frequency), which prevents part of the acoustic energy reaching chromospheric heights in the network and plage regions, similar to observations by Kontogiannis et al. (2014); Kontogiannis et al. (2016). It is worth noting that the quiet-Sun magnetic network elements are surrounded by such a “magnetic shadows” (McIntosh & Judge, 2001), which are the regions that lack oscillatory power at higher frequencies. The magnetic shadows most likely correspond to the typical “acoustic halos”, which are the locations of the increased high-frequency (>3.3 mHz) power in the solar photosphere (Muglach et al., 2005). Rajaguru et al. (2019) shown that low-frequency waves in the range of 2–4 mHz can still channel a significant amount of energy to the low chromosphere at locations with relatively vertical magnetic

field (their frequencies are below the magnetic-field reduced acoustic cutoff). Propagation of these waves is probably assisted by the radiative transfer-related mechanisms as pointed out by Khomenko, Centeno, et al. (2008). These waves transport up to  $2.6 \text{ kW m}^{-2}$  to the chromosphere, which is about twice larger than estimated previously by Jefferies et al. (2006). Straus et al. (2008), using high-cadence IBIS measurements at mid-photospheric heights found up to  $5 \text{ kW m}^{-2}$  energy flux in low-frequency gravity waves.

There is still no agreement if high-frequency (magneto-) acoustic waves can supply enough energy to maintain a chromosphere (Cuntz et al., 2007; Fossum & Carlsson, 2005). Theoretical calculations by Musielak et al. (1994) reveal that acoustic flux has a broad maximum in the high frequency region around 100 mHz (periods  $\approx 10$  s). Ulmschneider et al. (2005) re-considered chromospheric heating by short-period acoustic waves arguing that one-dimensional simulations are inadequate since shock merging destroys much of such short period waves. Firm detection of the high-frequency part of the solar oscillation spectrum is still uncertain. According to Cuntz et al. (2007) the high-frequency energy flux was underestimated by Fossum and Carlsson (2005) due to the limited sensitivity of the TRACE data and for not fully assessing the three-dimensional chromospheric magnetic field topology. Using high resolution data by GFPI/VTT, Bello González et al. (2009) revealed the presence of significant acoustic flux into the quiet chromosphere of about  $3,000 \text{ W m}^{-2}$  carried by acoustic waves with frequencies in the 5–10 mHz range (about 2/3 of the flux) and in the 10–20 mHz range (about 1/3 of the flux) predominantly at locations above intergranular lanes. These fluxes can contribute to the basal heating of the quiet chromosphere. Almost twice large fluxes were found from the highest resolution IMAx/SUNRISE data by Bello González et al. (2010). These results are in contradiction to the earlier work by Fossum and Carlsson (2006) and Carlsson et al. (2007) using TRACE and Hinode data, respectively, but are in agreement with Cuntz et al. (2007).

When considering high-frequency waves and shocks, damping or dissipation effects become important. As discussed above, small-scale disturbances can be easily damped in the chromosphere through various non-ideal mechanisms such as viscosity, radiation, or electrical resistivity. Additionally, in the partially ionized chromosphere ion-neutral effects effectively assist the wave damping. In this regard, numerous works have been aimed at modeling strongly non-linear wave dynamics in the chromosphere in the presence of neutrals. At temporal and spatial scales larger than ion-neutral collisional scales the effect of neutrals can be taken into account using a single-fluid MHD like approximation. In this approximation, the ion-neutral interaction is expressed via the ambipolar diffusion mechanism (Spitzer, 1962). The ambipolar diffusion has been studied extensively in the context of chromospheric heating and structure formation, both using the analytical theory or idealized, and even realistic, numerical simulations (see the review by Ballester et al., 2018). It has been shown that ambipolar diffusion allows to dissipate into heat incompressible magnetic waves (e.g., Alfvén waves; Khomenko et al., 2018; González-Morales et al., 2020). Resistive dissipation of Alfvén waves, enhanced through ion-neutral interaction, has been considered by Song and Vasylūnas (2011); Tu and Song (2013); Shelyag et al. (2016), and Martínez-Sykora et al. (2016). Arber et al. (2016) argued that viscous damping of shock waves has more importance than ambipolar dissipation.

In the upper chromosphere, collisions may not be strong enough and the difference in the velocities of ions and neutrals (or between the different types of ions or neutrals themselves) may reach some fraction of the sound speed. In this situation, a simplified single-fluid treatment may not be sufficient and multi-fluid modeling should be applied. In a multi-fluid approach, the heating due to neutrals is expressed via the frictional heating term (Braginskii, 1965; Leake et al., 2014). The influence of multi-fluid effects on the formation and dissipation of chromospheric shock waves has been scarcely studied, see e.g., Hillier et al. (2016); Snow and Hillier (2019, 2020). Hillier et al. (2016) modeled the formation and evolution of slow-mode shocks driven by reconnection in a partially ionized plasma. A complex multi-fluid structure of the shock transition was modeled revealing structures similar to *C*-shocks or *J*-shocks in the classification by Draine and McKee (1993). The frictional heating associated with ion-neutral decoupling at the shock front was up to 2% of the available magnetic energy. In a recent study, Popescu Braileanu et al. (2019a, 2019b) have shown how the ion-neutral decoupling visibly affects waves in neutrals and charges in the chromosphere, and how these effects become more pronounced in shocks. Realistic multi-fluid modeling still remains a challenge due to its complexity, see recent works by Maneva et al. (2017); Kuźma et al. (2019). Apart from typical chromospheric shocks, recently Srivastava et al. (2018) have observed the presence of pseudo-shocks around a sunspot. Unlike a typical shock as described above, pseudo-shocks exhibit discontinuities only in

the mass density. A two-fluid numerical simulation reproduces such confined pseudo-shocks with rarefied plasma regions lagging behind them. It was conjectured that these pseudo-shocks carry an energy of  $10^3 \text{ W m}^{-2}$ , which is enough to locally power the inner corona and also generate bulk mass flows ( $10^{-5} \text{ kg m}^{-2} \text{ s}^{-1}$ ), contributing to the localized mass transport. If they are ubiquitous, such energized and bulky pseudo-shocks above active regions could provide an important contribution to the heating and mass transport in the overlying solar corona.

In summary, wave heating of the solar chromosphere is a promising mechanism which, despite being proposed long time ago, still provides grounds for discussions. While the chromosphere seems not to be hot at all times, but rather in an intermittent manner, acoustic waves might provide a basal heating in the quiet areas. Hypothesis of magneto-acoustic and Alfvén wave heating are getting more observational evidence as better observations become available. The role of magnetic topology is beginning to be recognized. A particular emphasis for the coming years should be put into the study of the high-frequency part of the spectrum, which also provides new dissipation mechanisms due to partial ionization effects.

#### 4.2. Energy Budget and Heating Capacity of MHD Waves in Localized Chromospheric Flux Tubes

While, the role of the MHD waves in large-scale solar chromosphere is still illusive and mainly predominant heating by acoustic waves/magneto-acoustic waves is known (see sub-section 4.1), the recent high-resolution observations detect a variety of MHD modes (kink, sausage, and torsional modes) in localized photospheric and chromospheric tubes (see Section 3), which carry substantial amount of energy flux that may balance the chromospheric huge radiative losses, as well as can enable the nascent solar wind plasma flows. Recent observations using high-resolution ground (e.g., SST, Rapid Oscillations in the Solar Atmosphere [ROSA]) and space-based (e.g., Interface Region Imaging Spectrograph (IRIS), Solar Dynamics Observatory (SDO)) observatories determine the presence of substantial energy flux associated with various MHD modes in different kinds of the magnetic structures coupling various layers of the Sun's atmosphere. In the photosphere and chromosphere, the wave behavior ubiquitously detected above pores, sunspots, EUV bright points, tubes related to the plage regions. Jess et al. (2009) have reported the detection of Alfvén waves with periods ranging between 126-400 s above bright-points with typical energy flux of  $1.5 \times 10^4 \text{ W m}^{-2}$  with a 42% transmission coefficient. Grant et al. (2015) has observed upwardly propagating slow sausage waves above magnetic pores carrying an energy flux of  $3.5 \times 10^4 \text{ W m}^{-2}$ . These observations infer that the magnetic pores transfer wave energy to the higher overlying atmosphere, and also inject substantial energy in the localized chromospheric plasma for its heating. The higher order non-axisymmetric modes magnetoacoustic oscillations ( $m \geq 1$ ) in the frame-work of both body and surface waves are also observationally detected in magnetic tubes rooted in the solar photosphere (Jess et al., 2017; Keys et al., 2018; Stangalini et al., 2018).

As far as the transverse waves are concerned, Morton et al. (2012) have reported the simultaneous presence of fast kink and sausage waves (Figure 3; subsection 3.2) in mottles and fibrils using ROSA  $H\alpha$  high-resolution observations. They have estimated that these wave modes carry an average energy of respectively 4,300  $\text{W m}^{-2}$ , and 11,700  $\text{W m}^{-2}$  in the solar chromosphere, which is still the large amount present in the lower solar atmosphere. Srivastava et al. (2017) have reported the ubiquitous presence of high frequency ( $\approx 12\text{--}42 \text{ MHz}$ ) torsional oscillations in spicular-type structures in the solar chromosphere (Figure 4, right-bottom box). Their numerical model have demonstrated that these high-resolution observations mimics torsional Alfvén waves associated with the high frequency drivers channeling a large amount of energy ( $10^5 \text{ W m}^{-2}$ ) in the chromosphere. A significant amount of wave energy ( $10^3 \text{ W m}^{-2}$ ) is transported into the overlying corona from the chromosphere to balance its radiative losses, even after partial reflection of the waves from the TR. Grant et al. (2018) have reported the evidence of Alfvén wave heating of the chromospheric plasma in an active region sunspot umbra in the frame-work of mode conversion and the formation of magnetoacoustic shocks. In conclusion, the various drivers in the chromosphere help in generating different MHD modes in magnetic flux tubes along with a sufficient amount of energy flux. The details of waves'energy budget in chromospheric tubes are given in details in Van Doorselaere et al. (2020). In the chromosphere, such magnetic structures exhibit a significant role in guiding MHD waves, and thus the related energy fluxes. However, the filling factor of these localized MHD waveguides in the lower solar atmosphere, and the global evolution of the particular wave mode is not possible eventually posing a question on over-all contributions



of these waves in the global heating of the solar corona. However, definitely the waves could play an important role in heating the localized chromosphere and corona.

In the next sub-section 4.3, we will illustrate the heating aspects of the chromospheric prominence plasma.

### 4.3. Wave Heating in Prominences

Solar prominences are structures with properties which resemble the chromosphere and are embedded in the solar corona. Due to their peculiar physical properties, low temperature and high density compared to that of the solar corona, and dynamic behavior, solar prominences are the subject of intense research. Due to their low temperature, the prominence plasma is partially ionized, although the exact degree of ionization is still unknown and, probably, is not a constant quantity inside each considered prominence. The origin of the prominence mass has been an open question for many years and, nowadays, we know that it must originate in the chromosphere (Pikel'Ner, 1971; Mackay et al., 2010), because there is not enough plasma in the corona for their formation (Song et al., 2017). Among the different models that have been proposed to explain how chromospheric plasma becomes prominence material the evaporation-condensation model (Antiochos et al., 1999; Luna et al., 2012; Mackay et al., 2010; Xia et al., 2014) is the one most rigorously studied for prominence formation. However, all the different models have been developed assuming fully ionized conditions, while partial ionization brings the presence of neutrals and electrons in addition to ions, thus collisions between the different species are possible and the effects on the prominence mass formation must be considered (Karpen et al., 2015). Another key problem in the physics of prominences is how these cool and dense structures are supported in the hotter, more rarefied solar corona. Considering the prominence as a partially ionized plasma, the problem of how neutrals are supported in prominences is a matter of great interest. Bakhareva et al. (1992) pointed out that, after perturbing a 2D Kippenhahn-Schlüter magnetic configuration, the system underwent amplified oscillations of density, magnetic field, and velocity which, finally, destroy the prominence. The instability is caused by the inability of the magnetic field to support the plasma's neutral component against gravity. However, Terradas et al. (2015) solved the two-fluid equations, including ion-neutral and charge-exchange collisions, to study the temporal behavior of a prominence plasma embedded in the solar corona. In their model, the prominence is represented by a large density enhancement, composed of neutrals and ions, and the magnetic configuration is quadrupolar with dips. The results showed that partially ionized prominence plasma can be efficiently supported when the coupling between ions and neutrals is very strong (see also H. Gilbert et al., 2007; H. R. Gilbert et al., 2002). Summarizing, since prominences are made of partially ionized plasmas, it is very important that we take into account ion-neutral coupling when describing the physics of prominence formation, support and stability.

The heating of solar prominence plasma has been a matter of intense debate. In order to exist, prominences need mechanical equilibrium as well as a detailed energy balance between heating and radiative cooling. Energy balance studies suggest that incident radiation provides most of the heating of prominence plasma (H. Gilbert, 2015), however, this radiative heating depends on the illumination from the surrounding atmosphere. Moreover, radiative equilibrium prominence models, constructed from a balance between incident radiation and cooling (Anzer & Heinzel, 1999; Heinzel & Anzer, 2012; Heinzel et al., 2010), as well as differential emission measures have pointed out that a further unknown heating is required in order to reproduce the observed temperatures in the prominence cores (Heinzel, 2015; Heinzel & Anzer, 2012; Labrosse et al., 2010) and to balance the radiative losses (Parenti, 2014; Parenti & Vial, 2007).

On the other hand, ground- and space-based observations have confirmed the presence of oscillatory motions in prominences, which have been interpreted in terms of standing or propagating MHD waves (Arregui et al., 2018; Aschwanden, 2004; Ballester, 2015; Erdélyi & Goossens, 2011; Roberts, 2000, 2008; Nakariakov & Verwichte, 2005; Nakariakov, Pilipenko, et al., 2016; Oliver, 1999, 2009; Oliver & Ballester, 2002). Observational studies of small amplitude prominence oscillations have shown the existence of periods which can be distributed in three groups: of a few minutes, between 10 and 40 min and between 40 and 90 min. Furthermore, observations have also provided evidence about the damping of prominence/filament oscillations. In most of the observations in which the damping time has been determined, those damping times are between 1 and 4 times the corresponding period, and large regions of prominences/filaments display similar damping times (Arregui et al., 2018). The observational evidence about wave activity in prominences together with theoretical developments about MHD waves have boosted the development

of prominence seismology (Arregui et al., 2018) which allows the determination of the prominence physical parameters from the comparison of observed and theoretical wave properties. However, much work remains to incorporate partial ionization effects, in particular multi-fluid physics, into existing models of oscillatory phenomena in prominences.

Mechanisms based on wave dissipation have been proposed for the heating of the solar atmosphere (see Arregui, 2015 for a review), therefore, an additional source of energy to heat prominences could be provided by these mechanisms. Kalkofen (2008) estimated the acoustic flux in the photosphere and found that it is much smaller than the energy radiated by the chromosphere. Therefore, it seems that sound waves are not the source of chromosphere and prominence heating, while Alfvén waves could be a good candidate. However, Pécseli and Engvold (2000) estimated the wave heating associated to Alfvén wave dissipation in prominence plasma finding that the contribution is very small. Parenti and Vial (2007) derived the distribution of nonthermal velocities at various temperatures in a prominence observed with SOHO/SUMER. They assumed that these velocities were the signatures of wave propagation, and computed the energy flux for Alfvén and sound waves. Using differential emission measure analysis, they computed the radiative losses in the prominence, and made a comparison between both estimations. They concluded that the radiative losses in the PCTR could be compensated by Alfvén wave heating. Hillier et al. (2013) made a comparison between power spectra coming from prominence waves with that of photospheric horizontal motions. They found that for frequencies less than 7 mHz, the frequency dependence of the velocity power is consistent with the velocity power spectra generated from observations of the horizontal motions of magnetic elements in the photosphere, suggesting that the prominence transverse waves are driven by photospheric motions. Then, the excited MHD waves at the photospheric level could transport energy from the photosphere to the prominences located in the solar corona.

Several studies have considered the damping of Alfvén waves in partially ionized plasmas, like the solar chromosphere, by means of ion-neutral collisions (De Pontieu et al., 2001; Haerendel, 1992; James et al., 2003; Leake et al., 2005; Soler, Ballester, & Zaqarashvili, 2015; Soler, Carbonell, & Ballester, 2015; Song & Vasylunas, 2011), and since prominence plasmas are akin to chromospheric plasmas, wave dissipation in partially ionized plasmas could be the source of the required additional heating. However, it is important to keep in mind that the efficiency of waves to heat the plasma depends on the efficiency of the dissipation mechanism locally (Soler et al., 2016). In this sense, Khodachenko et al. (2004 and 2006) made a qualitative study of the damping of MHD waves in a partially ionized plasma considering viscosity, collisional friction and thermal conduction as potential damping mechanisms. From this study, they concluded that collisional friction is the dominant damping mechanism for MHD waves in prominences. Using the single-fluid approximation, further studies on the temporal and spatial damping of Alfvén and magnetoacoustic waves in unbounded and structured partially ionized plasmas with prominence physical properties, but without computing heating estimations, were made by Barceló et al. (2011); Carbonell et al. (2010); Forteza et al. (2007, 2008); Soler et al. (2008, 2009, 2010), while Martínez-Gómez et al. (2018) have computed the heating in a three-fluid prominence plasma

With the aim to explore prominence heating by means of damped Alfvén waves, first of all, Soler et al. (2016) considered an unbounded homogeneous and partially ionized prominence plasma, with a straight and constant magnetic field, and studied the propagation and spatial damping of linear Alfvén waves. The plasma was considered to be composed of partially ionized hydrogen and neutral helium at  $T < 10^4$  K. To study wave propagation, the multifluid formalism (Zaqarashvili, Khodachenko, & Rucker, 2011) was used, assuming that ions and electrons formed a single fluid while neutral hydrogen and neutral helium formed two separate neutral fluids. Then, from the linearized equations for Alfvén waves, an expression for the evolution of wave energy was derived,

$$\frac{\partial U}{\partial t} + \nabla \cdot \Pi = -Q. \quad (18)$$

This equation includes the temporal evolution of wave energy density,  $U$ , corresponding to the sum of kinetic energies of ions, neutral hydrogen, neutral helium and magnetic energy; the divergence of wave energy flux,  $\Pi$ , corresponding to the amount of energy propagated by the wave; and the loss of wave energy,  $Q$ , due to dissipation by collisions. As the wave propagates, wave energy is absorbed by the plasma and converted

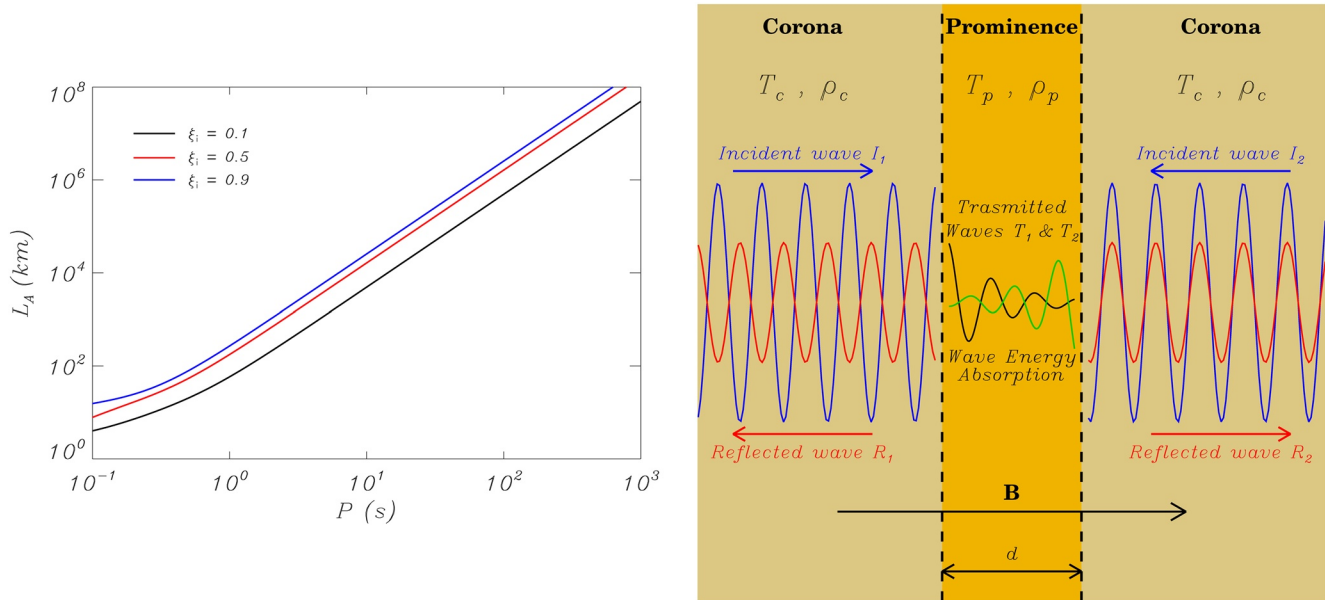


**Figure 5.** Left panel: Energy absorption length,  $L_A$ , as a function of the wave period,  $P = 2\pi/\omega$ , for Alfvén waves propagating in a prominence plasma when different values of the hydrogen ionization ratio,  $\xi_i$ , are assumed. The meaning of the various line styles is indicated within the figure. Logarithmic scale has been used in both axes. Right panel: Sketch of the prominence slab model. Credit: Soler et al., 2016, A&A, 592, A28, reproduced with permission © ESO.

into internal energy, and the quantity,  $Q$ , can be identified as the wave heating rate. The Alfvén energy flux can be computed from  $\Pi$ , and the time-averaged energy flux for a forward-propagating wave is,

$$\langle \Pi \rangle = \frac{B^2}{2\mu} \frac{\text{Re}(k)}{\omega} V^2 \exp[-2\text{Im}(k)s] \hat{e}_B. \quad (19)$$

in  $W \cdot m^{-2}$ . The time-averaged energy flux is proportional to  $\exp[-2\text{Im}(k)s]$ , with  $\text{Im}(k)$  the imaginary part of the wavenumber and,  $s$ , the propagation distance, indicating that the net energy carried by the Alfvén wave exponentially decreases, because of collisions, as the wave propagates (see Soler et al., 2016 for details). Then, a characteristic energy absorption length scale,  $L_A$ , can be defined as

$$L_A = \frac{1}{2\text{Im}(k)}, \quad (20)$$

which represents the length scale at which the energy absorbed is deposited in the plasma. Figure 5 (left panel) displays the energy absorption length,  $L_A$ , computed from Equation 20, as a function of the wave period,  $P$ , for different values of the hydrogen ionization ratio,  $\xi_i = \rho_i/(\rho_i + \rho_H)$ , and typical prominence parameters ( $\rho = 5 \cdot 10^{11} \text{ kg m}^{-3}$ ,  $T = 8,000 \text{ K}$ ,  $B = 10 \text{ G}$ , and abundance ratio,  $A_{He}/A_H = 0.1$ ). As it can be expected, when the hydrogen ionization degree decreases, the wave damping is stronger. Also, Figure 5 (left panel) shows that low period waves are efficiently damped in the plasma, while for long periods waves the damping is less efficient. These results indicate that for waves with periods  $P > 100 \text{ s}$ , typical of waves in prominences, the wave energy absorption and associated heating are negligible since the energy absorption length is of the order of  $10^6 \text{ km}$ , which is unrealistic for prominence's length scales.

Next, Soler et al. (2016) investigated whether the energy of Alfvén waves incident on a solar prominence can be deposited in the prominence medium because of this damping. To this end, they represented the prominence by a slab with a transverse magnetic field embedded in the solar corona (see Figure 5, right panel) and assume the presence of Alfvén waves that are incident on the prominence-corona interface. These Alfvén waves come from the footpoints of the magnetic field lines which support the prominence, propagating along these field lines. In solar prominences, the strong discontinuity in density between the prominence and the corona could lead to Alfvén wave reflection and decrease the amount of heat released

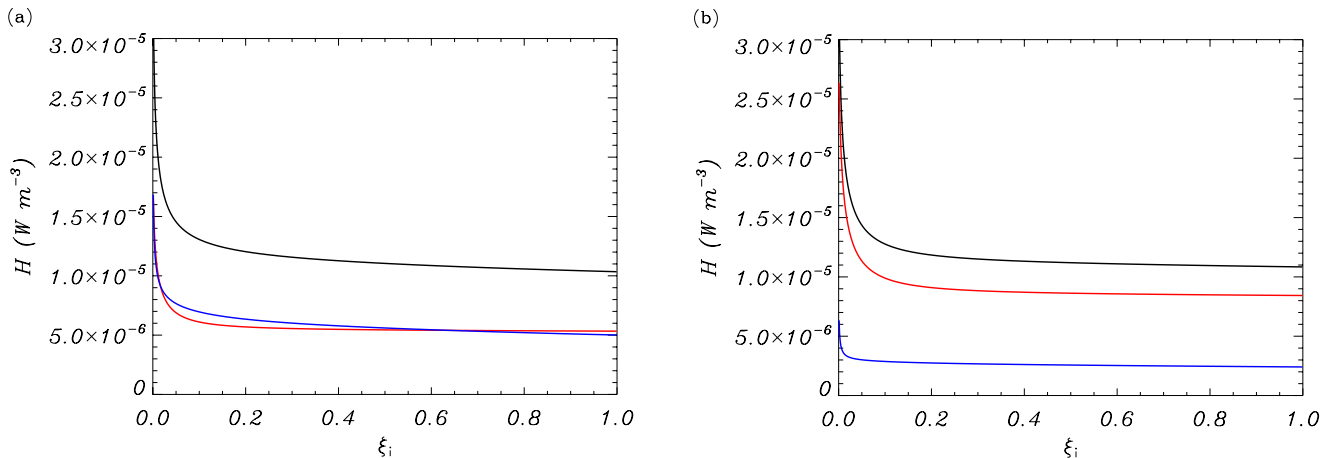


**Figure 6.** (a) Total integrated heating,  $H$ , as a function of the hydrogen ionization ratio,  $\xi_i$ , when the velocity amplitude of the incident waves is  $10 \text{ km s}^{-1}$ . The black line indicates the full result, the red line indicates the contribution of short periods ( $0.1 \text{ s} \leq P \leq 1 \text{ s}$ ), and the blue line indicates the contribution of intermediate periods ( $1 \text{ s} \leq P \leq 100 \text{ s}$ ). (b) Same as panel (a) but for the velocity power law of Hillier et al. (2013). Credit: Soler et al., 2016, A&A, 592, A28, reproduced with permission © ESO.

inside the prominence. However, Hollweg (1984) suggested that the decrease of the Alfvén wave velocity inside a prominence slab could act as a resonant cavity for incident Alfvén waves. Using this approach, Soler et al. (2016) studied the trapping of energy of Alfvén waves incident on a prominence and the associated heating rate. The incident Alfvén waves on the prominence-corona interface (see Figure 5, right panel) are partly transmitted into the prominence slab and partly reflected back to the corona. The condition for the excitation of cavity resonances is that the frequency of the incident waves matches a natural frequency (eigenmode) of the prominence, then, the trapping of wave energy within the prominence slab can be very efficient when the period of the incident Alfvén waves matches a resonance period. The channeled energy into the prominence is then dissipated by ion-neutral collisions, and can efficiently contribute to the heating of the plasma. The heating rate within the slab caused by the Alfvén wave dissipation,  $Q$ , is computed using the ion velocity amplitude of the waves transmitted into the slab. First of all, this heating rate is time-averaged over one wave period and, next, it is spatially averaged within the slab. The obtained volumetric heating rate depends on the power spectrum of the waves incident on the prominence which, unfortunately, is not well known from observations and needs to be assumed (see below). Finally, the total heating produced by a broadband driver is obtained by integrating the volumetric heating rate over a range of periods. Then, to estimate this total heating rate, Soler et al. (2016) used two different power spectra: a flat power spectrum with a constant velocity amplitude of  $10 \text{ km s}^{-1}$ , and a velocity amplitude which decreases with a power law following the observations by Hillier et al. (2013) (see Figures 6a and 6b), and compared the obtained heating rates with the prominence radiative losses. Using different approaches, and for typical prominence parameters, the radiative losses from the prominence slab were estimated to be in the range  $10^{-5} \text{ W m}^{-3}$  and  $10^{-4} \text{ W m}^{-3}$ . The comparison of the integrated heating rates of Figure 6 with the estimated radiative losses indicates that wave heating may compensate for a non-negligible fraction ( $\sim 10\%$ ) of the energy lost by radiation. Therefore, the estimated wave heating rate represents a small contribution to the total heating necessary to balance the emitted radiation, but it can possibly account for the additional heating necessary to explain the observed prominence core temperatures (Heinzel et al., 2010). This model is rather simple, but it is a first attempt to try to understand how the damping of Alfvén waves due to dissipation by collisions can contribute to prominence heating. In order to develop more accurate and efficient prominence heating mechanisms, realistic 2D or 3D numerical models of prominence support, prominence fine structure, ionization equilibrium and energy balance are needed as initial configurations for further studies.

In general, the fluid (magnetized or non-magnetized) systems are subjected to the arbitrary perturbations. There are likely physical scenario that either the fluid system evolves waves & oscillatory phenomenon, or it will experience the instabilities. In the next Section 5, we describe the magnetic instabilities that arise in the structured chromospheric plasma.



## 5. MHD Instabilities in the Chromospheric Plasma

While wave dynamics is potentially influenced by the structured chromosphere, there may be certain physical conditions that may lead to a subsequent growth of the perturbations in the form of various instabilities. The most common instabilities that are observed and studied in the large-scale chromospheric structures “(e.g., solar prominences)” are driven by respectively the gravity and sheared flow: (i) Rayleigh-Taylor (RT) and (ii) Kelvin-Helmholtz (KH) instabilities (T. E. Berger et al., 2008; Ryutova et al., 2010; T. E. Berger et al., 2010; Hillier et al., 2011; T. Berger et al., 2017; Mishra & Srivastava, 2019). The RT instability was originally proposed by Rayleigh (1899) and Taylor (1950) to explain the growth of small-amplitude perturbations at the interface between two fluids. This instability takes place when a denser fluid caps a lighter fluid, while the interface between these fluids is perturbed against the gravity. According to Priest (2014), the dispersion relation for the uniformly magnetized fluid can be expressed as

$$\omega_{th}^2 = -gk \frac{(\rho_h - \rho_l)}{(\rho_h + \rho_l)} + \frac{2B^2 k_x^2}{\mu(\rho_h + \rho_l)}. \quad (21)$$

Here  $g$  is the gravitational acceleration of the Sun,  $B$  is the horizontal component of the magnetic field,  $k = 2\pi/\lambda$  is the wavenumber with  $\lambda$  being the characteristic wavelength of the RT instability. The symbols  $\rho_h$  and  $\rho_l$  denote the densities of the heavy and lighter fluids, respectively. The dispersion relation as given in Equation 21 describes that in the absence of the magnetic field the interface will be RT unstable as  $\omega_{th}^2 < 0$  providing the condition that heavy fluid ( $\rho_h$ ) lies above lighter one ( $\rho_l$ ). The oscillations of the interface along the magnetic field renders the stabilizing effects as the second term in Equation 21 becomes positive. A representative evolution of RT instability in the solar prominence system, resulting from the above equation, is shown in Figure 7 both in the observations (left) and numerical modeling (right).

The evolution of the bubbles and plumes are characteristic features associated with the RT instabilities evolved in the solar chromospheric prominence plasma (T. E. Berger et al., 2010; Hillier et al., 2012; Mishra & Srivastava, 2019).

The linear theory of the RT instability in the partially ionized plasma was developed by Diaz et al. (2012). Additionally, Khomenko, Diaz, et al. (2014) showed that the non-ideal, partially ionized chromospheric plasma with resistive and ambipolar diffusion taken into account experiences larger growth rate of the RT instability (RTI), faster plasma flows, rapid downflows, evolution of the high temperature bubbles, and the asymmetry between large rising bubbles and small-scale down-flowing fingers, compared to the plasma evolution in the framework of ideal MHD. Such dynamical plasma processes, elevated temperatures, and RT features are well observed by Mishra and Srivastava (2019). Usually, the ideal MHD is sufficient to explain the RT instability. However, in order to explain generation of fine structures, their dynamics, and plasma heating the non-ideal effects are required.

KH instability takes place in a medium with a sufficiently strong sheared flow. In a magnetic-free fluid the dispersion relation for the KH instability resulting at the interface which separates two different states of a gas is given as Chandrasekhar (1961) and Choudhuri (1998):

$$\frac{\omega_{th}}{k} = \frac{\rho_1 U_1 + \rho_2 U_2}{\rho_1 + \rho_2} \pm \left[ \frac{g}{k} \frac{\rho_1 - \rho_2}{\rho_1 + \rho_2} - \frac{\rho_1 \rho_2 (U_1 - U_2)^2}{(\rho_1 + \rho_2)^2} \right]^{\frac{1}{2}} \quad (22)$$

where  $U_1$  and  $U_2$  are gas velocities at both sides of the interface and  $\rho_1$  and  $\rho_2$  the corresponding mass densities. When, the expression within the square root of Equation 22 becomes negative then,

$$\rho_1 \rho_2 (U_1 - U_2)^2 > (\rho_1^2 - \rho_2^2) \frac{g}{k} \quad (23)$$

depicts the evolution of the Kelvin-Helmholtz instability when the two fluid layers move with the different speeds (Choudhuri, 1998). Perturbations with the small wavelengths become unstable when the velocity difference in both the layers is small. These basic equations (Equations 21 and 22) respectively for RT and

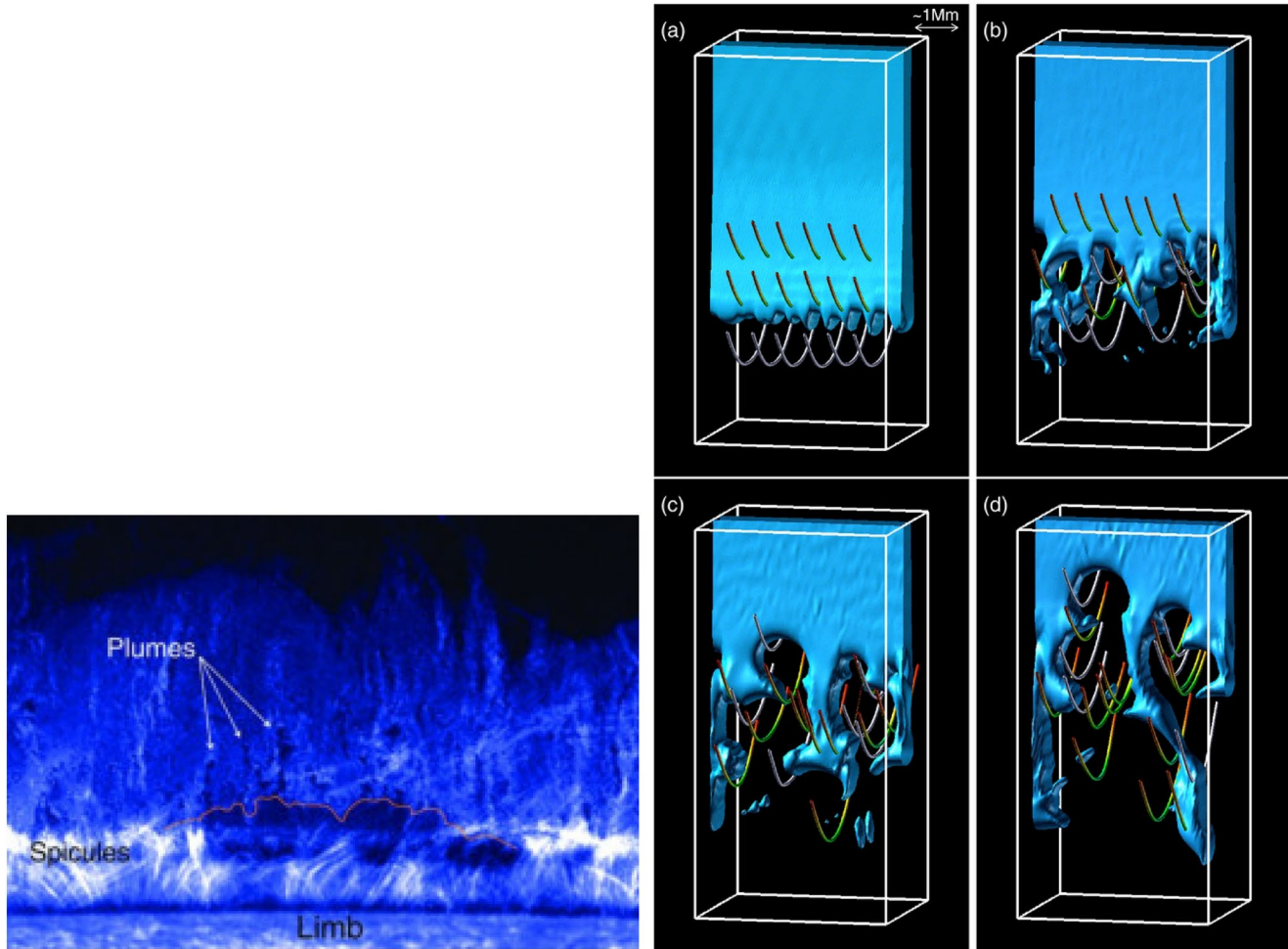


**Figure 7.** Left: The 30 November 2006 Ca II H-line prominence observed on the west limb at 04:50:10 UT, in which RT instability-related plumes, upflows, and cavities are well seen (image adapted from Berger et al., 2010). Right: The numerically simulated RT instability evolution in form of the growth of plumes/bubbles are seen, which match the observational data (image adapted from Hillier et al., 2012). © AAS Reproduced with permission.

KHI instabilities can be applied in the incompressible limit. In the presence of the magnetic fields, the onset condition for the K-H instability will be (Chandrasekhar, 1961; Yuan et al., 2019):

$$\left[ \bar{k} \cdot \Delta \bar{U} \right]^2 = \frac{\rho_1 + \rho_2}{\mu(\rho_1 \rho_2)} \left[ (\bar{k} \cdot \bar{B}_1)^2 + (\bar{k} \cdot \bar{B}_2)^2 \right]. \quad (24)$$

Here,  $\bar{k} = 2\pi / \lambda$  is the wave vector,  $\lambda$  is the characteristic wavelength of the perturbations, and  $\Delta \bar{U}$  is the velocity difference in fluid layers.

It is noteworthy that the KH instability is the most common instability that is observed and modeled in the cool chromospheric plasma, cool jets, and in spicules (Antolin et al., 2018; Zhelyazkov et al., 2015; Kuridze et al., 2016). An example of the unstable upflows in the Mg II k and Si IV channels is observed by Interface Region Spectrograph (IRIS) in the solar prominence (Figure 8, top and middle panels), while the simulation of the resulting KH instability is displayed in the bottom panel of Figure 8, that arises due to the counter-propagating flows generating the shear motion at the fluid interface (Hillier & Polito, 2018). In the example shown in Figure 8, in the middle, we note that the instability leads to the growth of perturbations with a specific parallel wavelength. Moreover, simulations illustrated in the bottom panels of Figure 8, display the appearance of coherent structures, rather than the nonlinear cascade to shorter wavelengths. The one most important implications of KH instability may be that it can result in turbulent flows in the chromospheric

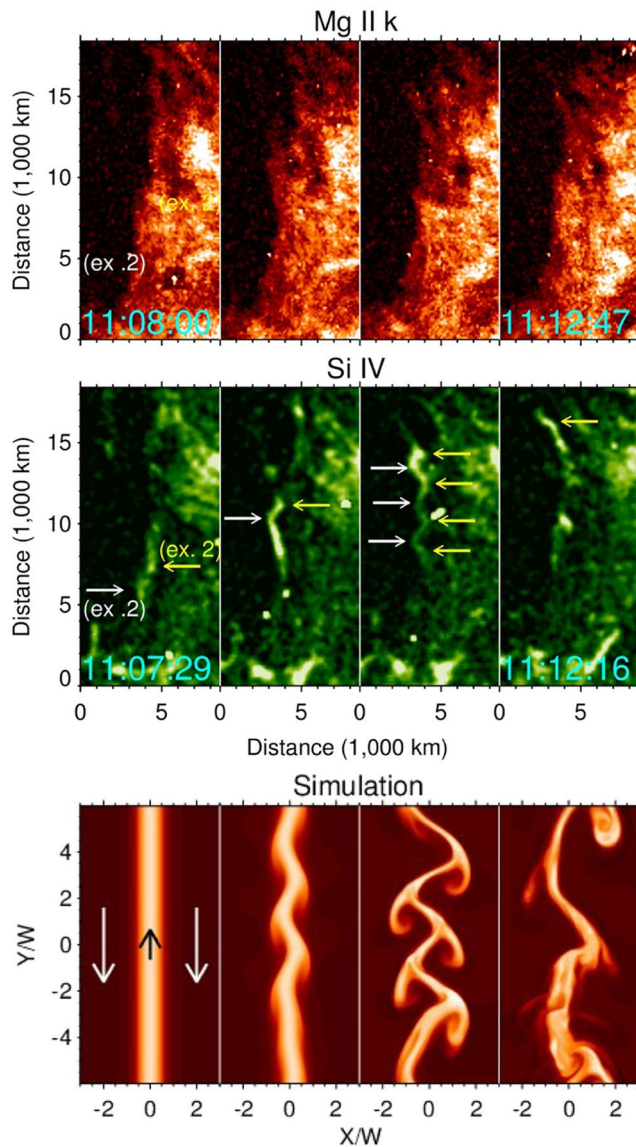


**Figure 8.** The observational data of the KH unstable upflowing plasma in the solar prominence (top and middle) and the results of MHD numerical simulations of the instability driven by shear motion at the interface between two fluids (bottom) (Image adapted from Hillier & Polito, 2018). © AAS Reproduced with permission. KH, Kelvin-Helmholtz; MHD, magnetohydrodynamic.

plasma, however, it is theorized in the observations of thin and cool chromospheric jets (Kuridze et al., 2016). The KHI was studied in the partially ionized plasma by Soler et al. (2012). The analysis of the instability in the partially ionized plasma shows that the ion-neutral collisions may lead to the fast heating of the generated KH instability vortices (Soler et al., 2012). These vortices, in the presence of non-ideal effects, may have a capability to heat the chromospheric plasma. Using simple analytical methods, Ballai et al. (2015) have shown that the dissipative instabilities appear for the flow speeds that are lower than the KHI threshold at the fluid interfaces. While viscosity tends to destabilize the plasma, the effect of partial ionisation through the Cowling resistivity will act toward stabilizing the interface. However, more observations and numerical simulations have to be performed to improve our knowledge in this area.

Cylindrical jets are subject to the  $m = 1$  kink instability which depends on the Alfvén Mach number (specified as the ratio of Alfvén and flow speeds) (Zaqarashvili, 2020). The kink instability is related to the flow instability (i.e., KHI, see above), where the centripetal force increases the transverse displacement of the jet when it overcomes the Lorentz force of magnetic field lines (panel A2 of Figure 9). It is shown that the kink instability may be important for spicules that rise up at the peripheries of vertically expanding magnetic flux tubes (panel A1 of Figure 9) (Zaqarashvili, 2020). Therefore, inclined spicules may be more unstable and have higher transverse speeds. Periods and growth times of unstable modes are comparable to the life time of type II spicules. Therefore, it may indicate an interconnection between high-speed flows and the rapid disappearance of type II spicules in chromospheric spectral lines (Sekse et al., 2012).

Chromospheric magnetic flux tubes may also become unstable owing to their twist. Twisted flux tubes can be subject to magnetic kink instability. It is shown that the motion of twisted tubes reduces classical Kruskal-Shafranov instability threshold for the kink instability (Zaqarashvili, Díaz, et al., 2010). Hence, this instability can be important in spicules. Another possibility is the  $m = 0$  sausage or pinch instability. However, there is no evidence of the sausage instability in the solar atmosphere. The only exception can be the one originally excited in the eruptive solar prominence (Figure 9, bottom panel), and also visible in its activation and heating phase (Srivastava et al., 2013). If the azimuthal component of the magnetic field ( $B_\theta$ ) at any point in the magnetic flux tube becomes larger than  $B_\theta$  outside the tube, the enhanced magnetic pressure makes that point on the tube pinched, and triggers the sausage instability. In the case of the sausage instability related perturbations, the axial field is compressed at the locations inside the flux tube, where pinching generated and the enhanced magnetic pressure there, further opposes the growth of pinching

and thus the growth of the sausage instability. In other words, the condition of  $B_z > B_\theta$  should be the most general criterion for the stability against the sausage instability.

Apart from above mentioned standard instabilities, there are several other plasma instabilities that are evolved under specific physical conditions, and they become highly important in determining the energy and mass transport in the chromosphere and its coupling with other layers of the solar atmosphere. The chromospheric heating may also be linked with the convective overshooting motions in the lower chromosphere driving the “Farley-Buneman (FB) instability” (Fontenla et al., 2008; Gogoberidze et al., 2009; Madsen et al., 2014). Some studies also advocate the liberation of the energy due to the fast magnetic reconnection which develops as a consequence of the “plasmoid instability” without anomalous resistivity



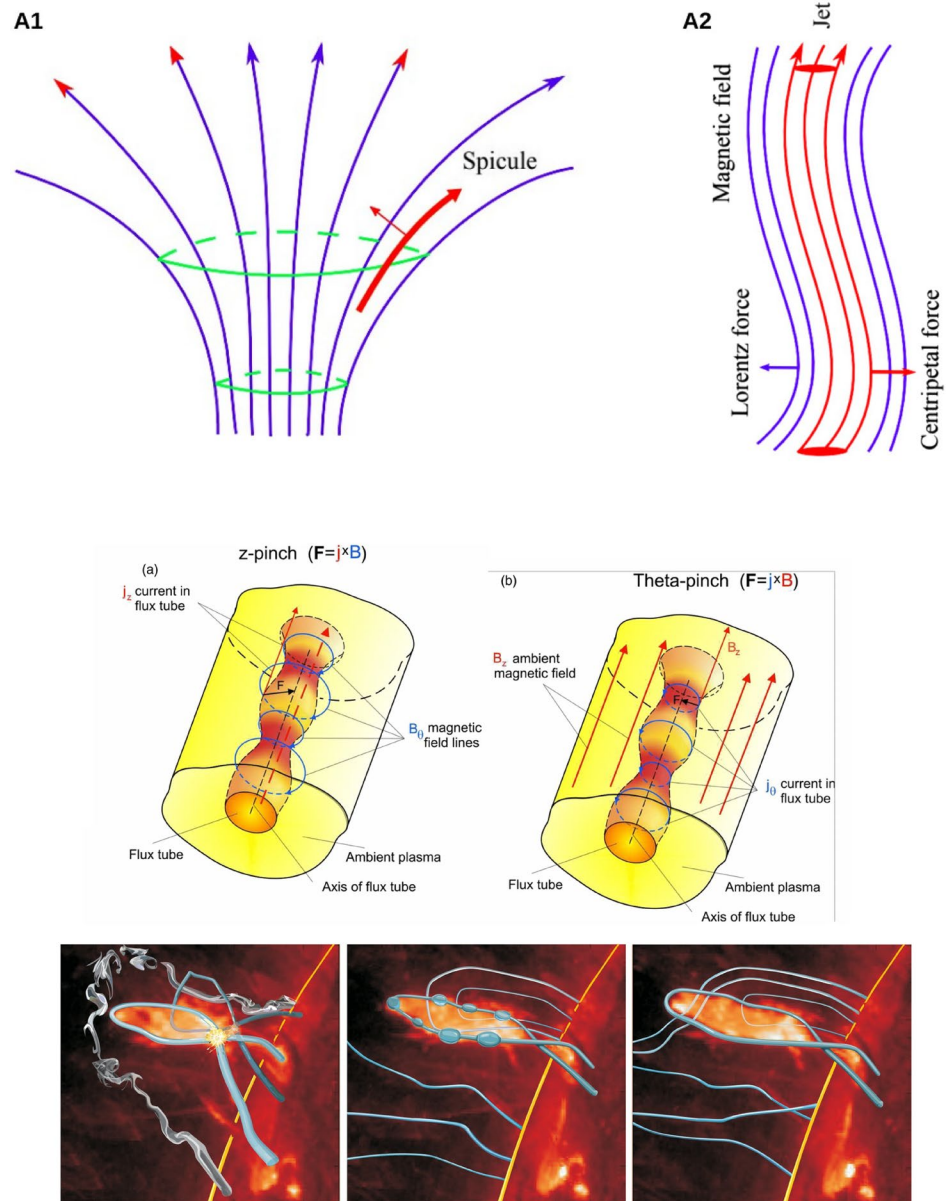


**Figure 9.** Top: The schematic view of the evolution of kink instability in the chromospheric jets (adapted from Zaqarashvili et al., 2020). Middle: A schematic view related to the physical mechanism of sausage instability in z-pinch (panel “a”) and  $\theta$ -pinch (panel “b”), shown in the context of Sun’s magnetized plasma. Bottom: The sketch of the sausage instability (middle-panel) in an active prominence on September 12, 2011 overlaid on SDO/AIA 304 Å image (image adapted from Srivastava et al., 2013). © AAS Reproduced with permission.

enhancements in the middle of the solar chromosphere (Ni et al., 2015). Under specific conditions of local thermal equilibrium in the solar corona, the “thermal instability” can also be evolved, which further leads to the initiation of the condensations locally in the corona with the plasma material cooling down to the chromospheric temperature there. Such plasma condensations may form a cool prominence, or evacuate downwards under the influence of the gravity and gas pressure constituting the coronal rain (Antolin, 2020).



## 6. Discussion, Conclusions, and Some Outstanding Questions

The complexity of the plasma conditions in the solar chromosphere pose a number of challenges when we try to understand the coupling between the *in situ* generation of various MHD wave modes in the photosphere, and their propagation into the overlying solar atmosphere. Since the chromosphere affects wave propagation and alters the overall plasma dynamics in an intrinsic manner, some of the main issues that need to be addressed may be outlined as follows:

- (i) Contemporary models of the solar chromosphere are still overly simple and do not take into account a number of important factors. Widely used one- or multi-fluid models need further improvement, particularly in the lower and upper chromospheric layers presenting challenges for accurate models of the solar atmosphere

Once this issue has been satisfactorily addressed, the next important task is to improve our knowledge and understanding of the drivers of MHD waves. Recent high-resolution ground-based observations (e.g., SST, ROSA, etc) reveal the presence of a variety of such drivers (e.g., Bonet et al., 2008; De Pontieu, Rouppe van der Voort, et al., 2014; Liu et al., 2019; Morton et al., 2013; Wedemeyer-Böhm et al., 2012). These drivers produce a variety of wave modes (kink, sausage, and torsional modes) in strongly magnetized flux tubes (see Section 3). Once MHD waves have been generated their propagation is influenced by the magnetic field and plasma properties of the chromospheric flux tube and the ambient medium. This can further enable the evolution of the mixed or individual modes (see sub-section 3.1) depending upon the local plasma conditions (e.g., Grant et al., 2018; Jess et al., 2009; McIntosh et al., 2011; Morton et al., 2012, 2015; Srivastava & Goossens, 2013; Srivastava et al., 2017). Despite significant theoretical developments (Section 3), outstanding questions remain, specifically:

- (ii) Which observables best reveal generation (e.g., resonant coupling of different tube modes in non-uniform media) and dissipation (e.g., resonant absorption) of MHD modes (e.g., kink/Alfvén waves)? (sub-section 3.1, and, e.g., Goossens et al., 2011)
- (iii) How can we determine the isolated symmetric modes of flux tubes (see sausage waves in sub-section 3.2) in the solar chromosphere when these are strongly structured in the radial direction? (e.g., Chen et al., 2016; Li et al., 2018, 2020; Lopin & Nagorny, 2015)
- (iv) Are we currently in a position to estimate waves' exact roles in the heating/energy budget of the chromosphere, as well as that of the TR and inner corona? Can we bring together observations and theory under realistic atmospheric conditions to provide a precise determination of wave energetics?
- (v) How efficient are the various wave dissipation mechanisms in prominences and how important is the dissipated energy to the prominence energy balance?

The answers to many of these outstanding questions will come through the continuous development and improvement of observational capabilities in the spatial, spectral and temporal and spatial domains. Spectropolarimetric observations from a wide range of instruments (e.g., IRIS, 1m-SST, 4m-DKIST, upcoming 4m-EST and 2m-NLST) will allow us to constrain models of the chromosphere and its local dynamics in such a way that existing physical models will need to be adapted and refined, improving our understanding of the role of MHD waves.

The “whole chromosphere” perspective was emphasized in Section 2, where we saw that MHD waves in a magnetic atmosphere display a different nature as the relative importance of the sound and Alfvén speeds change drastically over 15 or more scale heights. The conversion of acoustic waves into magnetoacoustic waves in the lower chromosphere and their upward propagation crucially depends on the local plasma and magnetic field conditions, and the wave orientation with respect to the magnetic field. Some outstanding questions are:

- (vi) Why are theoretical models unable to reproduce the observed variation of acoustic cutoff in the solar atmosphere? (e.g., Felipe et al., 2018; Murawski et al., 2016; Wiśniewska et al., 2016).
- (vii) How do the transverse cut-off frequency and longitudinal cut-off frequency for longitudinal waves (magnetoacoustic waves, or sausage waves in flux tubes) and transverse waves (e.g., Alfvén waves; or Alfvénic/kink waves in tubes) respectively depend upon local plasma conditions (e.g., density,

magnetic field and its inclination) and differ from the local acoustic cut-off frequency, and how do they further affect mode-coupling (McAteer et al., 2003)?

Even as we continuously make progress refining our understanding on (vi) and (vii), new imaging, spectral and spectropolarimetric observations challenge our models (e.g., Centeno et al., 2009; Heggland et al., 2011; Kayshap et al., 2020; Kayshap, Murawski, Srivastava, Musielak, & Dwivedi, 2018). Further physical insight is yet required to broaden the entire scientific context of mass and energy supply in the solar atmosphere, which again poses a question:

(viii) Are omnipresent jets/plasma flows in the solar chromosphere responsible for plasma heating in addition to waves? How do these contribute to the fast component of the solar wind at higher altitudes?

Despite significant observational and theoretical developments over two decades on magnetic waves, shocks, instabilities, and formation of the jets/flows, their respective roles or inter-relationships in a variety of chromospheric magnetic structures are not yet fully understood (e.g., Brady & Arber, 2016; De Pontieu et al., 2004; Iijima & Yokoyama, 2015; Kayshap, Murawski, Srivastava, & Dwivedi, 2018; Kudoh & Shibata, 1999; Kuźma et al., 2017; Mishra & Srivastava, 2019; Nishizuka et al., 2011; Shibata et al., 2007; Srivastava et al., 2013; Wang & Yokoyama, 2020; Wójcik et al., 2019; Zaqarashvili, 2020; Zhelyazkov et al., 2015).

(ix) The question of how the solar chromosphere is heated remains open. Do compressible (magnetoacoustic) waves make a significant contribution in this process in the large-scale chromosphere? Is the amount of thermal energy released during ion-neutral-electron collisions sufficient to balance the radiative losses?

(x) How does the thermal energy released by wave dissipation and plasma instabilities compare with thermal energy associated with the reconnection of magnetic field lines on various scales?

Answers to these outstanding questions will only come through simultaneous high spatial resolution observations over multiple heights. Specific tasks are to estimate the thickness of resonant layers (e.g., following on from Jess et al., 2020); resolve magnetic surfaces (iso-frequency surfaces) in pure torsional motions; determine characteristic length scales in instabilities; etc (e.g., see some science cases planned with DKIST; Rast et al., 2021). Moreover, spectral or spectro-polarimetric observations of the localized chromosphere should be made in such a manner that we detect the ultra-high cadence (temporal) variations revealing the high-frequency part of the (magneto-) acoustic and Alfvénic wave modes as they evolve in particular magnetic structures (e.g., see some science cases planned with DKIST; Rast et al., 2021). Moreover, there should be an appropriate estimation of the various cut-off frequencies with respect to the local acoustic cut-off frequency throughout the chromosphere, which sensitively depends upon the accurate estimation of density and magnetic field there, and also requires the consideration of appropriate model atmospheres (e.g., Avrett & Loeser, 2008). Moreover, the most sensitive measurements of chromospheric magnetic fields should be utilized in re-constructing localized magnetic tubes along which these waves may channel their energy (e.g., Lagg et al., 2017).

These sophisticated measurements of plasma properties, and magnetic fields will lead to convincing observations of various physical properties of MHD waves, shocks, and instabilities (see Sections 2-4) in the localized chromosphere along with dynamical plasma processes (e.g., waves and flows) to determine their role in its heating and mass transport. The upcoming/existing ultra-high resolution observatories (e.g., 1m SST, 4m DKIST, 4m EST, 2m NLST, GREGOR, etc) from the ground, and space (e.g., IRIS, ADITYA-L1/SUIT), which are equipped with cutting-edge spectrographs/spectro-polarimeters, magnetograms, imagers, etc., will be able to fill important gaps in our observations. They will provide appropriate measurements and detection of dynamical processes in the solar chromosphere (e.g., waves, shocks, and instabilities), which will further refine our theoretical understanding/numerical modeling to answer many unresolved questions related to this highly dynamic layer of the solar atmosphere.

### **Data Availability Statement**

In this review study, the data were not used, nor created for this research.

**Acknowledgments**

The authors thank both the reviewers for their comments that improved our manuscript. JLB acknowledges support from MINECO and FEDER funds through project AYA2017-85465-P. JLB acknowledges discussions within the team on “The eruption of solar filaments and the associated mass and energy transport,” led by JC Vial and PF Chen, and thanks ISSI for their support. The work of TVZ was funded by the Austrian Science Fund (FWF, project P30695-N27). DBJ wishes to thank Invest NI and Randox Laboratories Ltd for the award of a Research & Development Grant (059RDEN-1), in addition to the UK Science and Technology Facilities Council (STFC) for the award of a Consolidated Grant (ST/T00021X/1). DBJ also wishes to acknowledge scientific discussions with the Waves in the Lower Solar Atmosphere (WaLSA; <https://www.WaLSA.team>) team, which is supported by the Research Council of Norway and the Royal Society (Hooke18b/SCTM). This research was supported by the Research Council of Norway through its Centers of Excellence scheme, project number 262622, and through grants of computing time from the Program for Supercomputing. KM’s work was done within the framework of the projects from the Polish Science Center (NCN) Grant Nos. 2017/25/B/ST9/00,506 and 2020/37/B/ST9/00,184. AKS and MM acknowledge support from the UK-India Education and Research Initiative under grant agreement UGC-UKIERI-2017/18-014-A2.

**References**

Abbasvand, V., Sobotka, M., Heinzel, P., Švanda, M., Jurčák, J., del Moro, D., & Berrilli, F. (2020). Chromospheric heating by acoustic waves compared to radiative cooling. II. Revised grid of models. *The Astrophysical Journal*, 890(1), 22. <https://doi.org/10.3847/1538-4357/ab665f>

Abbasvand, V., Sobotka, M., Švanda, M., Heinzel, P., García-Rivas, M., Denker, C., et al. (2020). Observational study of chromospheric heating by acoustic waves. *Astronomy & Astrophysics*, 642, A52. <https://doi.org/10.1051/0004-6361/202038559>

Afanasyev, A. N., & Nakariakov, V. M. (2015). Cut-off period for slow magnetoacoustic waves in coronal plasma structures. *Astronomy & Astrophysics*, 582, A57. <https://doi.org/10.1051/0004-6361/201526530>

Al Shidi, Q., Cohen, O., Song, P., & Tu, J. (2019). Time-dependent two-fluid magnetohydrodynamic model and simulation of the chromosphere. *Solar Physics*, 294(9), 124. <https://doi.org/10.1007/s11207-019-1513-8>

Alfvén, H. (1942). Existence of electromagnetic-hydrodynamic waves. *Nature*, 150(3805), 405–406. <https://doi.org/10.1038/150405d0>

Alfvén, H., Lindblad, P. (1947). Granulation, magneto-hydrodynamic waves, and the heating of the solar corona. *Monthly Notices of the Royal Astronomical Society*, 107, 211, 219. <https://doi.org/10.1093/mnras/107.2.211>

Antiochos, S. K., MacNeice, P. J., Spicer, D. S., & Klimchuk, J. A. (1999). The dynamic formation of prominence condensations. *The Astrophysical Journal*, 512(2), 985–991. <https://doi.org/10.1086/306804>

Antolin, P. (2020). Thermal instability and non-equilibrium in solar coronal loops: from coronal rain to long-period intensity pulsations. *Plasma Physics and Controlled Fusion*, 62(014016). <https://doi.org/10.1088/0004-637X/799/1/7910.1088/1361-6587/ab5406>

Antolin, P., Schmit, D., Pereira, T. M. D., De Pontieu, B., & De Moortel, I. (2018). Transverse wave induced kelvin-helmholtz rolls in spicules. *The Astrophysical Journal*, 856(1), 44. <https://doi.org/10.3847/1538-4357/aab34f>

Anzer, U., & Heinzel, P. (1999). The energy balance in solar prominences. *Astronomy and Astrophysics*, 349, 974–984.

Arber, T. D., Brady, C. S., & Shelyag, S. (2016). Alfvén wave heating of the solar chromosphere: 1.5d models. *The Astrophysical Journal*, 817(2), 94. <https://doi.org/10.3847/0004-637X/817/2/94>

Arregui, I. (2015). Wave heating of the solar atmosphere. *Philosophical Transactions of the Royal Society A: Mathematical, Physical and Engineering Sciences*, 373(2042), 20140261. <https://doi.org/10.1098/rsta.2014.0261>

Arregui, I., Oliver, R., & Ballester, J. L. (2018). Prominence oscillations. *Living Reviews in Solar Physics*, 15(1), 3. <https://doi.org/10.1007/s41116-018-0012-6>

Aschwanden, M. J. (2004). *Physics of the solar corona: An introduction with problems and solutions*. Springer Science & Business Media.

Aschwanden, M. J. (2019). *New Millennium Solar Physics*. Springer International Publishing. <https://doi.org/10.1007/978-3-030-13956-8>

Aschwanden, M. J., Nakariakov, V. M., & Melnikov, V. F. (2004). Magnetohydrodynamic Sausage-mode oscillations in coronal loops. *The Astrophysical Journal*, 600(1), 458–463. <https://doi.org/10.1086/379789>

Asgari-Targhi, M., & van Ballegooijen, A. A. (2012). Model for Alfvén wave turbulence in solar coronal loops: Heating rate profiles and temperature fluctuations. *The Astrophysical Journal*, 746(1), 81. <https://doi.org/10.1088/0004-637X/746/1/81>

Avrett, E. H. (1981). Energy balance in solar and stellar chromospheres. In R. M. Bonnet & A. K. Dupree (Eds.), *Solar phenomena in stars and stellar systems* (Vol. 68, p. 173–198). [https://doi.org/10.1007/978-94-009-8479-0\\_9](https://doi.org/10.1007/978-94-009-8479-0_9)

Avrett, E. H., & Loeser, R. (2008). Models of the solar chromosphere and transition region from SUMER and HRTS observations: Formation of the extreme-ultraviolet spectrum of hydrogen, carbon, and oxygen. *The Astrophysical Journal: Supplement Series*, 175(1), 229–276. <https://doi.org/10.1086/523671>

Bakhareva, N. M., Zaitsev, V. V., & Khodachenko, M. L. (1992). Dynamic regimes of prominence evolution. *Solar Physics*, 139(2), 299–314. <https://doi.org/10.1007/BF00159156>

Ballai, I., Forgács-Dajka, E., & Marcu, A. (2019). Dispersive shock waves in partially ionized plasmas. *Advances in Space Research*, 63(4), 1472–1482. <https://doi.org/10.1016/j.asr.2018.10.024>

Ballai, I., Oliver, R., & Alexandrou, M. (2015). Dissipative instability in partially ionized prominence plasmas. *Astronomy & Astrophysics*, 577, A82. <https://doi.org/10.1051/0004-6361/201423973>

Ballester, J. L. (2015). Magnetism and dynamics of prominences: MHD waves. In J.-C. Vial & O. Engvold (Eds.), *Solar prominences* (415, pp. 259–296). [https://doi.org/10.1007/978-3-319-10416-4\\_1110.1007/978-3-319-10416-4\\_11](https://doi.org/10.1007/978-3-319-10416-4_1110.1007/978-3-319-10416-4_11)

Ballester, J. L., Alexeev, I., Collados, M., Downes, T., Pfaff, R. F., Gilbert, H., et al. (2018). Partially ionized plasmas in astrophysics. *Space Science Reviews*, 214(2), 58. <https://doi.org/10.1007/s11214-018-0485-6>

Ballester, J. L., Soler, R., Terradas, J., & Carbonell, M. (2020). Nonlinear coupling of Alfvén and slow magnetoacoustic waves in partially ionized solar plasmas. *Astronomy & Astrophysics*, 641, A48. <https://doi.org/10.1051/0004-6361/202038220>

Balmforth, N. J. (1992). Solar pulsational stability—III. Acoustical excitation by turbulent convection. *Monthly Notices of the Royal Astronomical Society*, 255, 639, 649. <https://doi.org/10.1093/mnras/255.4.639>

Barbulescu, M., & Erdélyi, R. (2016). Propagation of long-wavelength nonlinear slow sausage waves in stratified magnetic flux tubes. *Solar Physics*, 291(5), 1369–1384. <https://doi.org/10.1007/s11207-016-0906-1>

Barceló, S., Carbonell, M., & Ballester, J. L. (2011). Time damping of non-adiabatic magnetohydrodynamic waves in a partially ionized prominence medium: Effect of a background flow. *Astronomy & Astrophysics*, 525, A60. <https://doi.org/10.1051/0004-6361/201015499>

Beck, C., Khotenko, E., Rezaei, R., & Collados, M. (2009). The energy of waves in the photosphere and lower chromosphere. *Astronomy & Astrophysics*, 507(1), 453–467. <https://doi.org/10.1051/0004-6361/200911851>

Beck, C., Rezaei, R., & Puschmann, K. G. (2013). The energy of waves in the photosphere and lower chromosphere. *Astronomy & Astrophysics*, 553, A73. <https://doi.org/10.1051/0004-6361/201220463>

Bel, N., & Leroy, B. (1977). Analytical study of magnetoacoustic gravity waves. *Astronomy and Astrophysics*, 55, 239.

Bello González, N., Flores Soriano, M., Kneer, F., & Okunev, O. (2009). Acoustic waves in the solar atmosphere at high spatial resolution. *Astronomy & Astrophysics*, 508(2), 941–950. <https://doi.org/10.1051/0004-6361/200912275>

Bello González, N., Franz, M., Martínez Pillet, V., Bonet, J. A., Solanki, S. K., del Toro Iniesta, J. C., et al. (2010). Detection of large acoustic energy flux in the solar atmosphere. *The Astrophysical Journal Letters*, 723(2), L134–L138. <https://doi.org/10.1088/2041-8205/723/2/L134>

Berger, T., Hillier, A., & Liu, W. (2017). Quiescent prominence dynamics observed with the hinosolar optical telescope. II. Prominence bubble boundary layer characteristics and the onset of a coupled Kelvin-Helmholtz Rayleigh-Taylor instability. *The Astrophysical Journal Letters*, 850(1), 60. <https://doi.org/10.3847/1538-4357/aa95b6>

Berger, T. E., Shine, R. A., Slater, G. L., Tarbell, T. D., Title, A. M., Okamoto, T. J., et al. (2008). Hinode SOT observations of solar quiescent prominence dynamics. *The Astrophysical Journal Letters*, 676(1), L89, L92. <https://doi.org/10.1086/587171>

- Berger, T. E., Slater, G., Hurlburt, N., Shine, R., Tarbell, T., Title, A., et al. (2010). Quiescent prominence dynamics observed with the Hinode solar optical telescope. I. Turbulent upflow plumes. *The Astrophysical Journal*, 716(2), 1288–1307. <https://doi.org/10.1088/0004-637X/716/2/1288>
- Bogdan, T. J., Hansteen, M. C. V., McMurry, A., Rosenthal, C. S., Johnson, M., Petty-Powell, S., et al. (2003). Waves in the magnetized solar atmosphere. II. Waves from localized sources in magnetic flux concentrations. *The Astrophysical Journal*, 599(1), 626–660. <https://doi.org/10.1086/378512>
- Bogdan, T. J., & Judge, P. G. (2006). Observational aspects of sunspot oscillations. *Philosophical Transactions of the Royal Society A: Mathematical, Physical and Engineering Sciences*, 364(1839), 313–331. <https://doi.org/10.1098/rsta.2005.1701>
- Bonet, J. A., Márquez, I., Sánchez Almeida, J., Cabello, I., & Domingo, V. (2008). Convectively driven vortex flows in the Sun. *The Astrophysical Journal Letters*, 687(2), L131, L134. <https://doi.org/10.1086/593329>
- Bose, S., Henriques, V. M. J., Joshi, J., & Rouppe van der Voort, L. (2019). Characterization and formation of on-disk spicules in the Ca II K and Mg II k spectral lines. *Astronomy & Astrophysics*, 631, L5. <https://doi.org/10.1051/0004-6361/201936617>
- Botha, G. J. J., Arber, T. D., Nakariakov, V. M., & Zhugzhda, Y. D. (2011). Chromospheric resonances above sunspot umbrae. *The Astrophysical Journal*, 728(2), 84. <https://doi.org/10.1088/0004-637X/728/2/84>
- Brady, C. S., & Arber, T. D. (2016). Simulations of Alfvén and Kink wave driving of the solar chromosphere: Efficient heating and spicule launching. *The Astrophysical Journal*, 829(2), 80. <https://doi.org/10.3847/0004-637X/829/2/80>
- Braginskii, S. I. (1965). *Transport processes in a plasma*. Reviews in plasma physics (p. 205).
- Braun, D. C., Labonte, B. J. T. L., & Duvall, T. L. J. (1987). Acoustic absorption by sunspots. *The Astrophysical Journal Letters*, 319, L27. <https://doi.org/10.1086/184949>
- Browning, P. K., & Priest, E. R. (1984). Kelvin-Helmholtz instability of a phased-mixed Alfvén wave. *Astronomy and Astrophysics*, 131(2), 283–290.
- Biermann, L. (1946). Zur Deutung der chromosphärischen turbulenz und des exzesses der UV-strahlung der sonne. *Naturwissenschaften*, 33(4), 118–119. <https://doi.org/10.1007/BF00738265>
- Cally, P. S. (2006). Dispersion relations, rays and ray splitting in magnetohelioseismology. *Philosophical Transactions of the Royal Society A: Mathematical, Physical and Engineering Sciences*, 364(1839), 333–349. <https://doi.org/10.1098/rsta.2005.1702>
- Cally, P. S. (2009). Phase jumps in local helioseismology. *Solar Physics*, 254(2), 241–257. <https://doi.org/10.1007/s11207-008-9290-9>
- Cally, P. S., & Goossens, M. (2008). Three-Dimensional MHD wave propagation and conversion to Alfvén waves near the solar surface. I. Direct numerical solution. *Solar Physics*, 251(1–2), 251–265. <https://doi.org/10.1007/s11207-007-9086-3>
- Cally, P. S., & Hansen, S. C. (2011). Benchmarking Fast-to-alfvén mode conversion in a cold magnetohydrodynamic plasma. *The Astrophysical Journal*, 738(2), 119. <https://doi.org/10.1088/0004-637X/738/2/119>
- Cally, P. S., & Khomenko, E. (2015). Fast-to-alfvén mode conversion mediated by the hall current. I. Cold plasma model. *The Astrophysical Journal*, 814(2), 106. <https://doi.org/10.1088/0004-637X/814/2/106>
- Cally, P. S., & Khomenko, E. (2019). Fast-to-Alfvén mode conversion and ambipolar heating in structured media. I. Simplified cold plasma model. *The Astrophysical Journal*, 885(1), 58. <https://doi.org/10.3847/1538-4357/ab3bce>
- Cally, P. S., & Moradi, H. (2013). Seismology of the wounded Sun. *Monthly Notices of the Royal Astronomical Society*, 435(3), 2589–2597. <https://doi.org/10.1093/mnras/stt1473>
- Campbell, W. R., & Roberts, B. (1989). The influence of a chromospheric magnetic field on the solar p- and f-modes. *The Astrophysical Journal*, 338, 538. <https://doi.org/10.1086/167216>
- Carbonell, M., Forteza, P., Oliver, R., & Ballester, J. L. (2010). The spatial damping of magnetohydrodynamic waves in a flowing partially ionised prominence plasma. *Astronomy & Astrophysics*, 515, A80. <https://doi.org/10.1051/0004-6361/200913024>
- Cargill, P. J., & Klimchuk, J. A. (2004). Nanoflare heating of the corona revisited. *The Astrophysical Journal*, 605(2), 911–920. <https://doi.org/10.1086/382526>
- Carlsson, M., Hansteen, V. H., de Pontieu, B., McIntosh, S., Tarbell, T. D., Shine, D., et al. (2007). Can high frequency acoustic waves heat the quiet sun chromosphere? *Pacific Astronomical Society of Japan*, 59, S663, S668. <https://doi.org/10.1093/pasj/59.sp3.S663>
- Carlsson, M., & Stein, R. F. (1995). Does a nonmagnetic solar chromosphere exist? *The Astrophysical Journal Letters*, 440, L29. <https://doi.org/10.1086/187753>
- Carlsson, M., & Stein, R. F. (1997). Formation of solar calcium H and K bright grains. *The Astrophysical Journal*, 481(1), 500–514. <https://doi.org/10.1086/304043>
- Carlsson, M., & Stein, R. F. (1998). The new chromosphere. In F.-L. Deubner, J. Christensen-Dalsgaard, & D. Kurtz (Eds.), *New eyes to see inside the sun and stars* (Vol. 185, p. 435, 446). [https://doi.org/10.1007/978-94-011-4982-2\\_96](https://doi.org/10.1007/978-94-011-4982-2_96)
- Centeno, R., Collados, M., & Bueno, J. T. (2009). Wave propagation and shock formation in different magnetic structures. *The Astrophysical Journal*, 692(2), 1211–1220. <https://doi.org/10.1088/0004-637X/692/2/1211>
- Chandrasekhar, S. (1961). *Hydrodynamic and hydromagnetic stability*. Courier Corporation.
- Chen, S.-X., Li, B., Shi, M., & Yu, H. (2018). Damping of slow surface sausage modes in photospheric waveguides. *The Astrophysical Journal*, 868(1), 5. <https://doi.org/10.3847/1538-4357/aae68610.3847/1538-4357/aae686>
- Chen, S.-X., Li, B., Xiong, M., Yu, H., & Guo, M.-Z. (2016). Fast sausage modes in magnetic tubes with continuous transverse profiles: Effects of a finite plasma beta. *The Astrophysical Journal*, 833(1), 114. <https://doi.org/10.3847/1538-4357/833/1/114>
- Chitta, L. P., van Ballegooijen, A. A., Rouppe van der Voort, L., DeLuca, E. E., & Kariyappa, R. (2012). Dynamics of the solar magnetic bright points derived from their horizontal motions. *The Astrophysical Journal*, 752(1), 48. <https://doi.org/10.1088/0004-637X/752/1/48>
- Cho, K., & Chae, J. (2020). Source depth of three-minute umbral oscillations. *The Astrophysical Journal Letters*, 892(2), L31. <https://doi.org/10.3847/2041-8213/ab8295>
- Choudhuri, A. R. (1998). *The physics of fluids and plasmas: An introduction for astrophysicists*. Cambridge University Press. <https://doi.org/10.1017/cbo9781139171069>
- Christensen-Dalsgaard, J. (2002). Helioseismology. *Reviews of Modern Physics*, 74(4), 1073–1129. <https://doi.org/10.1103/RevModPhys.74.1073>
- Cohen, R. H., & Kulsrud, R. M. (1974). Nonlinear evolution of parallel-propagating hydromagnetic waves. *Physics of Fluids*, 17, 2215–2225. <https://doi.org/10.1063/1.1694695>
- Cranmer, S. R., & van Ballegooijen, A. A. (2005). On the generation, propagation, and reflection of Alfvén waves from the solar photosphere to the distant heliosphere. *The Astrophysical Journal Supplement Series*, 156(2), 265–293. <https://doi.org/10.1086/426507>
- Crouch, A. D., & Cally, P. S. (2005). Mode conversion of solar p-modes in non-vertical magnetic fields. *Solar Physics*, 227(1), 1–26. <https://doi.org/10.1007/s11207-005-8188-z>



- Cuntz, M., Rammacher, W., & Musielak, Z. E. (2007). Acoustic heating of the solar chromosphere: Present indeed and locally dominant. *The Astrophysical Journal Letters*, 657(1), L57–L60. <https://doi.org/10.1086/512973>
- Davila, J. M. (1987). Heating of the solar corona by the resonant absorption of Alfvén waves. *The Astrophysical Journal*, 317, 514. <https://doi.org/10.1086/165295>
- De Pontieu, B., Carlsson, M., Rouppe van der Voort, L. H. M., Rutten, R. J., Hansteen, V. H., & Watanabe, H. (2012). Ubiquitous torsional motions in type II spicules. *The Astrophysical Journal Letters*, 752(1), L12. <https://doi.org/10.1088/2041-8205/752/1/L12>
- De Pontieu, B., Erdélyi, R., & James, S. P. (2004). *Solar chromospheric spicules from the leakage of photospheric oscillations and flows*. 430(6999), 536–539. <https://doi.org/10.1038/nature02749>
- De Pontieu, B., Martens, P. C. H., & Hudson, H. S. (2001). Chromospheric damping of Alfvén waves. *The Astrophysical Journal*, 558(2), 859–871. <https://doi.org/10.1086/322408>
- De Pontieu, B., McIntosh, S. W., Carlsson, M., Hansteen, V. H., Tarbell, T. D., Schrijver, C. J., et al. (2007). Chromospheric Alfvénic waves strong enough to power the solar wind. *Science*, 318(5856), 1574–1577. <https://doi.org/10.1126/science.1151747>
- De Pontieu, B., Rouppe van der Voort, L., McIntosh, S. W., Pereira, T. M. D., Carlsson, M., Hansteen, V., et al. (2014). On the prevalence of small-scale twist in the solar chromosphere and transition region. *Science*, 346(6207), 1255732. <https://doi.org/10.1126/science.1255732>
- De Pontieu, B., Title, A. M., Lemen, J. R., Kushner, G. D., Akin, D. J., Allard, B., et al. (2014). The interface region imaging spectrograph (IRIS). *Solar Physics*, 289(7), 2733–2779. <https://doi.org/10.1007/s11207-014-0485-y>
- Del Zanna, L. (2001). Parametric decay of oblique arc-polarized Alfvén waves. *Geophysical Research Letters*, 28(13), 2585–2588. <https://doi.org/10.1029/2001GL012911>
- Deubner, F.-L., & Gough, D. (1984). Helioseismology: Oscillations as a diagnostic of the solar interior. *Annual Review in Astronomy and Astrophysics*, 22, 593–619. <https://doi.org/10.1146/annurev.aa.22.090184.003113>
- Deubner, F. L., Waldschik, T., & Steffens, S. (1996). Dynamics of the solar atmosphere. VI. Resonant oscillations of an atmospheric cavity: Observations. *Annual Review in Astronomy and Astrophysics*, 307, 936–946.
- Díaz, A. J., Soler, R., & Ballester, J. L. (2012). Rayleigh-taylor instability in partially ionized compressible plasmas. *The Astrophysical Journal*, 754(1), 41. <https://doi.org/10.1088/0004-637X/754/1/41>
- Díaz-Suárez, S., & Soler, R. (2021). Transition to turbulence in nonuniform coronal loops driven by torsional Alfvén waves. *Astronomy & Astrophysics*, 648, A22.
- Dinesh Singh, H., & Singh Jatav, B. (2019). Anisotropic turbulence of kinetic Alfvén waves and heating in solar corona. *Research in Astronomy and Astrophysics*, 19(12), 185. <https://doi.org/10.1088/1674-4527/19/12/185>
- Dorotovič, I., Erdélyi, R., Freij, N., Karlovský, V., & Márquez, I. (2014). Standing sausage waves in photospheric magnetic waveguides. *Astronomy and Astrophysics*, 563, A12. <https://doi.org/10.1051/0004-6361/201220542>
- Dorotovič, I., Erdélyi, R., & Karlovský, V. (2008). Identification of linear slow sausage waves in magnetic pores. In R. Erdélyi & C. A. Mendoza-Briceno (Eds.), *Waves & oscillations in the solar atmosphere: Heating and magneto-seismology* (Vol. 247, p. 351–354). <https://doi.org/10.1017/S174392130801507X>
- Draine, B. T., & McKee, C. F. (1993). Theory of interstellar shocks. *Annual Reviews in Astronomy and Astrophysics*, 31, 373–432. <https://doi.org/10.1146/annurev.aa.31.090193.002105>
- Ebadí, H., Hosseinpour, M., & Altafi-Mehrabani, H. (2012). Phase mixing of propagating Alfvén waves in a stratified atmosphere: Solar spicules. *Astrophysics and Space Sciences*, 340(1), 9–15. <https://doi.org/10.1007/s10509-012-1036-3>
- Edwin, P. M., & Roberts, B. (1983). Wave propagation in a magnetic cylinder. *Solar Physics*, 88(1–2), 179–191. <https://doi.org/10.1007/BF00196186>
- Erdélyi, R. (2006). Magnetic coupling of waves and oscillations in the lower solar atmosphere: Can the tail wag the dog? *Astrophysics and Space Sciences*, 364(1839), 351–381. <https://doi.org/10.1098/rsta.2005.1703>
- Erdélyi, R., & Fedun, V. (2006). Solitary wave propagation in solar flux tubes. *Physics of Plasmas*, 13(3), 032902. <https://doi.org/10.1063/1.2176599>
- Erdélyi, R., & Fedun, V. (2007). Are there Alfvén waves in the solar atmosphere? *Science*, 318(5856), 1572, 1574. <https://doi.org/10.1126/science.1153006>
- Erdélyi, R., & Goossens, M. (2011). Magnetohydrodynamic waves and seismology of the solar atmosphere. *Space Science Reviews*, 158(2–4), 167–168. <https://doi.org/10.1007/s11214-011-9800-1>
- Espagnet, O., Müller, R., Roudier, T., & Mein, N. (1993). Turbulent power spectra of solar granulation. *Astronomy and Astrophysics*, 271, 589–600.
- Evans, D. J., & Roberts, B. (1991). The sensitivity of chromospherically induced p- and f-mode frequency shifts to the height of the magnetic canopy. *The Astrophysical Journal*, 371, 387. <https://doi.org/10.1086/169899>
- Fedun, V., Shelyag, S., & Erdélyi, R. (2011). Numerical modeling of footpoint-driven magneto-acoustic wave propagation in a localized solar flux tube. *The Astrophysical Journal*, 727(1), 17. <https://doi.org/10.1088/0004-637X/727/1/17>
- Fedun, V., Verth, G., Jess, D. B., & Erdélyi, R. (2011). Frequency filtering of torsional Alfvén waves by chromospheric magnetic field. *The Astrophysical Journal Letters*, 740(2), L46. <https://doi.org/10.1088/2041-8205/740/2/L46>
- Felipe, T. (2012). Three-dimensional numerical simulations of fast-to-Alfvén conversion in sunspots. *The Astrophysical Journal*, 758(2), 96. <https://doi.org/10.1088/0004-637X/758/2/96>
- Felipe, T., Khomeenko, E., & Collados, M. (2010). Magneto-acoustic waves in sunspots: First results from a new three-dimensional nonlinear magnetohydrodynamic code. *The Astrophysical Journal*, 719(1), 357–377. <https://doi.org/10.1088/0004-637X/719/1/357>
- Felipe, T., Kuckein, C., & Thaler, I. (2018). Height variation of the cutoff frequency in a sunspot umbra. *Astronomy and Astrophysics*, 617, A39. <https://doi.org/10.1051/0004-6361/201833155>
- Ferraro, V. C. A. (1955). Hydromagnetic waves in a rare ionized gas and galactic magnetic fields. *Proceedings of Royal Society London A*, 233(1194), 310–318. <https://doi.org/10.1098/rspa.1955.0267>
- Fleck, B., & Schmitz, F. (1991). The 3-min oscillations of the solar chromosphere—A basic physical effect? *Astronomy and Astrophysics*, 250(1), 235–244.
- Fontenla, J. M., Peterson, W. K., & Harder, J. (2008). Chromospheric heating by the Farley-Buneman instability. *Astronomy and Astrophysics*, 480(3), 839–846. <https://doi.org/10.1051/0004-6361:20078517>
- Forteza, P., Oliver, R., & Ballester, J. L. (2008). Time damping of non-adiabatic MHD waves in an unbounded partially ionized prominence plasma. *Astronomy and Astrophysics*, 492, 223–231. <https://doi.org/10.1051/0004-6361:200810370>
- Forteza, P., Oliver, R., Ballester, J. L., & Khodachenko, M. L. (2007). Damping of oscillations by ion-neutral collisions in a prominence plasma. *Astronomy and Astrophysics*, 461(2), 731–739. <https://doi.org/10.1051/0004-6361:20065900>

- Fossum, A., & Carlsson, M. (2005). High-frequency acoustic waves are not sufficient to heat the solar chromosphere. *Nature*, 435(7044), 919–921. <https://doi.org/10.1038/nature03695>
- Fossum, A., & Carlsson, M. (2006). Determination of the acoustic wave flux in the lower solar chromosphere. *The Astrophysical Journal*, 646(1), 579–592. <https://doi.org/10.1086/504887>
- Freij, N., Dorotovič, I., Morton, R. J., Ruderman, M. S., Karlovský, V., & Erdélyi, R. (2016). On the properties of slow MHD sausage waves within small-scale photospheric magnetic structures. *The Astrophysical Journal*, 817(1), 44. <https://doi.org/10.3847/0004-637X/817/1/44>
- Fujimura, D., & Tsuneta, S. (2009). Properties of magnetohydrodynamic waves in the solar photosphere obtained within a node. *The Astrophysical Journal Letters*, 702(2), 1443–1457. <https://doi.org/10.1088/0004-637X/702/2/1443>
- Gafeira, R., Jafarzadeh, S., Solanki, S. K., Lagg, A., van Noort, M., Barthol, P., et al. (2017). Oscillations on width and intensity of slender Ca II H fibrils from sunrise/SuFI. *The Astrophysical Journal Supplement Series*, 229(1), 7. <https://doi.org/10.3847/1538-4365/229/1/7>
- Giagkiozis, I., Goossens, M., Verth, G., Fedun, V., & Doorselaere, T. V. (2016). Resonant absorption of axisymmetric modes in twisted magnetic flux tubes. *The Astrophysical Journal*, 823(2), 71. <https://doi.org/10.3847/0004-637X/823/2/71>
- Gilbert, H. (2015). Energy Balance. In J.-C. Vial, & O. Engvold (Eds.), *Solar prominences* (415, pp. 157–178). [https://doi.org/10.1007/978-3-319-10416-4\\_710.1007/978-3-319-10416-4\\_7](https://doi.org/10.1007/978-3-319-10416-4_710.1007/978-3-319-10416-4_7)
- Gilbert, H., Kilper, G., & Alexander, D. (2007). Observational evidence supporting cross-field diffusion of neutral material in solar filaments. *The Astrophysical Journal*, 671(1), 978–989. <https://doi.org/10.1086/522884>
- Gilbert, H. R., Hansteen, V. H., & Holzer, T. E. (2002). Neutral atom diffusion in a partially ionized prominence plasma. *The Astrophysical Journal*, 577, 464–474. <https://doi.org/10.1086/342165>
- Gilchrist-Millar, C. A., Jess, D. B., Grant, S. D. T., Keys, P. H., Beck, C., Jafarzadeh, S., et al. (2021). Magnetoacoustic wave energy dissipation in the atmosphere of solar pores. *Philosophical Transactions of the Royal Society of London Series A*, 379(2190), 20200172. <https://doi.org/10.1098/rsta.2020.0172>
- Gizon, L., & Birch, A. C. (2005). Local helioseismology. *Living Reviews in Solar Physics*, 2(1), 6. <https://doi.org/10.12942/lrsp-2005-6>
- Gogoberidze, G., Voitenko, Y., Poedts, S., & Goossens, M. (2009). Farley-Buneman instability in the solar chromosphere. *The Astrophysical Journal Letters*, 706(1), L12–L16. <https://doi.org/10.1088/0004-637X/706/1/L12>
- Goldreich, P., & Keeley, D. A. (1977). Solar seismology. II—The stochastic excitation of the solar p-modes by turbulent convection. *The Astrophysical Journal Letters*, 212, 243–251. <https://doi.org/10.1086/155043>
- González-Morales, P. A., Khomenko, E., & Cally, P. S. (2019). Fast-to-Alfvén mode conversion mediated by hall current. II. Application to the solar atmosphere. *The Astrophysical Journal*, 870(2), 94. <https://doi.org/10.3847/1538-4357/aaf1a9>
- González-Morales, P. A., Khomenko, E., Vitas, N., & Collados, M. (2020). Joint action of Hall and bipolar effects in 3D magneto-convection simulations of the quiet Sun. *Astronomy and Astrophysics*, 642, A220. <https://doi.org/10.1051/0004-6361/202037938>
- Goodman, M. L. (1996). Heating of the solar middle chromospheric network and internetwork by large-scale electric currents in weakly ionized magnetic elements. *The Astrophysical Journal*, 463, 784. <https://doi.org/10.1086/177290>
- Goodman, M. L. (2011). Conditions for photospherically driven Alfvénic oscillations to heat the solar chromosphere by Pedersen current dissipation. *The Astrophysical Journal*, 735(1), 45. <https://doi.org/10.1088/0004-637X/735/1/45>
- Goodman, M. L., & Kazeminezhad, F. (2010). Simulation of magnetohydrodynamic shock wave generation, propagation, and heating in the photosphere and chromosphere using a complete electrical conductivity tensor. *The Astrophysical Journal*, 708(1), 268–287. <https://doi.org/10.1088/0004-637X/708/1/268>
- Goossens, M., Andries, J., & Arregui, I. (2006). Damping of magnetohydrodynamic waves by resonant absorption in the solar atmosphere. *Philosophical Transaction of the Royal Society of Astronomy*, 364(1839), 433–446. <https://doi.org/10.1098/rsta.2005.1708>
- Goossens, M., Andries, J., & Aschwanden, M. J. (2002). Coronal loop oscillations. *Astronomy and Astrophysics*, 394, L39–L42. <https://doi.org/10.1051/0004-6361:20021378>
- Goossens, M., Andries, J., Soler, R., Van Doorselaere, T., Arregui, I., & Terradas, J. (2012). Surface Alfvén Waves in solar flux tubes. *The Astrophysical Journal*, 753(2), 111. <https://doi.org/10.1088/0004-637X/753/2/111>
- Goossens, M., Arregui, I., Soler, R., & Van Doorselaere, T. (2020). Resonant absorption: Transformation of compressive motions into vortical motions. *Astronomy and Astrophysics*, 641, A106. <https://doi.org/10.1051/0004-6361/202038394>
- Goossens, M., Chen, S.-X., Geeraerts, M., Li, B., & Van Doorselaere, T. (2021). Mixed properties of magnetohydrodynamic waves undergoing resonant absorption in the cusp continuum. *Astronomy and Astrophysics*, 646, A86. <https://doi.org/10.1051/0004-6361/202039780>
- Goossens, M., Erdélyi, R., & Ruderman, M. S. (2011). Resonant MHD waves in the solar atmosphere. *Space Science Reviews*, 158(2–4), 289–338. <https://doi.org/10.1007/s11214-010-9702-7>
- Goossens, M., Hollweg, J. V., & Sakurai, T. (1992). Resonant behaviour of MHD waves on magnetic flux tubes. *Solar Physics*, 138(2), 233–255. <https://doi.org/10.1007/BF00151914>
- Goossens, M., Soler, R., Terradas, J., Van Doorselaere, T., & Verth, G. (2014). The transverse and rotational motions of magnetohydrodynamic kink waves in the solar atmosphere. *The Astrophysical Journal*, 788(1), 9. <https://doi.org/10.1088/0004-637X/788/1/9>
- Goossens, M., Terradas, J., Andries, J., Arregui, I., & Ballester, J. L. (2009). On the nature of kink MHD waves in magnetic flux tubes. *Astronomy and Astrophysics*, 503(1), 213–223. <https://doi.org/10.1051/0004-6361/200912399>
- Goossens, M., Van Doorselaere, T., Soler, R., & Verth, G. (2013a). Energy content and propagation in transverse solar atmospheric waves. *The Astrophysical Journal*, 768(2), 191. <https://doi.org/10.1088/0004-637X/768/2/191>
- Goossens, M., Van Doorselaere, T., Soler, R., & Verth, G. (2013b). ERRATUM: "Energy content and propagation in transverse solar atmospheric waves" (2013, ApJ, 768, 191). *The Astrophysical Journal*, 771(1), 74. <https://doi.org/10.1088/0004-637X/771/1/74>
- Goossens, M. L., Arregui, I., & Van Doorselaere, T. (2019). Mixed properties of MHD waves in non-uniform plasmas. *Frontiers in Astronomy and Space Sciences*, 6, 20. <https://doi.org/10.3389/fspas.2019.00020>
- Grant, S. D. T., Jess, D. B., Moreels, M. G., Morton, R. J., Christian, D. J., Giagkiozis, I., et al. (2015). Wave damping observed in upwardly propagating sausage-mode oscillations contained within a magnetic pore. *The Astrophysical Journal*, 806(1), 132. <https://doi.org/10.1088/0004-637X/806/1/132>
- Grant, S. D. T., Jess, D. B., Zaqarashvili, T. V., Beck, C., Socas-Navarro, H., Aschwanden, M. J., et al. (2018). Alfvén wave dissipation in the solar chromosphere. *Nature Physics*, 14(5), 480–483. <https://doi.org/10.1038/s41567-018-0058-3>
- Gruszecki, M., Nakariakov, V. M., & Van Doorselaere, T. (2012). Intensity variations associated with fast sausage modes. *Astronomy and Astrophysics*, 543, A12. <https://doi.org/10.1051/0004-6361/201118168>
- Guo, M., Van Doorselaere, T., Karampelas, K., Li, B., Antolin, P., & De Moortel, I. (2019). Heating effects from driven transverse and Alfvén waves in coronal loops. *The Astrophysical Journal*, 870(2), 55. <https://doi.org/10.3847/1538-4357/aaf1d0>
- Haerendel, G. (1992). Weakly damped Alfvén waves as drivers of solar chromospheric spicules. *Nature*, 360(6401), 241–243. <https://doi.org/10.1038/360241a0>

- Hansen, S. C., & Cally, P. S. (2012). Benchmarking Fast-to-Alfvén mode conversion in a cold MHD plasma. II. How to get Alfvén waves through the solar transition region. *The Astrophysical Journal*, 751(1), 31. <https://doi.org/10.1088/0004-637X/751/1/31>
- Hansteen, V. H., Carlsson, M., & Gudiksen, B. (2007). 3D numerical models of the chromosphere, transition region, and corona. In P. Heinzel, I. Dorotovič, & R. J. Rutten (Eds.), *The physics of chromospheric plasmas* (Vol. 368, p. 107).
- Hasan, S. S., Kalkofen, W., van Ballegoijen, A. A., & Ulmschneider, P. (2003). Kink and longitudinal oscillations in the magnetic network on the sun: nonlinear effects and mode transformation. *The Astrophysical Journal*, 585(2), 1138–1146. <https://doi.org/10.1086/346102>
- Hasegawa, A., & Uberoi, C. (1982). *The Alfvén wave*. Bell Labs. <https://doi.org/10.2172/5259641>
- Heggland, L., Hansteen, V. H., De Pontieu, B., & Carlsson, M. (2011). Wave propagation and jet formation in the chromosphere. *The Astrophysical Journal*, 743(2), 142. <https://doi.org/10.1088/0004-637X/743/2/142>
- Heinzel, P. (2015). Radiative transfer in solar prominences. In J.-C. Vial, & O. Engvold (Eds.), *Solar prominences* (415, pp. 103–130). [https://doi.org/10.1007/978-3-319-10416-4\\_510.1007/978-3-319-10416-4\\_5](https://doi.org/10.1007/978-3-319-10416-4_510.1007/978-3-319-10416-4_5)
- Heinzel, P., & Anzer, U. (2012). Radiative equilibrium in solar prominences reconsidered. *Astronomy and Astrophysics*, 539, A49. <https://doi.org/10.1051/0004-6361/200913537>
- Heinzel, P., Anzer, U., & Gunár, S. (2010). Solar quiescent prominences. Filamentary structure and energetics. *Mem. Soc. Astr. It.*, 81, 654.
- Heyvaerts, J., & Priest, E. R. (1983). Coronal heating by phase-mixed shear Alfvén waves. *Astronomy and Astrophysics*, 117, 220–234.
- Hillier, A., Berger, T., Isobe, H., & Shibata, K. (2012). Numerical simulations of the magnetic Rayleigh-taylor instability in the Kippenhahn-Schlüter prominence model. I. Formation of upflows. *The Astrophysical Journal*, 746(2), 120. <https://doi.org/10.1088/0004-637X/746/2/120>
- Hillier, A., Isobe, H., Shibata, K., & Berger, T. (2011). Numerical simulations of the magnetic Rayleigh-taylor instability in the Kippenhahn-schlüter prominence model. *The Astrophysical Journal Letters*, 736(1), L1. <https://doi.org/10.1088/2041-8205/736/1/L1>
- Hillier, A., Morton, R. J., & Erdélyi, R. (2013). A statistical study of transverse oscillations in a quiescent prominence. *The Astrophysical Journal*, 779(2), L16. <https://doi.org/10.1088/2041-8205/779/2/L16>
- Hillier, A., & Polito, V. (2018). Observations of the Kelvin-Helmholtz instability driven by dynamic motions in a solar prominence. *The Astrophysical Journal Letters*, 864(1), L10. <https://doi.org/10.3847/2041-8213/aad9a5>
- Hillier, A., Takasao, S., & Nakamura, N. (2016). The formation and evolution of reconnection-driven, slow-mode shocks in a partially ionised plasma. *Astronomy and Astrophysics*, 591, A112. <https://doi.org/10.1051/0004-6361/201628215>
- Hollweg, J. V. (1984). Alfvénic resonant cavities in the solar atmosphere: Simple aspects. *Solar Physics*, 91(2), 269–288. <https://doi.org/10.1007/BF00146299>
- Hollweg, J. V., & Yang, G. (1988). Resonance absorption of compressible magnetohydrodynamic waves at thin “surfaces”. *Journal of Geophysical Research*, 93(A6), 5423–5436. <https://doi.org/10.1029/JA093iA06p05423>
- Howson, T. A., De Moortel, I., Antolin, P., Van Doorselaere, T., & Wright, A. N. (2019). Resonant absorption in expanding coronal magnetic flux tubes with uniform density. *Astronomy and Astrophysics*, 631, A105. <https://doi.org/10.1051/0004-6361/201936146>
- Iijima, H., & Yokoyama, T. (2015). Effect of coronal temperature on the scale of solar chromospheric jets. *The Astrophysical Journal Letters*, 812(2), L30. <https://doi.org/10.1088/2041-8205/812/2/L30>
- Innes, D. E., Cameron, R. H., Fletcher, L., Inhester, B., & Solanki, S. K. (2012). Break up of returning plasma after the 7 June 2011 filament eruption by Rayleigh-Taylor instabilities. *Astronomy and Astrophysics*, 540, L10. <https://doi.org/10.1051/0004-6361/201118530>
- Ionson, J. A. (1978). Resonant absorption of Alfvénic surface waves and the heating of solar coronal loops. *The Astrophysical Journal*, 226, 650–673. <https://doi.org/10.1086/156648>
- Jafarzadeh, S., Solanki, S. K., Gafeira, R., Noort, M. v., Barthol, P., Rodríguez, J. B., et al. (2017). Transverse oscillations in slender Ca II H fibrils observed with sunrise/SuFI. *The Astrophysical Journal Supplement Series*, 229(1), 9. <https://doi.org/10.3847/1538-4365/229/1/9>
- Jefferies, S. M., McIntosh, S. W., Armstrong, J. D., Bogdan, T. J., Cacciani, A., & Fleck, B. (2006). Magnetoacoustic portals and the basal heating of the solar chromosphere. *The Astrophysical Journal Letters*, 648(2), L151–L155. <https://doi.org/10.1086/508165>
- Jess, D. B., Doorselaere, T. V., Verth, G., Fedun, V., Prasad, S. K., Erdélyi, R., et al. (2017). An inside look at sunspot oscillations with higher azimuthal wavenumbers. *The Astrophysical Journal*, 842(1), 59. <https://doi.org/10.3847/1538-4357/aa73d6>
- Jess, D. B., Mathioudakis, M., Erdélyi, R., Crockett, P. J., Keenan, F. P., & Christian, D. J. (2009). Alfvén waves in the lower solar atmosphere. *Science*, 323(5921), 1582, 1585. <https://doi.org/10.1126/science.1168680>
- Jess, D. B., Morton, R. J., Verth, G., Fedun, V., Grant, S. D. T., & Giagkiozis, I. (2015). Multiwavelength studies of MHD waves in the solar chromosphere. An overview of recent results. *Space Science Reviews*, 190(1–4), 103–161. <https://doi.org/10.1007/s11214-015-0141-3>
- Jess, D. B., Pascoe, D. J., Christian, D. J., Mathioudakis, M., Keys, P. H., & Keenan, F. P. (2012). The origin of type I spicule oscillations. *The Astrophysical Journal Letters*, 744(1), L5. <https://doi.org/10.1088/2041-8205/744/1/L5>
- Jess, D. B., Snow, B., Houston, S. J., Botha, G. J. J., Fleck, B., Krishna Prasad, S., et al. (2020). A chromospheric resonance cavity in a sunspot mapped with seismology. *Nature Astronomy*, 4, 220–227. <https://doi.org/10.1038/s41550-019-0945-2>
- Jess, D. B., & Verth, G. (2016). Ultra-high-resolution observations of MHD waves in photospheric magnetic structures. *Geophysics Monograph Series*, 216, 449–465. <https://doi.org/10.1002/9781119055006.ch26>
- James, S. P., Erdélyi, R., & De Pontieu, B. (2003). Can ion-neutral damping help to form spicules? *Astronomy and Astrophysics*, 406, 715–724. <https://doi.org/10.1051/0004-6361:20030685>
- Kalkofen, W. (2008). Wave heating of the solar chromosphere. *Journal of Astrophysics and Astronomy*, 29(1–2), 163–166. <https://doi.org/10.1007/s12036-008-0020-3>
- Kang, J., Chae, J., Nakariakov, V. M., Cho, K., Kwak, H., & Lee, K. (2019). The Physical nature of spiral wave patterns in sunspots. *The Astrophysical Journal Letters*, 877(1), L9. <https://doi.org/10.3847/2041-8213/ab1f6c>
- Karpen, J. T., Olson, K., DeVore, C. R., Martinez Gomez, D., & Sokolov, I. (2015). The effects of partial ionization on prominence mass formation. In *Agu fall meeting abstracts*.
- Kayshap, P., Murawski, K., Srivastava, A. K., & Dwivedi, B. N. (2018). Rotating network jets in the quiet Sun as observed by IRIS. *Astronomy and Astrophysics*, 616, A99. <https://doi.org/10.1051/0004-6361/201730990>
- Kayshap, P., Murawski, K., Srivastava, A. K., Musielak, Z. E., & Dwivedi, B. N. (2018). Vertical propagation of acoustic waves in the solar internetwork as observed by IRIS. *Monthly Notices of Royal Astronomical Society*, 479(4), 5512–5521. <https://doi.org/10.1093/mnras/sty1861>
- Kayshap, P., Srivastava, A. K., Tiwari, S. K., Jelinek, P., & Mathioudakis, M. (2020). Propagation of waves above a plage as observed by IRIS and SDO. *Astronomy and Astrophysics*, 634, A63. <https://doi.org/10.1051/0004-6361/201936070>
- Keiling, A. (2009). Alfvén waves and their roles in the dynamics of the Earth’s magnetotail: A review. *Space Science Reviews*, 142(1–4), 73–156. <https://doi.org/10.1007/s11214-008-9463-8>



- Kudoh, T., & Shibata, K. (1999). Alfvén wave model of spicules and coronal heating. *The Astrophysical Journal*, 514(1), 493–505. <https://doi.org/10.1086/306930>
- Kuridze, D., Verth, G., Mathioudakis, M., Erdélyi, R., Jess, D. B., Morton, R. J., et al. (2013). Characteristics of transverse waves in chromospheric mottles. *The Astrophysical Journal*, 779(1), 82. <https://doi.org/10.1088/0004-637X/779/1/82>
- Keys, P. H., Morton, R. J., Jess, D. B., Verth, G., Grant, S. D. T., Mathioudakis, M., et al. (2018). Photospheric observations of surface and body modes in solar magnetic pores. *The Astrophysical Journal*, 857(1), 28. <https://doi.org/10.3847/1538-4357/aab432>
- Khodachenko, M. L., Rucker, H. O., Oliver, R., Arber, T. D., & Hanslmeier, A. (2006). On the mechanisms of MHD wave damping in the partially ionized solar plasmas. *Advances in Space Research*, 37, 447–455. <https://doi.org/10.1016/j.asr.2005.02.025>
- Khomenko, E., & Cally, P. S. (2012). Numerical simulations of conversion to Alfvén waves in sunspots. *The Astrophysical Journal*, 746(1), 68. <https://doi.org/10.1088/0004-637X/746/1/68>
- Khomenko, E., & Cally, P. S. (2019). Fast-to-Alfvén mode conversion and ambipolar heating in structured media. II. Numerical simulation. *The Astrophysical Journal*, 883(2), 179. <https://doi.org/10.3847/1538-4357/ab3d28>
- Khomenko, E., Centeno, R., Collados, M., & Trujillo Bueno, J. (2008). Channeling 5 minute photospheric oscillations into the solar outer atmosphere through small-scale vertical magnetic flux tubes. *The Astrophysical Journal Letters*, 676(1), L85–L88. <https://doi.org/10.1086/587057>
- Khomenko, E., & Collados, M. (2009). Sunspot seismic halos generated by fast MHD wave refraction. *Astronomy and Astrophysics*, 506(2), L5–L8. <https://doi.org/10.1051/0004-6361/200913030>
- Khomenko, E., & Collados, M. (2012). Heating of the magnetized solar chromosphere by partial ionization effects. *The Astrophysical Journal*, 747(2), 87. <https://doi.org/10.1088/0004-637X/747/2/87>
- Khomenko, E., & Collados, M. (2015). Oscillations and waves in sunspots. *Living Reviews in Solar Physics*, 12(1), 6. <https://doi.org/10.1007/lrsp-2015-6>
- Khomenko, E., Collados, M., Díaz, A., & Vitas, N. (2014). Fluid description of multi-component solar partially ionized plasma. *Physics of Plasmas*, 21(9), 092901. <https://doi.org/10.1063/1.4894106>
- Khomenko, E., Collados, M., & Felipe, T. (2008). Nonlinear numerical simulations of magneto-acoustic wave propagation in small-scale flux tubes. *Solar Physics*, 251(1–2), 589–611. <https://doi.org/10.1007/s11207-008-9133-8>
- Khomenko, E., Díaz, A., de Vicente, A., Collados, M., & Luna, M. (2014). Rayleigh-Taylor instability in prominences from numerical simulations including partial ionization effects. *Astronomy and Astrophysics*, 565, A45. <https://doi.org/10.1051/0004-6361/201322918>
- Khomenko, E., & Santamaria, I. C. (2013). Magnetohydrodynamic waves driven by modes. In *Journal of Physics Conference Series* (Vol. 440, p. 012048). <https://doi.org/10.1088/1742-6596/440/1/012048>
- Khomenko, E., Vitas, N., Collados, M., & de Vicente, A. (2018). Three-dimensional simulations of solar magneto-convection including effects of partial ionization. *Astronomy and Astrophysics*, 618, A87. <https://doi.org/10.1051/0004-6361/201833048>
- Kiselman, D., Pereira, T. M. D., Gustafsson, B., Asplund, M., Meléndez, J., & Langhans, K. (2011). Is the solar spectrum latitude-dependent? *Astronomy and Astrophysics*, 535, A14. <https://doi.org/10.1051/0004-6361/201117553>
- Khodachenko, M. L., Arber, T. D., Rucker, H. O., & Hanslmeier, A. (2004). Collisional and viscous damping of MHD waves in partially ionized plasmas of the solar atmosphere. *Astronomy and Astrophysics*, 422, 1073–1084. <https://doi.org/10.1051/0004-6361:20034207>
- Klimchuk, J. A. (2015). Key aspects of coronal heating. *Philosophical Transactions of the Royal Society of London Series A*, 373(2042), 20140256. <https://doi.org/10.1098/rsta.2014.0256>
- Kohutova, P., Verwichte, E., & Froment, C. (2020). First direct observation of a torsional Alfvén oscillation at coronal heights. *Astronomy and Astrophysics*, 633, L6. <https://doi.org/10.1051/0004-6361/201937144>
- Kontogiannis, I., Tsiropoula, G., & Tziotziou, K. (2014). Transmission and conversion of magnetoacoustic waves on the magnetic canopy in a quiet Sun region. *Astronomy and Astrophysics*, 567, A62. <https://doi.org/10.1051/0004-6361/201423986>
- Kontogiannis, I., Tsiropoula, G., & Tziotziou, K. (2016). Wave propagation in a solar quiet region and the influence of the magnetic canopy. *Astronomy and Astrophysics*, 585, A110. <https://doi.org/10.1051/0004-6361/201527053>
- Kosugi, T., Matsuzaki, K., Sakao, T., Shimizu, T., Sone, Y., Tachikawa, S., et al. (2007). The Hinode (Solar-B) mission: An overview. *Solar Physics*, 243(1), 3–17. <https://doi.org/10.1007/s11207-007-9014-6>
- Kuźma, B., Murawski, K., Kayshap, P., Wójcik, D., Srivastava, A. K., & Dwivedi, B. N. (2017). Two-fluid numerical simulations of solar spicules. *The Astrophysical Journal*, 849(2), 78. <https://doi.org/10.3847/1538-4357/aa8ea1>
- Kuźma, B., Wójcik, D., & Murawski, K. (2019). Heating of a quiet region of the solar chromosphere by ion and neutral acoustic waves. *The Astrophysical Journal*, 878(2), 81. <https://doi.org/10.3847/1538-4357/ab1b4a>
- Kukhianidze, V., Zaqarashvili, T. V., & Khutsishvili, E. (2006). Observation of kink waves in solar spicules. *Astronomy and Astrophysics*, 449(2), L35–L38. <https://doi.org/10.1051/0004-6361:200600018>
- Kuridze, D., Henriques, V., Mathioudakis, M., Erdélyi, R., Zaqarashvili, T. V., Shelyag, S., et al. (2015). The dynamics of rapid redshifted and blueshifted excursions in the solar H $\alpha$  line. *The Astrophysical Journal*, 802(1), 26. <https://doi.org/10.1088/0004-637X/802/1/26>
- Kuridze, D., & Zaqarashvili, T. V. (2008). Resonant energy conversion of 3-min intensity oscillations into Alfvén waves in the solar atmosphere. *Journal of Atmospheric and Solar-Terrestrial Physics*, 70(2–4), 351–355. <https://doi.org/10.1016/j.jastp.2007.08.059>
- Kuridze, D., Zaqarashvili, T. V., Henriques, V., Mathioudakis, M., Keenan, F. P., & Hanslmeier, A. (2016). Kelvin-Helmholtz instability in solar chromospheric jets: Theory and observation. *Journal of Atmospheric and Solar-Terrestrial Physics*, 830(2), 133. <https://doi.org/10.3847/0004-637X/830/2/133>
- Labrosse, N., Heinzel, P., Vial, J.-C., Kucera, T., Parenti, S., Guнар, S., et al. (2010). Physics of solar prominences: I—spectral diagnostics and non-LTE modelling. *Space Science Reviews*, 151(4), 243–332. <https://doi.org/10.1007/s11214-010-9630-6>
- Lagg, A., Lites, B., Harvey, J., Gosain, S., & Centeno, R. (2017). Measurements of photospheric and chromospheric magnetic fields. *Space Science Reviews*, 210(1–4), 37–76. <https://doi.org/10.1007/s11214-015-0219-y>
- Laming, J. M. (2009). Non-WKB models of the first ionization potential effect: Implications for solar coronal heating and the coronal helium and neon abundances. *Space Science Reviews*, 695(2), 954–969. <https://doi.org/10.1088/0004-637X/695/2/954>
- Langangen, O., Carlsson, M., van der Voort, L. R., & Stein, R. F. (2007). Velocities measured in small-scale solar magnetic elements. *The Astrophysical Journal*, 655(1), 615–623. <https://doi.org/10.1086/509754>
- Leake, J. E., Arber, T. D., & Khodachenko, M. L. (2005). Collisional dissipation of Alfvén waves in a partially ionised solar chromosphere. *Astronomy and Astrophysics*, 442, 1091–1098. <https://doi.org/10.1051/0004-6361:20053427>
- Leake, J. E., DeVore, C. R., Thayer, J. P., Burns, A. G., Crowley, G., Gilbert, H. R., et al. (2014). Ionized plasma and neutral gas coupling in the Sun's chromosphere and Earth's ionosphere/thermosphere. *Space Science Reviews*, 184(1–4), 107–172. <https://doi.org/10.1007/s11214-014-0103-1>



- Lee, D., & Deane, A. E. (2009). An unsplit staggered mesh scheme for multidimensional magnetohydrodynamics. *Journal of Computational Physics*, 228(4), 952–975. <https://doi.org/10.1016/j.jcp.2008.08.026>
- Li, B., Antolin, P., Guo, M.-Z., Kuznetsov, A. A., Pascoe, D. J., Van Doorselaere, T., & Vasheghani Farahani, S. (2020). Magnetohydrodynamic fast sausage waves in the solar corona. *Space Science Reviews*, 216(8), 136. <https://doi.org/10.1007/s11214-020-00761-z>
- Li, B., Guo, M.-Z., Yu, H., & Chen, S.-X. (2018). Impulsively generated wave trains in coronal structures. II. Effects of transverse structuring on sausage waves in pressureless slabs. *The Astrophysical Journal*, 855(1), 53. <https://doi.org/10.3847/1538-4357/aaaf19>
- Liu, J., Nelson, C. J., Snow, B., Wang, Y., & Erdélyi, R. (2019). Evidence of ubiquitous Alfvén pulses transporting energy from the photosphere to the upper chromosphere. *Nature Communications*, 10, 3504. <https://doi.org/10.1038/s41467-019-11495-0>
- Lopin, I., & Nagorny, I. (2015). Sausage waves in transversely nonuniform monolithic coronal tubes. *The Astrophysical Journal*, 810(2), 87. <https://doi.org/10.1088/0004-637X/810/2/87>
- Luna, M., Karpen, J. T., & DeVore, C. R. (2012). Formation and evolution of a multi-threaded solar prominence. *The Astrophysical Journal*, 746(1), 30. <https://doi.org/10.1088/0004-637X/746/1/30>
- Luo, Q. Y., Wei, F. S., & Feng, X. S. (2002). Excitation and dissipation of torsional modes in solar photospheric magnetic flux tubes. *Astronomy and Astrophysics*, 395, 669–675. <https://doi.org/10.1051/0004-6361/20021292>
- Mackay, D. H., Karpen, J. T., Ballester, J. L., Schmieder, B., & Aulanier, G. (2010). Physics of solar prominences: II-Magnetic structure and dynamics. *Space Science Reviews*, 151, 333–399. <https://doi.org/10.1007/s11214-010-9628-0>
- Madsen, C. A., Dimant, Y. S., Oppenheim, M. M., & Fontenla, J. M. (2014). The Multi-species Farley-Buneman instability in the solar chromosphere. *The Astrophysical Journal*, 783(2), 128. <https://doi.org/10.1088/0004-637X/783/2/128>
- Malara, F., Primavera, L., & Veltri, P. (2000). Nonlinear evolution of parametric instability of a large-amplitude nonmonochromatic Alfvén wave. *Physics of Plasmas*, 7(7), 2866–2877. <https://doi.org/10.1063/1.874136>
- Malara, F., & Velli, M. (1996). Parametric instability of a large-amplitude nonmonochromatic Alfvén wave. *Physics of Plasmas*, 3(12), 4427–4433. <https://doi.org/10.1063/1.872043>
- Maneva, Y. G., Laguna, A. A., Lani, A., & Poedts, S. (2017). Multi-fluid modeling of magnetosonic wave propagation in the solar chromosphere: Effects of impact ionization and radiative recombination. *Physics of Plasmas*, 836(2), 197. <https://doi.org/10.3847/1538-4357/aa5b83>
- Martínez-Gómez, D., Soler, R., & Terradas, J. (2018). Multi-fluid approach to high-frequency waves in plasmas. III. Nonlinear regime and plasma heating. *The Astrophysical Journal*, 856(1), 16. <https://doi.org/10.3847/1538-4357/aab156>
- Martínez-Sykora, J., De Pontieu, B., Hansteen, V., & Carlsson, M. (2015). The role of partial ionization effects in the chromosphere. *Philosophical Transactions of the Royal Society of London Series A*, 373(2042), 20140268. <https://doi.org/10.1098/rsta.2014.0268>
- Martínez-Sykora, J., Pontieu, B. D., Carlsson, M., & Hansteen, V. (2016). On the misalignment between chromospheric features and the magnetic field on the Sun. *The Astrophysical Journal Letters*, 831(1), L1. <https://doi.org/10.3847/2041-8205/831/1/L1>
- Mathioudakis, M., Jess, D. B., & Erdélyi, R. (2013). Alfvén waves in the solar atmosphere. *Space Science Reviews*, 175(1–4), 1–27. <https://doi.org/10.1007/s11214-012-9944-7>
- Matsumoto, T., & Shibata, K. (2010). Nonlinear propagation of Alfvén Waves driven by observed photospheric motions: Application to the coronal heating and spicule formation. *The Astrophysical Journal*, 710(2), 1857–1867. <https://doi.org/10.1088/0004-637X/710/2/1857>
- Mattig, W., Mehlretter, J. P., & Nesis, A. (1981). Granular-size horizontal velocities in the solar atmosphere. *Astronomy and Astrophysics*, 96(1–2), 96–101.
- McAteer, R. T. J., Gallagher, P. T., Williams, D. R., Mathioudakis, M., Bloomfield, D. S., Phillips, K. J. H., & Keenan, F. P. (2003). Observational evidence for mode coupling in the chromospheric network. *The Astrophysical Journal*, 587(2), 806–817. <https://doi.org/10.1086/368304>
- McClements, K. G., Harrison, R. A., & Alexander, D. (1991). The detection of wave activity in the solar corona using UV line spectra. *Solar Physics*, 131(1), 41–48. <https://doi.org/10.1007/BF00151742>
- McIntosh, S. W., & De Pontieu, B. (2012). Estimating the “dark” energy content of the solar corona. *The Astrophysical Journal*, 761(2), 138. <https://doi.org/10.1088/0004-637X/761/2/138>
- McIntosh, S. W., de Pontieu, B., Carlsson, M., Hansteen, V., Boerner, P., & Goossens, M. (2011). Alfvénic waves with sufficient energy to power the quiet solar corona and fast solar wind. *Nature*, 475(7357), 477–480. <https://doi.org/10.1038/nature10235>
- McIntosh, S. W., & Jefferies, S. M. (2006). Observing the modification of the acoustic cutoff frequency by field inclination angle. *The Astrophysical Journal Letters*, 647(1), L77–L81. <https://doi.org/10.1086/507425>
- McIntosh, S. W., & Judge, P. G. (2001). On the nature of magnetic shadows in the solar chromosphere. *The Astrophysical Journal*, 561(1), 420–426. <https://doi.org/10.1086/323068>
- Medvedev, M. V. (1999). Collisionless dissipative nonlinear Alfvén waves: Nonlinear steepening, compressible turbulence, and particle trapping. *Physics of Plasmas*, 6(5), 2191–2197. <https://doi.org/10.1063/1.873471>
- Mishra, S. K., Singh, T., Kayshap, P., & Srivastava, A. K. (2018). Evolution of magnetic Rayleigh-Taylor instability into the outer solar corona and low interplanetary space. *The Astrophysical Journal*, 856(1), 86. <https://doi.org/10.3847/1538-4357/aaae03>
- Mishra, S. K., & Srivastava, A. K. (2019). The Evolution of magnetic Rayleigh-Taylor unstable plumes and hybrid KH-RT instability into a loop-like eruptive prominence. *The Astrophysical Journal*, 874(1), 57. <https://doi.org/10.3847/1538-4357/ab06f2>
- Montgomery, D. (1959). Development of hydromagnetic shocks from large-amplitude Alfvén waves. *Physical Review Letters*, 2(2), 36–37. <https://doi.org/10.1103/PhysRevLett.2.36>
- Moreels, M. G., Freij, N., Erdélyi, R., Van Doorselaere, T., & Verth, G. (2015). Observations and mode identification of sausage waves in a magnetic pore. *Astronomy and Astrophysics*, 579, A73. <https://doi.org/10.1051/0004-6361/201425096>
- Moreels, M. G., Goossens, M., & Van Doorselaere, T. (2013). Cross-sectional area and intensity variations of sausage modes. *Astronomy and Astrophysics*, 555, A75. <https://doi.org/10.1051/0004-6361/201321545>
- Moreels, M. G., Van Doorselaere, T., Grant, S. D. T., Jess, D. B., & Goossens, M. (2015). Energy and energy flux in axisymmetric slow and fast waves. *Astronomy and Astrophysics*, 578, A60. <https://doi.org/10.1051/0004-6361/201425468>
- Moretti, P. F., Jefferies, S. M., Armstrong, J. D., & McIntosh, S. W. (2007). Observational signatures of the interaction between acoustic waves and the solar magnetic canopy. *Astronomy and Astrophysics*, 471(3), 961–965. <https://doi.org/10.1051/0004-6361:20077247>
- Morton, R. J., Erdélyi, R., Jess, D. B., & Mathioudakis, M. (2011). Observations of sausage modes in magnetic pores. *The Astrophysical Journal Letters*, 729(2), L18. <https://doi.org/10.1088/2041-8205/729/2/L18>
- Morton, R. J., Tomczyk, S., & Pinto, R. (2015). Investigating Alfvénic wave propagation in coronal open-field regions. *Nature Communications*, 6, 7813. <https://doi.org/10.1038/ncomms8813>
- Morton, R. J., Tomczyk, S., & Pinto, R. F. (2016). A global view of velocity fluctuations in the corona below 1.3r<sub>☉</sub> with comp. *The Astrophysical Journal*, 828(2), 89. <https://doi.org/10.3847/0004-637X/828/2/89>

- Morton, R. J., Verth, G., Fedun, V., Shelyag, S., & Erdélyi, R. (2013). Evidence for the photospheric excitation of incompressible chromospheric waves. *The Astrophysical Journal*, 768(1), 17. <https://doi.org/10.1088/0004-637X/768/1/17>
- Morton, R. J., Verth, G., Hillier, A., & Erdélyi, R. (2014). The generation and damping of propagating MHD kink waves in the solar atmosphere. *The Astrophysical Journal*, 784(1), 29. <https://doi.org/10.1088/0004-637X/784/1/29>
- Morton, R. J., Verth, G., Jess, D. B., Kuridze, D., Ruderman, M. S., Mathioudakis, M., & Erdélyi, R. (2012). Observations of ubiquitous compressive waves in the Sun's chromosphere. *Nature Communications*, 3, 1315. <https://doi.org/10.1038/ncomms2324>
- Morton, R. J., Weberg, M. J., & McLaughlin, J. A. (2019). A basal contribution from p-modes to the Alfvénic wave flux in the Sun's corona. *Nature Astronomy*, 3(3), 223–229. Retrieved from <https://doi.org/10.1038/s41550-018-0668-9>
- Muglach, K., Hofmann, A., & Staudé, J. (2005). Dynamics of solar active regions. *Astronomy and Astrophysics*, 437(3), 1055–1060. <https://doi.org/10.1051/0004-6361/20041164>
- Murawski, K., Musielak, Z. E., Konkol, P., & Wiśniewska, A. (2016). Variation of acoustic cutoff period with height in the solar atmosphere: Theory versus observations. *Astrophysical Journal*, 827(1), 37. <https://doi.org/10.3847/0004-637X/827/1/37>
- Murawski, K., Solov'ev, A., Musielak, Z. E., Srivastava, A. K., & Kraškievich, J. (2015). Torsional Alfvén waves in solar magnetic flux tubes of axial symmetry. *Astronomy and Astrophysics*, 577, A126. <https://doi.org/10.1051/0004-6361/201424545>
- Musielak, Z. E., Rosner, R., Stein, R. F., & Ulmschneider, P. (1994). On sound generation by turbulent convection: a new look at old results. *The Astrophysical Journal*, 423, 474. <https://doi.org/10.1086/173825>
- Nakariakov, V. M., Anfinogentov, S. A., Nisticò, G., & Lee, D.-H. (2016). Undamped transverse oscillations of coronal loops as a self-oscillatory process. *Astronomy and Astrophysics*, 591, L5. <https://doi.org/10.1051/0004-6361/201628850>
- Nakariakov, V. M., Pilipenko, V., Heilig, B., Jelinek, P., Karlický, M., Klimushkin, D. Y., et al. (2016). Magnetohydrodynamic oscillations in the solar corona and Earth's magnetosphere: Towards consolidated understanding. *Space Science Reviews*, 200(1–4), 75–203. <https://doi.org/10.1007/s11214-015-0233-0>
- Nakariakov, V. M., & Verwichte, E. (2005). Coronal waves and oscillations. *Living Reviews in Solar Physics*, 2(1), 3. <https://doi.org/10.12942/lrsp-2005-3>
- Narain, U., & Ulmschneider, P. (1996). Chromospheric and coronal heating mechanisms II. *Space Science Reviews*, 75, 453–509. <https://doi.org/10.1007/BF00833341>
- Nakariakov, V. M., & Roberts, B. (1999). Solitary autowaves in magnetic flux tubes. *Physics Letters A*, 254(6), 314–318. [https://doi.org/10.1016/S0375-9601\(99\)00136-X](https://doi.org/10.1016/S0375-9601(99)00136-X)
- Nechaeva, A., Zimovets, I. V., Nakariakov, V. M., & Goddard, C. R. (2019). Catalog of decaying kink oscillations of coronal loops in the 24th solar cycle. *Catalog of Decaying Kink Oscillations of Coronal Loops in the 24th Solar Cycle*, 241(2), 31. <https://doi.org/10.3847/1538-4365/ab0e86>
- Ni, L., Kliem, B., Lin, J., & Wu, N. (2015). Fast magnetic reconnection in the solar chromosphere mediated by the plasmoid instability. *The Astrophysical Journal*, 799(1), 79. <https://doi.org/10.1088/0004-637X/799/1/79>
- Nishizuka, N., Nakamura, T., Kawate, T., Singh, K. A. P., & Shibata, K. (2011). Statistical study of chromospheric anemone jets observed withinode/sot. *The Astrophysical Journal*, 731(1), 43. <https://doi.org/10.1088/0004-637X/731/1/43>
- Nordlund, A., Spruit, H. C., Ludwig, H. G., & Trampedach, R. (1997). Is stellar granulation turbulence? *The Astrophysical Journal*, 328, 229–234.
- Nordlund, A., & Stein, R. F. (2001). Solar oscillations and convection. I. Formalism for radial oscillations. *The Astrophysical Journal*, 546(1), 576–584. <https://doi.org/10.1086/318217>
- Ofman, L., & Aschwanden, M. J. (2002). Damping time scaling of coronal loop oscillations deduced from [ITAL] transition region and coronal explorer/[ITAL] observations. *The Astrophysical Journal Letters*, 576(2), L153–L156. <https://doi.org/10.1086/343886>
- Ofman, L., Davila, J. M., & Steinolfson, R. S. (1994). Coronal heating by the resonant absorption of Alfvén waves: The effect of viscous stress tensor. *The Astrophysical Journal*, 421, 360. <https://doi.org/10.1086/173654>
- Ofman, L., Davila, J. M., & Steinolfson, R. S. (1995). Coronal heating by the resonant absorption of Alfvén waves: Wavenumber scaling laws. *The Astrophysical Journal*, 444, 471. <https://doi.org/10.1086/175621>
- Oliver, R. (1999). Prominence oscillations: Observations and theory. In A. Wilson & et al. (Eds.), *Magnetic fields and solar processes* (Vol. 9, p. 425).
- Oliver, R. (2009). Prominence seismology using small amplitude oscillations. *Space Science Reviews*, 149(1–4), 175–197. <https://doi.org/10.1007/s11214-009-9527-4>
- Oliver, R., & Ballester, J. L. (2002). Oscillations in quiescent solar prominences observations and theory (invited review). *Solar Physics*, 206, 45–67. <https://doi.org/10.1023/A:1014915428440>
- Oran, R., Landi, E., Holst, B. v. d., Sokolov, I. V., & Gombosi, T. I. (2017). Alfvén wave turbulence as a coronal heating mechanism: Simultaneously predicting the heating rate and the wave-induced emission line broadening. *The Astrophysical Journal*, 845(2), 98. <https://doi.org/10.3847/1538-4357/aa7fec>
- Pagano, P., & De Moortel, I. (2017). Contribution of mode-coupling and phase-mixing of Alfvén waves to coronal heating. *Astronomy and Astrophysics*, 601, A107. <https://doi.org/10.1051/0004-6361/201630059>
- Parenti, S. (2014). Solar prominences: Observations. *Living Reviews in Solar Physics*, 11(1), 1. <https://doi.org/10.12942/lrsp-2014-1>
- Parenti, S., & Vial, J.-C. (2007). Prominence and Quiet-Sun plasma parameters derived from FUV spectral emission. *Living Reviews in Solar Physics*, 469(3), 1109–1115. <https://doi.org/10.1051/0004-6361/20077196>
- Pécselei, H., & Engvold, O. (2000). Modeling of prominence threads in magnetic fields: Levitation by incompressible MHD waves. *Solar Physics*, 194, 73–86. <https://doi.org/10.1023/A:1005242609261>
- Pennicott, J. D., & Cally, P. S. (2019). Smoothing of MHD shocks in mode conversion. *Solar Physics*, 881(1), L21. <https://doi.org/10.3847/2041-8213/ab3423>
- Pikel'Ner, S. B. (1971). Origin of quiescent prominences. *Solar Physics*, 17(1), 44–49. <https://doi.org/10.1007/BF00152860>
- Poedts, S., Goossens, M., & Kerner, W. (1989). Numerical simulation of coronal heating by resonant absorption of Alfvén waves. *Solar Physics*, 123(1), 83–115. <https://doi.org/10.1007/BF00150014>
- Poedts, S., Goossens, M., & Kerner, W. (1990). On the efficiency of coronal loop heating by resonant absorption. *The Astrophysical Journal*, 360, 279. <https://doi.org/10.1086/169118>
- Popescu Braileanu, B., Lukin, V. S., Khomenko, E., & de Vicente, Á. (2019a). Two-fluid simulations of waves in the solar chromosphere. *The Astrophysical Journal*, 630, A79. <https://doi.org/10.1051/0004-6361/201935844>
- Popescu Braileanu, B., Lukin, V. S., Khomenko, E., & de Vicente, Á. (2019b). Two-fluid simulations of waves in the solar chromosphere. *Astronomy and Astrophysics*, 627, A25. <https://doi.org/10.1051/0004-6361/201834154>

- Primavera, L., Malara, F., Servidio, S., Nigro, G., & Veltri, P. (2019). Parametric instability in two-dimensional Alfvénic turbulence. *The Astrophysical Journal*, 880(2), 156. <https://doi.org/10.3847/1538-4357/ab29f5>
- Prokopyshyn, A. P. K., & Hood, A. W. (2019). Investigating the damping rate of phase-mixed Alfvén waves. *Astronomy and Astrophysics*, 632, A93. <https://doi.org/10.1051/0004-6361/201936658>
- Rajaguru, S. P., Couvidat, S., Sun, X., Hayashi, K., & Schunker, H. (2013). Properties of high-frequency wave power halos around active regions: An analysis of multi-height data from HMI and AIA onboard SDO. *Solar Physics*, 287(1–2), 107–127. <https://doi.org/10.1007/s11207-012-0180-9>
- Rajaguru, S. P., Sangeetha, C. R., & Tripathi, D. (2019). Magnetic fields and the supply of low-frequency acoustic wave energy to the solar chromosphere. *The Astrophysical Journal*, 871(2), 155. <https://doi.org/10.3847/1538-4357/aaf883>
- Rast, M. P., Bello González, N., Bellot Rubio, L., Cao, W., Cauzzi, G., DeLuca, E., et al. (2021). Critical science plan for the Daniel K. Inouye solar telescope (DKIST). *Solar Physics*, 296, 70. <https://doi.org/10.1007/s11207-021-01789-2>
- Rayleigh, B. (1899). *The multi-species Farley-Buneman instability in the solar chromosphere. Scientific papers*, Cambridge: Cambridge University Press. <https://doi.org/10.1088/0004-637X/783/2/128>
- Reznikova, V. E., Van Doorslaere, T., & Kuznetsov, A. A. (2015). Perturbations of gyrosynchrotron emission polarization from solar flares by sausage modes: Forward modeling. *Astronomy and Astrophysics*, 575, A47. <https://doi.org/10.1051/0004-6361/201424548>
- Riedl, J. M., Gilchrist-Millar, C. A., Van Doorslaere, T., Jess, D. B., & Grant, S. D. T. (2021). Finding the mechanism of wave energy flux damping in solar pores using numerical simulations. *Astronomy and Astrophysics*, 648, A77. <https://doi.org/10.1051/0004-6361/2020040163>
- Rijs, C., Rajaguru, S. P., Przybylski, D., Moradi, H., Cally, P. S., & Shelyag, S. (2016). 3D simulations of realistic power halos in magnetohydrostatic sunspot atmospheres: Linking theory and observation. *The Astrophysical Journal*, 817(1), 45. <https://doi.org/10.3847/0004-637X/817/1/45>
- Rimmele, T. R., Warner, M., Keil, S. L., Goode, P. R., Knölker, M., Kuhn, J. R., et al. (2020). The Daniel K. Inouye solar telescope—observatory overview. *Solar Physics*, 295(12), 172. <https://doi.org/10.1007/s11207-020-01736-7>
- Roberts, B. (2000). Waves and oscillations in the corona—(invited review). *Solar Physics*, 193, 139–152. <https://doi.org/10.1023/A:1005237109398>
- Roberts, B. (2008). Progress in coronal seismology. In R. Erdélyi & C. A. Mendoza-Briceno (Eds.), *Oscillations in the solar atmosphere: Heating and magneto-seismology* (Vol. 3, p. 3–19). <https://doi.org/10.1017/S1743921308014609>
- Roberts, B., & Mangeney, A. (1982). Solitons in solar magnetic flux tubes. *Solar Physics*, 198, 7P–11P. <https://doi.org/10.1093/mnras/198.1.7P>
- Roupe van der Voort, L., Leenaarts, J., de Pontieu, B., Carlsson, M., & Vissers, G. (2009). On-disk counterparts of type II spicules in the Ca II 854.2 nm and H $\alpha$  lines. *The Astrophysical Journal*, 705(1), 272–284. <https://doi.org/10.1088/0004-637X/705/1/272>
- Ruderman, M. S. (1999). Coronal loop heating by torsional Alfvén waves directly driven by footpoint motions: Harmonic driving versus stochastic driving. *The Astrophysical Journal*, 521(2), 851–858. <https://doi.org/10.1086/307584>
- Ruderman, M. S. (2003). Nonlinear waves in the magnetically structured solar atmosphere. In *Turbulence* (pp. 239–274). [https://doi.org/10.1007/978-94-007-1063-4\\_12](https://doi.org/10.1007/978-94-007-1063-4_12)
- Ruderman, M. S., Berghmans, D., Goossens, M., & Poedts, S. (1997). Direct excitation of resonant torsional Alfvén waves by footpoint motions. *Astronomy and Astrophysics*, 320, 305–318.
- Ruderman, M. S., Goldstein, M. L., Roberts, D. A., Deane, A., & Ofman, L. (1999). Alfvén wave phase mixing driven by velocity shear in two-dimensional open magnetic configurations. *Journal of Geophysical Research*, 104(A8), 17057–17068. <https://doi.org/10.1029/1999JA900144>
- Ruderman, M. S., & Roberts, B. (2002). The damping of coronal loop oscillations. *The Astrophysical Journal*, 577(1), 475–486. <https://doi.org/10.1086/342130>
- Ryutova, M., Berger, T., Frank, Z., Tarbell, T., & Title, A. (2010). Observation of plasma instabilities in quiescent prominences. *Solar Physics*, 267(1), 75–94. <https://doi.org/10.1007/s11207-010-9638-9>
- Sakurai, T., Goossens, M., & Hollweg, J. V. (1991). Resonant behavior of MHD waves on magnetic flux tubes. *Solar Physics*, 133(2), 227–245. <https://doi.org/10.1007/BF00149888>
- Scharmer, G. B., Narayan, G., Hillberg, T., de la Cruz Rodriguez, J., Löfdahl, M. G., Kiselman, D., et al. (2008). CRISP spectropolarimetric imaging of penumbral fine structure. *The Astrophysical Journal Letters*, 689(1), L69, L72. <https://doi.org/10.1086/595744>
- Schmitz, F., & Fleck, B. (1998). On wave equations and cut-off frequencies of plane atmospheres. *Astronomy and Astrophysics*, 337, 487–494.
- Schmitz, F., & Fleck, B. (2003). Towards an explanation of features in the diagnostic diagram of a model atmosphere. *Astronomy and Astrophysics*, 399, 723–730. <https://doi.org/10.1051/0004-6361:20021815>
- Schrijver, C. J., & Title, A. M. (2003). The magnetic connection between the solar photosphere and the corona. *The Astrophysical Journal Letters*, 597(2), L165–L168. <https://doi.org/10.1086/379870>
- Schunker, H., & Cally, P. S. (2006). Magnetic field inclination and atmospheric oscillations above solar active regions. *Monthly Notices of the Royal Astronomical Society*, 372(2), 551–564. <https://doi.org/10.1111/j.1365-2966.2006.10855.x>
- Schwarzschild, M. (1948). On noise arising from the solar granulation. *The Astrophysical Journal*, 107, 1. <https://doi.org/10.1086/144983>
- Sekse, D. H., Roupe van der Voort, L., & De Pontieu, B. (2012). Statistical properties of the disk counterparts of type II spicules from simultaneous observations of rapid blueshifted excursions in Ca II 8542 and H $\alpha$ . *The Astrophysical Journal*, 752(2), 108. <https://doi.org/10.1088/0004-637X/752/2/108>
- Shelyag, S., Fedun, V., & Erdélyi, R. (2008). Magnetohydrodynamic code for gravitationally-stratified media. *Astronomy and Astrophysics*, 486(2), 655–662. <https://doi.org/10.1051/0004-6361:200809800>
- Shelyag, S., Khomenko, E., Vicente, A. d., & Przybylski, D. (2016). Heating of the partially ionized solar chromosphere by waves in magnetic structures. *The Astrophysical Journal Letters*, 819(1), L11. <https://doi.org/10.3847/2041-8205/819/1/L11>
- Shelyag, S., & Przybylski, D. (2014). Center-to-limb spectro-polarimetric diagnostics of simulated solar photospheric magneto-convection: Signatures of photospheric Alfvén waves. *Publication of Astronomical Society of Japan*, 66, S9. <https://doi.org/10.1093/pasj/psu085>
- Shestov, S. V., Nakariakov, V. M., Ulyanov, A. S., Reva, A. A., & Kuzin, S. V. (2017). Nonlinear evolution of short-wavelength torsional Alfvén waves. *The Astrophysical Journal*, 840(2), 64. <https://doi.org/10.3847/1538-4357/aa6c65>
- Shibata, K., Nakamura, T., Matsumoto, T., Otsuji, K., Okamoto, T. J., Nishizuka, N., et al. (2007). Chromospheric anemone jets as evidence of ubiquitous reconnection. *Science*, 318(5856), 1591, 1594. <https://doi.org/10.1126/science.1146708>
- Snow, B., Fedun, V., Gent, F. A., Verth, G., & Erdélyi, R. (2018). Magnetic shocks and substructures excited by torsional Alfvén wave interactions in merging expanding flux tubes. *The Astrophysical Journal*, 857(2), 125. <https://doi.org/10.3847/1538-4357/aab7f7>
- Snow, B., & Hillier, A. (2019). Intermediate shock sub-structures within a slow-mode shock occurring in partially ionised plasma. *Astronomy and Astrophysics*, 626, A46. <https://doi.org/10.1051/0004-6361/201935326>
- Snow, B., & Hillier, A. (2020). Mode conversion of two-fluid shocks in a partially-ionised, isothermal, stratified atmosphere. *Astronomy and Astrophysics*, 637, A97. <https://doi.org/10.1051/0004-6361/202037848>



- Soler, R., Ballester, J. L., & Zaqarashvili, T. V. (2015). Overdamped Alfvén waves due to ion-neutral collisions in the solar chromosphere. *Astronomy and Astrophysics*, 573, A79. <https://doi.org/10.1051/0004-6361/201423930>
- Soler, R., Carbonell, M., & Ballester, J. L. (2015). On the Spatial scales of wave heating in the solar chromosphere. *The Astrophysical Journal*, 810(2), 146. <https://doi.org/10.1088/0004-637X/810/2/146>
- Soler, R., Carbonell, M., Ballester, J. L., & Terradas, J. (2013). Alfvén waves in a partially ionized two-fluid plasma. *The Astrophysical Journal*, 767(2), 171. <https://doi.org/10.1088/0004-637X/767/2/171>
- Soler, R., Díaz, A. J., Ballester, J. L., & Goossens, M. (2012). Kelvin-Helmholtz instability in partially ionized compressible plasmas. *The Astrophysical Journal*, 749(2), 163. <https://doi.org/10.1088/0004-637X/749/2/163>
- Soler, R., Oliver, R., & Ballester, J. L. (2008). Nonadiabatic magnetohydrodynamic waves in a cylindrical prominence thread with mass flow. *The Astrophysical Journal*, 684, 725–735. <https://doi.org/10.1086/590244>
- Soler, R., Oliver, R., & Ballester, J. L. (2009). Magnetohydrodynamic waves in a partially ionized filament thread. *The Astrophysical Journal*, 699, 1553–1562. <https://doi.org/10.1088/0004-637X/699/2/1553>
- Soler, R., Oliver, R., & Ballester, J. L. (2010). Time damping of non-adiabatic magnetohydrodynamic waves in a partially ionized prominence plasma: effect of helium. *Astronomy and Astrophysics*, 512, A28. <https://doi.org/10.1051/0004-6361/200913478>
- Soler, R., Terradas, J., Oliver, R., & Ballester, J. L. (2016). The role of Alfvén wave heating in solar prominences. *Astronomy and Astrophysics*, 592, A28. <https://doi.org/10.1051/0004-6361/201628722>
- Soler, R., Terradas, J., Oliver, R., & Ballester, J. L. (2017). Propagation of torsional Alfvén waves from the photosphere to the corona: reflection, transmission, and heating in expanding flux tubes. *The Astrophysical Journal*, 840(1), 20. <https://doi.org/10.3847/1538-4357/aa6d7f>
- Soler, R., Terradas, J., Oliver, R., & Ballester, J. L. (2019). Energy transport and heating by torsional Alfvén waves propagating from the photosphere to the corona in the quiet Sun. *The Astrophysical Journal*, 871(1), 3. <https://doi.org/10.3847/1538-4357/aaf64c>
- Song, H. Q., Chen, Y., Li, B., Li, L. P., Zhao, L., He, J. S., et al. (2017). The origin of solar filament plasma inferred from in situ observations of elemental abundances. *The Astrophysical Journal Letters*, 836(1), L11. <https://doi.org/10.3847/2041-8213/aa5d54>
- Song, P., & Vasyliūnas, V. M. (2011). Heating of the solar atmosphere by strong damping of Alfvén waves. *Journal of Geophysical Research (Space Physics)*, 116(A9). <https://doi.org/10.1029/2011JA016679>
- Song, P., & Vasyliūnas, V. M. (2014). Effect of horizontally inhomogeneous heating on flow and magnetic field in the chromosphere of the Sun. *The Astrophysical Journal Letters*, 796(2), L23. <https://doi.org/10.1088/2041-8205/796/2/L23>
- Spitzer, L. (1962). *Physics of fully ionized gases*. Courier Corporation.
- Spruit, H. C. (1981). Motion of magnetic flux tubes in the solar convection zone and chromosphere. *Astronomy and Astrophysics*, 98, 155–160.
- Spruit, H. C., & Roberts, B. (1983). Magnetic flux tubes on the Sun. *Nature*, 304(5925), 401–406. <https://doi.org/10.1038/304401a0>
- Srivastava, A. K., & Dwivedi, B. N. (2010). Observations from Hinode/EIS of intensity oscillations above a bright point: Signature of the leakage of acoustic oscillations in the inner corona. *Monthly Notices of the Royal Astronomical Society*, 405(4). <https://doi.org/10.1111/j.1365-2966.2010.16651.x>
- Srivastava, A. K., Erdélyi, R., Tripathi, D., Fedun, V., Joshi, N. C., & Kayshap, P. (2013). Observational evidence of sausage-pinch instability in solar corona by Sdo/Aia. *The Astrophysical Journal Letters*, 765(2), L42. <https://doi.org/10.1088/2041-8205/765/2/L42>
- Srivastava, A. K., Murawski, K., Kuźma, B., Wójcik, D. P., Zaqarashvili, T. V., Stangalini, M., et al. (2018). Confined pseudo-shocks as an energy source for the active solar corona. *Nature Astronomy*, 2, 951–956. <https://doi.org/10.1038/s41550-018-0590-1>
- Srivastava, A. K., & Goossens, M. (2013). X6.9-class flare-induced vertical kink oscillations in a large-scale plasma curtain as observed by the solar dynamics observatory/atmospheric imaging assembly. *The Astrophysical Journal*, 777(1), 17. <https://doi.org/10.1088/0004-637X/777/1/17>
- Srivastava, A. K., Kuridze, D., Zaqarashvili, T. V., & Dwivedi, B. N. (2008). Intensity oscillations observed with Hinode near the south pole of the Sun: Leakage of low frequency magneto-acoustic waves into the solar corona. *Astronomy and Astrophysics*, 481(3), L95–L98. <https://doi.org/10.1051/0004-6361:20079328>
- Srivastava, A. K., Mishra, S. K., Jelínek, P., Samanta, T., Tian, H., Pant, V., et al. (2019). On the observations of rapid forced reconnection in the solar corona. *The Astrophysical Journal*, 887(2), 137. <https://doi.org/10.3847/1538-4357/ab4a0c>
- Srivastava, A. K., Shetye, J., Murawski, K., Doyle, J. G., Stangalini, M., Scullion, E., et al. (2017). High-frequency torsional Alfvén waves as an energy source for coronal heating. *Nature Scientific Reports*, 7, 43147. <https://doi.org/10.1038/srep43147>
- Stangalini, M., Del Moro, D., Berrilli, F., & Jefferies, S. M. (2011). MHD wave transmission in the Sun's atmosphere. *Astronomy and Astrophysics*, 534, A65. <https://doi.org/10.1051/0004-6361/201117356>
- Stangalini, M., Giannattasio, F., Erdélyi, R., Jafarzadeh, S., Consolini, G., Criscuolo, S., et al. (2017). Polarized kink waves in magnetic elements: Evidence for chromospheric helical waves. *The Astrophysical Journal*, 840(1), 19. <https://doi.org/10.3847/1538-4357/aa6c5e>
- Stangalini, M., Jafarzadeh, S., Ermolli, I., Erdélyi, R., Jess, D. B., Keys, P. H., et al. (2018). Propagating spectropolarimetric disturbances in a large sunspot. *The Astrophysical Journal*, 869(2), 110. <https://doi.org/10.3847/1538-4357/aaec7b>
- Stein, R. F. (1968). Waves in the solar atmosphere. I. The acoustic energy flux. *The Astrophysical Journal*, 154, 297. <https://doi.org/10.1086/149758>
- Stein, R. F., & Nordlund, A. (2001). Solar oscillations and convection. II. Excitation of radial oscillations. *The Astrophysical Journal*, 546(1), 585–603. <https://doi.org/10.1086/318218>
- Straus, T., Fleck, B., Jefferies, S. M., Cauzzi, G., McIntosh, S. W., Reardon, K., et al. (2008). The energy flux of internal gravity waves in the lower solar atmosphere. *The Astrophysical Journal Letters*, 681(2), L125, L128. <https://doi.org/10.1086/590495>
- Severino, T. K., & Inutsuka, S.-I. (2005). Making the corona and the fast solar wind: A self-consistent simulation for the low-frequency Alfvén waves from the photosphere to 0.3 AU. *The Astrophysical Journal Letters*, 632(1), L49–L52. <https://doi.org/10.1086/497536>
- Taylor, G. (1950). The instability of liquid surfaces when accelerated in a direction perpendicular to their planes. I. *Proceedings of the Royal Society of London Series A*, 201(1065), 192–196. <https://doi.org/10.1098/rspa.1950.0052>
- Tenerani, A., & Velli, M. (2013). Parametric decay of radial Alfvén waves in the expanding accelerating solar wind. *Journal of Geophysical Research*, 118(12), 7507–7516. <https://doi.org/10.1002/2013JA019293>
- Terradas, J., Soler, R., Luna, M., Oliver, R., & Ballester, J. L. (2015). Morphology and dynamics of solar prominences from 3D MHD simulations. *The Astrophysical Journal*, 799(1), 94. <https://doi.org/10.1088/0004-637X/799/1/94>



- Tian, H., DeLuca, E., Reeves, K. K., McKillop, S., De Pontieu, B., Martínez-Sykora, J., et al. (2014). High-resolution observations of the shock wave behavior for sunspot oscillations with the interface region imaging spectrograph. *The Astrophysical Journal*, 786(2), 137. <https://doi.org/10.1088/0004-637X/786/2/137>
- Title, A. (1984). The SOUP and CIP instruments. *Space Res.*, 4(8), 67–74. [https://doi.org/10.1016/0273-1177\(84\)90368-5](https://doi.org/10.1016/0273-1177(84)90368-5)
- Tomczyk, S., McIntosh, S. W., Keil, S. L., Judge, P. G., Schad, T., Seeley, D. H., & Edmondson, J. (2007). Alfvén waves in the solar corona. *Science*, 317(5842), 1192, 1196. <https://doi.org/10.1126/science.1143304>
- Tsap, Y. T., Stepanov, A. V., & Kopylova, Y. G. (2011). Energy flux of alfvén waves in weakly ionized plasma and coronal heating of the Sun. *Solar Physics*, 270(1), 205–211. <https://doi.org/10.1007/s11207-011-9727-4>
- Tsuneta, S., Ichimoto, K., Katsukawa, Y., Nagata, S., Otsubo, M., Shimizu, T., et al. (2008). The solar optical telescope for the hinode mission: An overview. *Solar Physics*, 249(2), 167–196. <https://doi.org/10.1007/s11207-008-9174-z>
- Tu, J., & Song, P. (2013). A study of Alfvén wave propagation and heating the chromosphere. *The Astrophysical Journal*, 777(1), 53. <https://doi.org/10.1088/0004-637X/777/1/53>
- Ulmshneider, P. (1971a). On the computation of shock heated models for the solar chromosphere and corona. *Astronomy and Astrophysics*, 12, 297.
- Ulmshneider, P. (1971b). On the propagation of a spectrum of acoustic waves in the solar atmosphere. *Astronomy and Astrophysics*, 14, 275.
- Ulmshneider, P., Rammacher, W., Musielak, Z. E., & Kalkofen, W. (2005). On the validity of acoustically heated chromosphere models. *The Astrophysical Journal Letters*, 631(2), L155–L158. <https://doi.org/10.1086/497395>
- Ulmshneider, P., Zaehring, K., & Musielak, Z. E. (1991). Propagation of nonlinear longitudinal-transverse waves along magnetic flux tubes in the solar atmosphere. I—Adiabatic waves. *Astronomy and Astrophysics*, 241(2), 625–634.
- Ulmshneider, R., Schmitz, F., Kalkofen, W., & Bohn, H. U. (1978). Acoustic waves in the solar atmosphere. V. On the chromospheric temperature rise. *Astronomy and Astrophysics*, 70, 487.
- Vögler, A., Shelyag, S., Schüssler, M., Cattaneo, F., Emonet, T., & Linde, T. (2005). Simulations of magneto-convection in the solar photosphere. *Astronomy and Astrophysics*, 429, 335–351. <https://doi.org/10.1051/0004-6361/20041507>
- van Ballegoijen, A. A., & Asgari-Targhi, M. (2016). Heating and acceleration of the fast solar wind by alfvén wave turbulence. *The Astrophysical Journal*, 821(2), 106. <https://doi.org/10.3847/0004-637X/821/2/106>
- van Ballegoijen, A. A., Asgari-Targhi, M., Cranmer, S. R., & DeLuca, E. E. (2011). Heating of the solar chromosphere and corona by alfvén wave turbulence. *The Astrophysical Journal*, 736(1), 3. <https://doi.org/10.1088/0004-637X/736/1/3>
- van Ballegoijen, A. A., Asgari-Targhi, M., & Voss, A. (2017). The heating of solar coronal loops by alfvén wave turbulence. *The Astrophysical Journal*, 849(1), 46. <https://doi.org/10.3847/1538-4357/aa9118>
- Van Damme, H. J., De Moortel, I., Pagano, P., & Johnston, C. D. (2020). Chromospheric evaporation and phase mixing of Alfvén waves in coronal loops. *Astronomy and Astrophysics*, 635, A174. <https://doi.org/10.1051/0004-6361/201937266>
- Van Doorselaere, T., Nakariakov, V. M., & Verwichte, E. (2008). Detection of waves in the solar corona: Kink or Alfvén? *The Astrophysical Journal Letters*, 676(1), L73, L75. <https://doi.org/10.1086/587029>
- Van Doorselaere, T., Srivastava, A. K., Antolin, P., Magyar, N., Vasheghani Farahani, S., Tian, H., et al. (2020). Coronal heating by MHD waves. *Space Science Reviews*, 216(8), 140. <https://doi.org/10.1007/s11214-020-00770-y>
- van Noort, M., Der Voort, L. R. V., & Löfdahl, M. G. (2005). Solar image restoration  $B_3$  use of multi-frame blind de-convolution with multiple objects and phase diversity. *Solar Physics*, 228(1–2), 191–215. <https://doi.org/10.1007/s11207-005-5782-z>
- Vasheghani Farahani, S., Nakariakov, V. M., van Doorselaere, T., & Verwichte, E. (2011). Nonlinear long-wavelength torsional Alfvén waves. *Astronomy and Astrophysics*, 526, A80. <https://doi.org/10.1051/0004-6361/201016063>
- Vasheghani Farahani, S., Nakariakov, V. M., Verwichte, E., & Van Doorselaere, T. (2012). Nonlinear evolution of torsional Alfvén waves. *Astronomy and Astrophysics*, 544, A127. <https://doi.org/10.1051/0004-6361/201219569>
- Vecchio, A., Cauzzi, G., Reardon, K. P., Janssen, K., & Rimmele, T. (2007). Solar atmospheric oscillations and the chromospheric magnetic topology. *Astronomy and Astrophysics*, 461(1), L1–L4. <https://doi.org/10.1051/0004-6361/20066415>
- Vernazza, J. E., Avrett, E. H., & Loeser, R. (1981). Structure of the solar chromosphere. III—Models of the EUV brightness components of the quiet-sun. *The Astrophysical Journal Supplement Series*, 45, 635–725. <https://doi.org/10.1086/190731>
- Verth, G., & Jess, D. B. (2016). MHD wave modes resolved in fine-scale chromospheric magnetic structures. *Geophysics Monograph Series*, 216, 431–448. <https://doi.org/10.1002/9781119055006.ch25>
- Vigeesh, G., Fedun, V., Hasan, S. S., & Erdélyi, R. (2012). Three-dimensional simulations of magnetohydrodynamic waves in magnetized solar atmosphere. *The Astrophysical Journal*, 755(1), 18. <https://doi.org/10.1088/0004-637X/755/1/18>
- Vranjes, J., Poedts, S., Pandey, B. P., & de Pontieu, B. (2008). Energy flux of Alfvén waves in weakly ionized plasma. *Astronomy and Astrophysics*, 478(2), 553–558. <https://doi.org/10.1051/0004-6361/20078274>
- Wang, Y., & Yokoyama, T. (2020). Simulation of Alfvén wave propagation in the magnetic chromosphere with radiative loss: Effects of nonlinear mode coupling on chromospheric heating. *Astronomy and Astrophysics*, 891(2), 110. <https://doi.org/10.3847/1538-4357/ab70b2>
- Wójcik, D., Kuźma, B., Murawski, K., & Srivastava, A. K. (2019). Two-fluid numerical simulations of the origin of the fast solar wind. *The Astrophysical Journal*, 884(2), 127. <https://doi.org/10.3847/1538-4357/ab26b1>
- Wedemeyer-Böhm, S., Scullion, E., Steiner, O., van der Voort, L. R., de La Cruz Rodriguez, J., Fedun, V., & Erdélyi, R. (2012, June). Magnetic tornadoes as energy channels into the solar corona. *Nature*, 486(7404), 505–508. <https://doi.org/10.1038/nature11202>
- Wentzel, D. G. (1979). Hydromagnetic surface waves on cylindrical fluxtubes. *Astronomy and Astrophysics*, 76(1), 20–23.
- Wiśniewska, A., Musielak, Z. E., Staiger, J., & Roth, M. (2016). Observational evidence for variations of the acoustic cutoff frequency with height in the solar atmosphere. *The Astrophysical Journal Letters*, 819(2), L23. <https://doi.org/10.3847/2041-8205/819/2/L23>
- Winebarger, A. R., Walsh, R. W., Moore, R., De Pontieu, B., Hansteen, V., Cirtain, J., et al. (2013). Detecting Nanoflare Heating Events in Subarcsecond Inter-moss Loops Using Hi-C. *Astronomy and Astrophysics*, 771(1), 21. <https://doi.org/10.1088/0004-637X/771/1/21>
- Withbroe, G. L., & Noyes, R. W. (1977). Mass and energy flow in the solar chromosphere and corona. *Annual Review of Astronomy and Astrophysics*, 15, 363–387. <https://doi.org/10.1146/annurev.aa.15.090177.002051>
- Xia, C., Keppens, R., Antolin, P., & Porth, O. (2014). Simulating the in situ condensation process of solar prominences. *The Astrophysical Journal*, 792(2), L38. <https://doi.org/10.1088/2041-8205/792/2/L38>
- Xue, Z., Yan, X., Cheng, X., Yang, L., Su, Y., Kliem, B., et al. (2016). Observing the release of twist by magnetic reconnection in a solar filament eruption. *Nature Communications*, 7, 11837. <https://doi.org/10.1038/ncomms11837>
- Yu, D. J., Van Doorselaere, T., & Goossens, M. (2017). Resonant absorption of surface sausage and surface kink modes under photospheric conditions. *The Astrophysical Journal*, 850(1), 44. <https://doi.org/10.3847/1538-4357/aa9223>

- Yuan, D., Shen, Y., Liu, Y., Li, H., Feng, X., & Keppens, R. (2019). Multilayered Kelvin-Helmholtz instability in the solar corona. *The Astrophysical Journal Letters*, *884*(2), L51. <https://doi.org/10.3847/2041-8213/ab4bcd>
- Zaqarashvili, T. V. (2003). Observation of coronal loop torsional oscillation. *Astronomy and Astrophysics*, *399*, L15–L18. <https://doi.org/10.1051/0004-6361/20030084>
- Zaqarashvili, T. V. (2020). Dynamic kink instability and transverse motions of solar spicules. *The Astrophysical Journal Letters*, *893*(2), L46. <https://doi.org/10.3847/2041-8213/ab881d>
- Zaqarashvili, T. V., Diaz, A. J., Oliver, R., & Ballester, J. L. (2010). Instability of twisted magnetic tubes with axial mass flows. *Astronomy and Astrophysics*, *516*, A84. <https://doi.org/10.1051/0004-6361/200913874>
- Zaqarashvili, T. V., & Erdélyi, R. (2009). Oscillations and waves in solar spicules. *Space Science Reviews*, *149*(1–4), 355–388. <https://doi.org/10.1007/s11214-009-9549-y>
- Zaqarashvili, T. V., Khodachenko, M. L., & Rucker, H. O. (2011a). Damping of Alfvén waves in solar partially ionized plasmas: Effect of neutral helium in multi-fluid approach. *Astronomy and Astrophysics*, *534*, A93. <https://doi.org/10.1051/0004-6361/201117380>
- Zaqarashvili, T. V., Khodachenko, M. L., & Rucker, H. O. (2011b). Magnetohydrodynamic waves in solar partially ionized plasmas: Two-fluid approach. *Astronomy and Astrophysics*, *529*, A82. <https://doi.org/10.1051/0004-6361/201016326>
- Zaqarashvili, T. V., Khodachenko, M. L., & Soler, R. (2013). Torsional Alfvén waves in partially ionized solar plasma: Effects of neutral helium and stratification. *Astronomy and Astrophysics*, *549*, A113. <https://doi.org/10.1051/0004-6361/201220272>
- Zaqarashvili, T. V., Khutsishvili, E., Kukhianidze, V., & Ramishvili, G. (2007). Doppler-shift oscillations in solar spicules. *Astronomy and Astrophysics*, *474*(2), 627–632. <https://doi.org/10.1051/0004-6361:20077661>
- Zaqarashvili, T. V., Kukhianidze, V., & Khodachenko, M. L. (2010). Propagation of a sausage soliton in the solar lower atmosphere observed by Hinode/SOT. *Monthly Notices of the Royal Astronomical Society*, *404*(1), L74–L78. <https://doi.org/10.1111/j.1745-3933.2010.00838.x>
- Zaqarashvili, T. V., Murawski, K., Khodachenko, M. L., Kukhianidze, V., & Rucker, H. O. (2011). Magnetohydrodynamic shocks and solitons in the solar atmosphere: Recent challenges in observations and theory. In H. O. Rucker, W. S. Kurth, P. Louarn, & G. Fischer (Eds.), *Planetary, solar and heliospheric radio emissions (pre vii)* (p. 465–470).
- Zaqarashvili, T. V., & Roberts, B. (2006). Two-wave interaction in ideal magnetohydrodynamics. *Astronomy and Astrophysics*, *452*(3), 1053–1058. <https://doi.org/10.1051/0004-6361:20053565>
- Zhelyazkov, I., Chandra, R., Srivastava, A. K., & Mishonov, T. (2015). Kelvin-Helmholtz instability of magnetohydrodynamic waves propagating on solar surges. *Astrophysics & Space Science*, *356*(2), 231–240. <https://doi.org/10.1007/s10509-014-2215-1>
- Zhugzhda, I. D., & Dzhalilov, N. S. (1984). Magneto-acoustic-gravity waves on the Sun. I—Exact solution for an oblique magnetic field. *Astronomy and Astrophysics*, *132*(1), 45–51.
- Zhugzhda, Y. D. (2005). Slow nonlinear waves in magnetic flux tubes. *Plasma Physics Reports*, *31*, 730–747. <https://doi.org/10.1134/1.2048832>
- Zhugzhda, Y. D., & Nakariakov, V. M. (1997). Non-linear body sausage waves in thin magnetic flux tubes. *Physics Letters A*, *233*(4), 413–417. [https://doi.org/10.1016/S0375-9601\(97\)82825-3](https://doi.org/10.1016/S0375-9601(97)82825-3)